Dickkopf proteins and their receptors in the adult lung and in idiopathic pulmonary fibrosis

Inauguraldissertation
zur Erlangung des Grades eines Doktors der Medizin
des Fachbereichs Medizin
der Justus-Liebig-Universität Gießen

vorgelegt von
Eva-Maria Pfaff
aus Herborn

Gießen 2013

Aus dem Zentrum für Innere Medizin
Medizinische Klinik II
Direktor: Prof. Dr. Werner Seeger
der Universitätsklinikum Gießen und Marburg GmbH
Standort Gießen

Gutachter: Prof. Dr. Oliver Eickelberg
Gutachter: Prof. Dr. Lienhard Schmitz
Tag der Disputation: 10.07.2015

Table of contents

1 Introduction

1.1 Idiopathic pulmonary fibrosis (IPF)

1.1.1 Classification

Idiopathic pulmonary fibrosis (IPF) is a fatal interstitial lung disease. It leads to a destruction of the lungs' architecture by accumulation of scar tissue and causes respiratory failure [1]. By classification, IPF belongs to the diffuse parenchymal lung diseases (DPLDs), more precisely to the idiopathic interstitial pneumonias (IIPs), a subset of the DLPDs with unknown etiology [2]. Seven IIP entities were specified in a Consensus Classification by the American Thoracic Society and the European Respiratory society in 2002 [2]: idiopathic pulmonary fibrosis (IPF), nonspecific interstitial pneumonia (NSIP), cryptogenic organizing pneumonia (COP), acute interstitial pneumonia (AIP), respiratory bronchiolitis-associated interstitial lung disease (RB-ILD), desquamative interstitial pneumonia (DIP) and lymphocytic interstitial pneumonia (LIP). A scheme of the DPLDs is depicted in ***figure 1***.

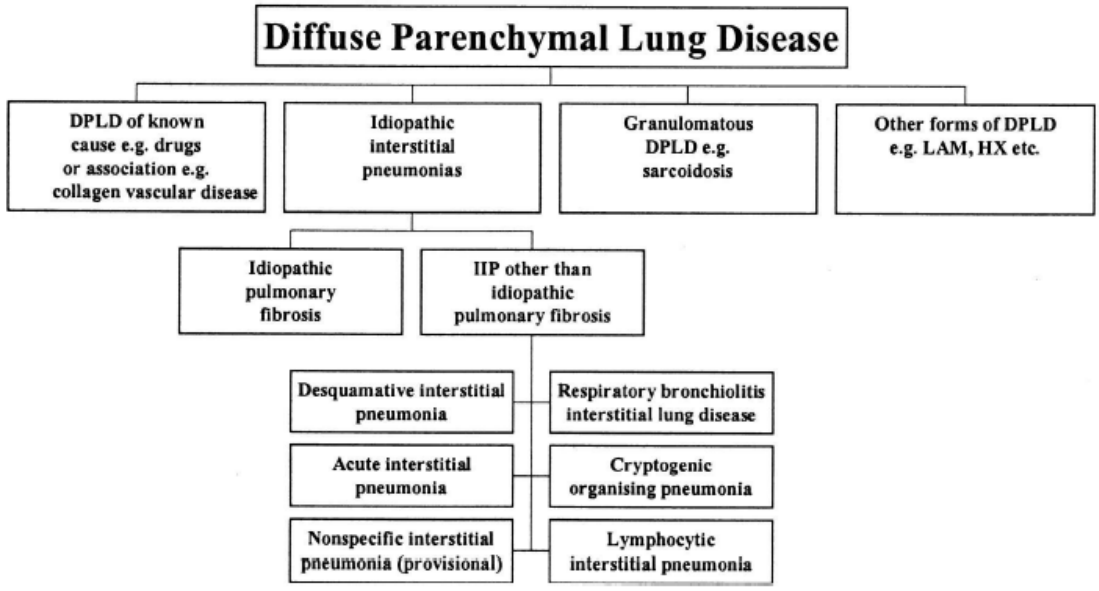

Figure 1. Diffuse parenchymal lung diseases [2]
The scheme depicts the group of diffuse parenchymal lung diseases (DPLDs), including the idiopathic interstitial pneumonias (IIPs). The IIPs can be divided into idiopathic pulmonary fibrosis (IPF) and IIPs other than IPF [2]. Reprinted with permission of the American Thoracic Society.

All IIPs affect the lung interstitium and cause respiratory deterioration [2]. However, IPF is the most frequent entity, as it is responsible for more than half of all cases [13,81]. It furthermore has a worse prognosis than other IIPs [2,13]. For precise diagnostic classification and assessment of therapeutic options, these several entities have to be distinguished by specific criteria on high-resolution computed tomography (HRCT) or lung biopsy [2].

1.1.2 Diagnostic criteria

The new, evidence-based guidelines implemented by cooperation of the American Thoracic Society (ATS), the European Respiratory Society (ERS), the Japanese Respiratory Society (JRS) and the Latin American Thoracic Association (ALAT) in 2011 define IPF as 'a specific form of chronic, progressive fibrosing interstitial pneumonia of unknown cause, occurring primarily in older adults, limited to the lungs, and associated with the histopathologic and / or radiologic pattern of UIP (usual interstitial pneumonia)' [133]. The revised diagnostic criteria for IPF demand the following [133]:

1. The exclusion of other known causes of interstitial lung disease, such as domestic and occupational environmental exposures, connective tissue disease and drug toxicity.
2. The presence of a UIP pattern on HRCT in patients not subjected to surgical lung biopsy.
3. Specific combinations of HRCT and surgical lung biopsy pattern in patients subjected to surgical lung biopsy [133].

It is emphasized that a multidisciplinary approach involving pulmonologists, radiologists and pathologists with experience in the field of interstitial lung diseases improves the validity of the diagnosis [133].

1.1.3 Clinical, histological and radiological characteristics

IPF can be found worldwide. The age of occurrence is usually 50 years or older, with a typical manifestation in the sixth and seventh decade of life [133]. Its incidence is estimated by 7 to 11 cases per 100000 persons a year, is higher in male than in female gender and increases with age [36,73,161]. There are cases of familial IPF that are considered to represent less than 4 % of all IPF cases [67,107] . These cases show similar characteristics and a similar outcome as the more frequent sporadic cases [14,93].

Clinical symptoms of IPF patients include dyspnea, nonproductive coughing, digital clubbing and "Velcro"-type inspiratory crackling at lung auscultation [2,133]. The respiratory function is impaired, especially under exertion, and pulmonary function testing reveals a restrictive pattern with deterioration of gas exchange. Pulmonary hypertension and cor pulmonale can develop in the course of the disease [1].

The histopathological equivalent of IPF is the usual interstitial pneumonia (UIP) pattern, which summarizes alterations of the lungs' architecture [2]. Prominent findings are an enhanced deposition of extracellular matrix components with formation of dense scars, honeycomb cysts (dilated bronchioles), an impaired alveolar epithelium and a mild interstitial inflammation [2,75,133,167]. The histological hallmark lesions of IPF are fibroblast foci, aggregates of activated myofibroblasts and fibroblasts [36] typically found in close relation to the alveolar septa [75,167] ***(figure 2A)***. In some studies their quantity has been associated with a worse prognosis [41,84,120], but deviating observations have been reported as well [43]. The pathological changes of lung architecture are predominantly located in the peripheral, subpleural and paraseptal parts of the lung tissue, arranged in heterogeneous patterns [133]. According to this, severely altered regions can be found next to areas with normal structural appearance [133].

Typical findings on HRCT are a bilateral, mainly basal and subpleural localized reticular pattern and structural alterations as honeycomb cysts, bronchiectasis and focal ground glass opacities [2,133] ***(figure 2B)***.

A. **B.**

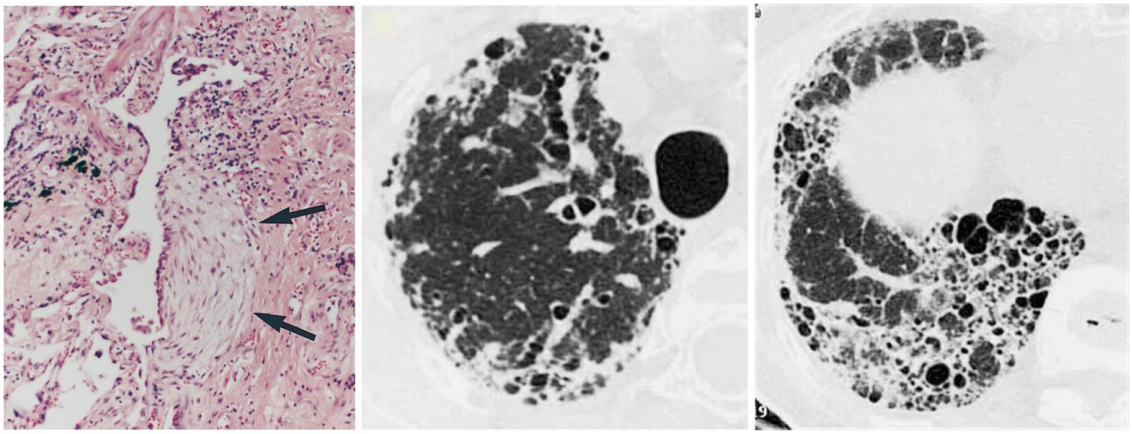

Figure 2. Histological and radiological characteristics of IPF.
(**A**) Histological alterations of the lung tissue in IPF, the arrows indicate a fibroblast focus [75].
(**B**) An IPF lung on HRCT [2]. Reprinted with permission of the American Thoracic Society.

1.1.4 Pathogenesis

Genetic predisposition as well as the influence of environmental factors have been investigated for identifying possible causes of IPF [14,36,57,133]. Thus, cigarette smoking has been associated with an increased risk to develop IPF [9,133] and several other potential risk factors such as a shortened telomere length, medication, chronic aspiration or viral infections are still under discussion [3,14,24,36,83,133]. However, there is no specific risk factor that can be considered as sole trigger for disease initiation and IPF still has to be classified as "idiopathic" [14,36].

The mechanisms underlying disease initiation and progression on the cellular and molecular level, leading to extensive fibrosis and destruction of the lungs' architecture, are not fully understood either [11,157]. More recent hypotheses about IPF pathophysiology have questioned its former understanding as a result of chronic inflammation [47,56,142]. These theories are supported by findings that inflammation in IPF lung tissues is not very prominent [75,142] and patients do not adequately respond to anti-inflammatory treatment [36,56]. It has rather been suggested that repetitive epithelial injuries in combination with a malfunction of repair processes, whether an inflammatory response may be included or not, are the key mechanisms of IPF pathogenesis [22,142]. An impaired epithelial function with disturbed re-epithelialization and hyperplasia of alveolar epithelial cells as well as an enhanced fibroblast activation are components of this process [142,160]. Fibroblast foci are seen as regions of an ongoing fibroblast / myofibroblast activation with the myofibroblast cell-type mainly responsible for extensive accumulation of extracellular matrix and therefore representing a key component of disease progression [75,128,141,171]. The origin of activated myofibroblasts is still under discussion. Hypotheses include the proliferation and activation of resident pulmonary fibroblasts, the recruitment of circulating progenitor cells that originate from the bone marrow and epithelial-mesenchymal transition (EMT), a process in which alveolar epithelial type II (ATII) cells can shift to a mesenchymal, fibroblast-like phenotype [39,141,157]. As fibroblast foci are primarily found in areas of impaired alveolar epithelium [75,167], epithelial-mesenchymal interactions via growth factors and cytokines are assumed to drive the fibrosing process [69,143]. However, despite the large number of investigations on underlying mechanisms and mediators, the exact nature of IPF pathogenesis has not been fully elucidated yet [11,42,123,157].

1.1.5 Course of disease and treatment

With a median survival between 2.5 and 3.5 years after diagnosis, the prognosis of IPF is poor [2,36]. It is a progressive disease that leads to the destruction of the lungs' architecture and causes respiratory failure [1,112]. Yet, the course of disease for an individual patient seems to be variable, with periods that appear fairly stable and periods of acute exacerbations that have a poor outcome [28,81,83,108,133]. Acute or subacute deterioration of respiratory function as well as respiratory infections or right heart failure were identified as disease related causes of death [1,108].

To date, a multitude of treatment studies for IPF have been initiated, including immunomodulatory, immunosuppressant, antioxidant, antifibrotic, vascular resistance modulatory and anticoagulatory approaches [36,38,48,58,124]. However, in almost all cases they either did not show a prominent effect on IPF progression or even turned out to be harmful, their therapeutic value has to be considered as unclear or they are still in the phase of clinical trials [38,45,58,112,168]. Therefore, for the majority of IPF patients, none of these treatment strategies has been recommended by the current ATS/ERS/JRS/ALAT guidelines [133]. There are some pharmacological treatments that may be considered as a reasonable choice for a minority of IPF patients, including pirfenidone [133]. Pirfenidone possesses antifibrotic, anti-inflammatory and antioxidant properties and can antagonize cellular mechanisms induced by transforming growth factor-β (TGF-β) [3,133]. It has recently been approved in Europe, India, Japan and China for the treatment of patients with mild to moderate IPF [64]. In a Cochrane review assessing several clinical trials, pirfenidone seemed to improve the progression-free survival of IPF patients by about 30 % [64,155]. Reliable data on the overall survival of patients treated with pirfenidone are still missing [64,155].

Lung transplantation is a therapeutical option with a proven and considerable benefit on survival of IPF patients [45,124,133,168]. However, access to donor organs is restricted and a comparatively high age or associated comorbidities of IPF patients represent limiting factors for a successful referral to transplantation [64,172]. Further recommendations include corticosteroid therapy in the event of acute exacerbations, the treatment of coexisting gastroesophageal reflux and long-term oxygen therapy [133].

Since the effects of present pharmaceutical treatments are limited, it emphasizes the need for a better understanding of the pathomechanisms that underlie disease initiation and progression. Hence, many recent studies have focused on molecular processes that

might be involved. Some proteins and signaling pathways have obtained particular attention, including WNT signaling [24,141].

1.2 WNT signaling

1.2.1 WNT proteins

WNTs are secreted glycoproteins, related by their amino acid sequences [101,114]. Their name derived from a combination of the gene names wingless and int-1, which were described independently, but were later identified to be homologous [135]. In mammals, 19 different WNT genes have been detected [101,114]. The signaling cascades of WNT proteins are of importance during embryogenesis and in the homeostasis of adult tissues [101]. Stem cell behavior, proliferation and differentiation processes as well as cell polarity are influenced by WNT [114,126]. Alterations of its signaling cascade were detected in various diseases and especially the role of WNT in cancer has been closely investigated [50,114]. Colorectal cancer, hepatocellular carcinoma and lung cancer are only some of the neoplasms that have been associated with mutations of WNT pathway components [27,50].

1.2.2 WNT signal transduction

WNT signaling is a complex process that involves several pathways with a number of ligands and receptors. There are different and so far incompletely understood crosslinks between the single participants and other transmitter cascades, as well as an extensive regulatory network [54,102,111,165].

At least three pathways of WNT signaling have been described [27,79,87]:

- WNT/β-catenin (canonical) pathway
- WNT/JNK planar cell polarity pathway
- WNT/Ca^{2+} pathway

Up to now, although several details of the molecular mechanisms still have to be clarified, the canonical pathway is the best studied WNT signaling cascade [5,7,27].

1.2.2.1 WNT/β-catenin signaling pathway

β-catenin, a protein also involved in cell adhesion, is the key molecule of signal transduction via the canonical pathway [16]. Under unstimulated conditions ***(figure 3A)***, cytoplasmic β-catenin is continuously phosphorylated by a complex consisting of glycogen synthase kinase 3β (GSK3β), casein kinase 1 (CK1), adenomatous polyposis coli (APC) and Axin [5,102]. Phosphorylated β-catenin is ubiquitinated and degraded by the pro-

teasome, with the result that cytoplasmic β-catenin levels are low [101,114]. WNT stimulation leads to changes in the β-catenin metabolism ***(figure 3B)***. For initiation of signal transduction, WNT has to interact with two different kinds of cell surface receptors. On the one hand, it binds to Frizzled proteins (FZD1-10) [125], a family of seven-transmembrane-spanning WNT receptors. On the other hand, it has to bind to single-pass transmembranous WNT coreceptors of the low density lipoprotein receptor-related protein family (LRP5 and LRP6) [29,101,114]. Following this interaction, LRP is phosphorylated by GSK-3β and casein kinase 1γ (CK1γ) at its intracytoplasmic portion [27,54,180]. Dishevelled (DSH) is phosphorylated and Axin is recruited, which directly binds to LRP [18,54,106]. The exact molecular mechanisms still have to be elucidated, but as a result of DSH phosphorylation and of the interaction of LRP and Axin, the GSK3β/APC/Axin complex is inhibited and therefore β-catenin phosphorylation and its degradation are prevented [18,54]. β-catenin accumulates in the cytoplasm and translocates to the nucleus, where it interacts with members of the T cell-specific transcription factor / lymphoid enhancer-binding factor (TCF/LEF) protein family, thereby modifying target gene expression [18,54,114].

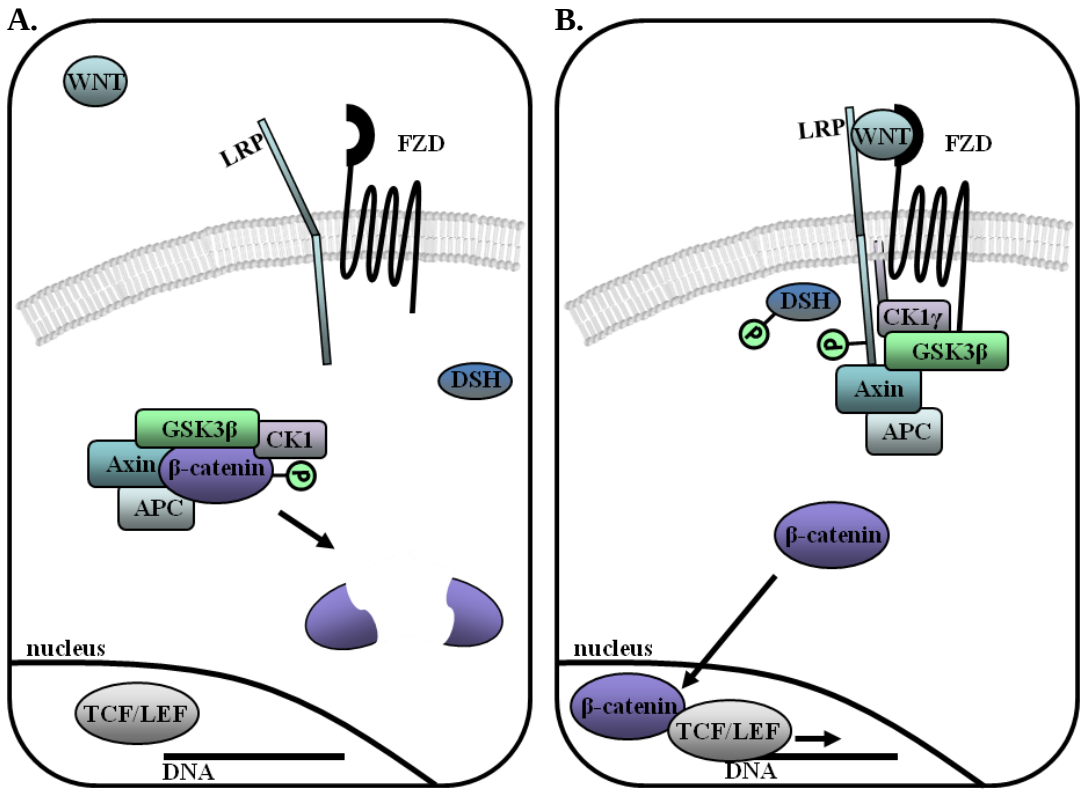

Figure 3. WNT/β-catenin signaling pathway.
(**A**) In the absence of WNT, β-catenin is degraded. (**B**) Changes induced by WNT stimulation. Inspired by an illustration by Michael D. Gordon and Roel Nusse [54].

1.2.3 WNT in the lung – embryogenesis and diseases of the adult

In mice, WNT signaling was found essential for several basic processes of lung development, including foregut specification [55], embryonic branching morphogenesis and distal airway formation [95,117]. A significant impact of WNT proteins on proper development and differentiation of the epithelial, mesenchymal, and vascular compartment of the lung has been stated [95,116,117,152].

Lung cancer has been related to alterations in WNT signaling, particularly non-small-cell lung carcinomas (NSCLCs) [87,109,166]. In detail, an overexpression of the proteins WNT1 [61] and WNT2 [177] was reported for NSCLC tissues and WNT1 overexpression has been associated with NSCLC proliferation [71]. An inhibition of these mediators was linked with apoptosis of cancer cells [61,177]. Furthermore, non-malignant lung diseases have been examined for an involvement of WNT signaling, such as pulmonary arterial hypertension and IPF [87].

1.2.3.1 WNT in IPF

By now there has been good evidence for an abnormal activation of the WNT/β-catenin pathway in IPF. An increase in nuclear β-catenin accumulation has been reported for bronchiolar lesions, atypical (cuboidal/hyperplastic) alveolar epithelial type II (ATII) cells and fibroblasts in the lung tissue of IPF patients, indicating an increase in active WNT/β-catenin signaling [26]. While WNT/β-catenin pathway activation in hyperplastic type II pneumocytes could also be demonstrated for other lung diseases involving alveolar damage and regeneration, the aberrant activation of WNT/β-catenin signaling in bronchiolar proliferative lesions and fibroblast foci was specific for IPF when compared to donor lungs and other interstitial lung diseases [26]. Further WNT/β-catenin pathway components were predominantly found in the bronchial and alveolar epithelium and some exhibited a significantly increased mRNA expression in lung tissue homogenates as well as in isolated ATII cells of IPF patients [86]. The presumed enhancement of pathway activation was supported by an increase in protein levels of phosphorylated GSK3β, phosphorylated LRP6 and β-catenin in IPF lung tissue homogenates [86]. Furthermore, an elevated expression of WNT/β-catenin target genes and their encoded proteins like Cyclin D1 [150] or matrix metalloproteinase 7 (MMP7) [15] was reported for IPF lung tissues by several studies [26,86,145,183]. The expression of WNT1-inducible-signaling pathway protein 1 (WISP1), another target gene of WNT signaling, was found increased

in alveolar epithelial type II cells of IPF patients [88]. WISP1 has been linked to the proliferation and epithelial-mesenchymal transition of ATII cells and moreover to an enhanced expression of extracellular matrix components by human lung fibroblasts [88].
In the mouse model of bleomycin-induced pulmonary fibrosis it could be demonstrated that *MMP7*-knockout [183] as well as WNT/β-catenin pathway inhibition via β-catenin small interfering RNA [82] or specific inhibition of WNT/β-catenin target gene transcription [63] are able to protect mice from fibrosis. The latter study actually reported a reversal of existing fibrotic changes [63].
It has been concluded that WNT signaling represents a developmental mechanism that is abnormally reactivated in IPF, a principle known from cancer pathogenesis [26,87,146].

1.2.4 Modulators of WNT signaling

Several proteins are able to modulate WNT activity, such as Dickkopf (DKK) [51], secreted frizzled-related protein (SFRP) [164], WNT inhibitory factor (WIF) [70] or Wise [72]. Two main mechanisms of interference with WNT signaling have been demonstrated. Thus, these factors either have the capability of direct interaction with WNT or to interfere with its receptors [76,87,102]. DKK proteins belong to the second category since they bind LRP receptors and therefore particularly affect the WNT/β-catenin pathway [102,121].

1.2.4.1 Dickkopf proteins and their interference with WNT

There are four known Dickkopf proteins in vertebrates, DKK1-4 [91,121]. They are secreted proteins sharing two cysteine rich domains, but they depict heterogeneity in structure and function [91,121]. DKK1 was initially discovered as WNT inhibitor and head-inducer in *Xenopus* embryos, where microinjection of *DKK1* mRNA led to formation of enlarged heads [51]. DKK2 and DKK4 are capable of WNT inhibition as well, whereas DKK2 can additionally act as a WNT activator, depending on molecular environment and cellular context [17,91,96,103,174].
Modulation of the WNT/β-catenin pathway is possible due to the ability of DKKs to bind LRP receptors. This has been demonstrated for DKK1 and DKK2 [8,17,105,147]. Additionally it has been discovered that DKK1 and DKK2 have high affinity for the Kremen (KRM) receptors KRM1 and KRM2 [104], single transmembrane-spanning proteins with a kringle domain in their extracellular region [119]. Although it seems that KRM proteins

are not necessarily required for WNT regulation via DKK [121,169], the presence of KRM receptors enhances the ability of DKK proteins 1, 2 and 4 to inhibit WNT signaling [103,104]. DKK2 with its context-dependent repressive or activating ability can actually be converted into a pure WNT inhibitor via interaction with KRM2 [103].

DKK3 demonstrates the highest discrepancy of the four family members in structure as well as in function [91,103]. It seems neither capable of binding LRP [105], nor KRM [103,104], nor was it considered to interfere with WNT signaling [91,103,174]. However, recent studies have reported WNT modulatory capabilities for DKK3, as it inhibited β-catenin accumulation in an osteosarcoma cell line [66] and reduced WNT/β-catenin target gene transcription in lung cancer cell lines [178]. So far, the exact mode of action remains unknown.

As mechanism of interference with WNT signaling it has been suggested that DKK proteins 1, 2 and 4 are able to form a ternary complex with LRP and KRM, which is removed from the cell surface via endocytosis [104,138]. Since LRP is no longer available for WNT binding, activation of the WNT/β-catenin pathway is prevented. However, there is contradictory data concerning the LRP internalization upon DKK stimulation. Authors of a more recent work criticize the usage of LRP6 overexpression in previous studies [148]. They favor the mere binding of DKK to LRP as sufficient mechanism for WNT modulation when experiments are performed at endogenous LRP6 levels [148].

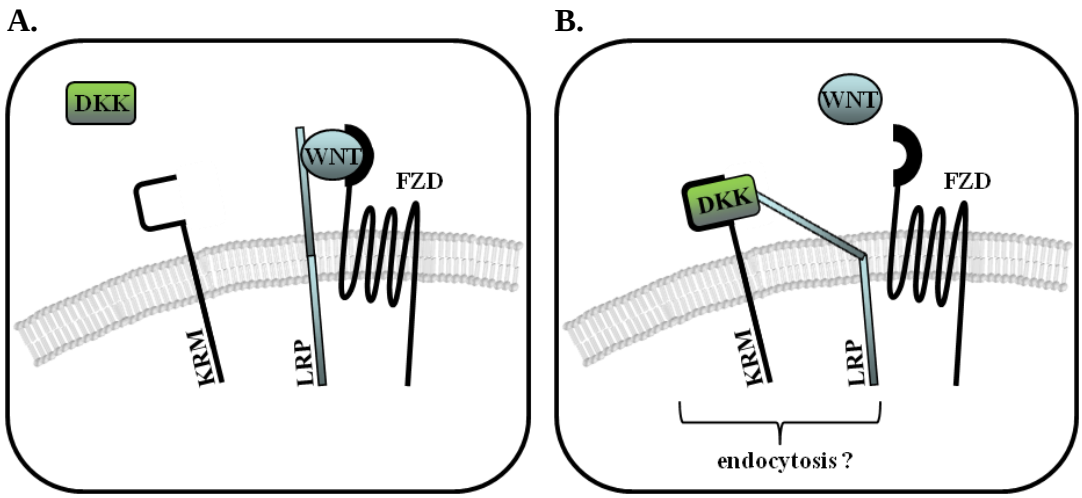

Figure 4. Mechanism of DKK interference with WNT.
(**A**) WNT interacts with FZD and LRP receptors to initiate canonical WNT signaling.
(**B**) DKK inhibits canonical WNT signaling by binding to LRP and KRM.

1.2.4.2 Dickkopf in the lung and in fibrosing diseases

Dickkopf proteins have been related to several diseases, for example DKK1 has been demonstrated to impair bone formation and to influence joint remodeling in rheumatoid arthritis [37,115]. It is overexpressed in several types of cancer [44,140] and it is also thought to promote osteolytic bone metastases [132].

Concerning the lung, DKK proteins seem to influence organ development and have been related to malignancies. In detail, it has been demonstrated that DKK1 is able to inhibit WNT/β-catenin signaling in the embryonic mouse lung and causes defects in distal airway and pulmonary vasculature formation [34,151]. DKK1 and DKK3 have both been related to lung cancer. More precisely, DKK1 expression was found increased in several lung cancer samples and it has been considered as a biomarker for lung carcinoma [149,175]. Anti-DKK1 is able to inhibit the growth of lung cancer cell lines *in vitro* and in a murine tumor graft model [140]. DKK3 expression was shown to be decreased in many human non-small-cell lung carcinoma (NSCLC) tissues and it has recently been suggested to prevent lung cancer cell growth by inhibition of the WNT/β-catenin pathway *in vitro* [109,178].

The role of DKK proteins in IPF had not been addressed before, but DKK1 has already been related to other fibrosing processes. Investigations on rat hepatic stellate cells and on a mouse model of cholestatic liver fibrosis have revealed an antifibrotic effect of DKK1 via WNT inhibition [23]. DKK1 also inhibited β-catenin accumulation in irradiated primary mouse fibroblasts, which is of importance since β-catenin is suggested to promote irradiation-induced fibrosis [59]. Furthermore, DKK1 mediated WNT inhibition was suggested to prevent renal fibrosis, because it decreased myofibroblast activation and collagen deposition in a mouse model of obstructive nephropathy [62]. A recent study has demonstrated that overexpression of DKK1 in transgenic mouse models can inhibit experimentally induced skin fibrosis, a fibrosing process suggested to result from an activated crosstalk between the transforming growth factor-β (TGF-β) and the WNT/β-catenin signaling pathway [4].

1.3 Aim of the study

The pathogenetic mechanisms underlying idiopathic pulmonary fibrosis are still not clarified. Impairment of the lung epithelium and epithelial-mesenchymal interactions are assumed to drive disease progression, but the exact mechanisms and mediators have to be further elucidated. A better understanding of the cellular and molecular processes would certainly contribute to an improvement in therapeutic strategies for this fatal disease.

The abnormal activation of the WNT/β-catenin pathway in the lung tissue of IPF patients seems to be a promising research subject. Even more since inhibition of its target genes' transcription has been demonstrated to prevent bleomycin-induced pulmonary fibrosis in mice [63,82,183]. Therefore regulators of WNT/β-catenin signaling are of particular interest.

Dickkopf proteins can effectively modulate the WNT/β-catenin signal transduction cascade and they have already demonstrated antifibrotic capabilities in mouse models of cholestatic liver fibrosis, renal fibrosis and skin fibrosis [4,23,62]. However, scarcely anything is known about their expression in healthy adult lungs, even less in IPF lungs. Thus, the aim of this study was to reveal and to compare the expression and localization of DKK proteins and their receptors in unaffected adult lungs and IPF lungs to provide a more detailed picture of WNT signaling and its modulation in IPF.

2 Material and Methods

2.1 Material

2.1.1 Human lung tissue

Lung tissue biopsies were obtained from 15 IPF patients with histological usual interstitial pneumonia (UIP) pattern (4 females, 11 males; age (mean ± standard deviation (stdev)): 58 years ± 10 years, vital capacity (VC) (mean ± stdev): 48 % ± 10 %, total lung capacity (TLC) (mean ± stdev): 50 % ± 7 %, diffusing capacity of the lung for CO per unit of alveolar volume (DL_{CO}/VA) (mean ± stdev): 23 % ± 4 % (all in % predicted), additional nasal oxygen supplementation (O_2): 2-4 l/min, partial pressure (Pa) of O_2 / CO_2 in the arterialized ear lobe blood sample: Pa_{O2}: 36–71 mmHg, Pa_{CO2}: 33-65 mmHg) and 13 organ donors (6 females, 7 males; age (mean ± stdev): 42 years ± 19 years). For individual patient characteristics see ***table 1*** (chapter ***10.1***). After explantation, tissue samples were immediately snap-frozen or placed in 4 % (w/v) paraformaldehyde. The study protocol was approved by the Ethics Committee of the Justus-Liebig-University School of Medicine, Giessen, Germany (AZ 31/93). Informed consent in written form was obtained from each subject.

2.1.2 Human bronchoalveolar lavage fluid (BALF)

Flexible fiber-optic bronchoscopy with extraction of bronchoalveolar lavage fluid was performed in a standardized manner by a physician at the Department of Medicine of the Justus-Liebig-University Giessen, Germany, in 2006 and 2007. Informed consent was obtained from each subject. The group of IPF patients consisted of 9 males (age (mean ± stdev): 68 years ± 6 years, VC (mean ± stdev): 59 % ± 19 %, TLC (mean ± stdev): 59 % ± 14 %, DL_{CO}/VA (mean ± stdev): 55 % ± 15 %, additional nasal oxygen supplementation (O_2): 0-5 l/min, Pa_{O2}: 45-90 mmHg, Pa_{CO2}: 34-46 mmHg). Individual patient characteristics are shown in ***table 2*** (chapter ***10.2***). The control group consisted of 4 healthy, non-smoking volunteers without a history of cardiac or lung disease (medical students from the Medical School of the Justus-Liebig-University Giessen, Germany).

2.1.3 Cell lines

cell line	specification	company, catalog number
BEAS-2B	human bronchial epithelial cell line (non-cancerous)	European Collection of Cell Cultures, Porton Down, UK; 95102433

2.1.4 Antibodies

2.1.4.1 Primary antibodies

Antibodies used for Western blot analysis (WB) and immunohistochemistry (IHC) are listed with the respective dilutions.

antibody	origin	company, catalog number	dilution WB	dilution IHC
anti-DKK1	rabbit	Santa Cruz Biotechnology, Santa Cruz, CA, USA, sc-25516	1:200	1:50
anti-DKK2	rabbit	Abcam, Cambridge, UK, ab38594	1:200	-
anti-DKK4	rabbit	Abcam, Cambridge, UK, ab38589	1:200	-
anti-DKK4	rabbit	Santa Cruz Biotechnology, Santa Cruz, CA, USA, sc-25519	-	1:100
anti-KRM1	goat	R&D Systems, Minneapolis, MN, USA, AF2127	1:1000	1:100
anti-KRM2	rabbit	Sigma-Aldrich, St. Louis, MO, USA, HP A003223	1:200	1:100
anti-LRP5	rabbit	Abcam, Cambridge, UK, ab38311	-	1:100
anti-β-actin	rabbit	Cell Signaling Technology, Beverly, MA, USA, #4967	1:1000	-

2.1.4.2 Secondary antibodies

antibody	origin	company, catalog number	dilution
anti-rabbit IgG, HRP conjugated	goat	Pierce Protein Research Products, Rockford, IL, USA,#31460	1:3000
anti-goat IgG, HRP conjugated	rabbit	Pierce Protein Research Products, Rockford, IL, USA, #31402	1:3000
biotinylated anti-rabbit IgG	goat	Invitrogen, Carlsbad, CA, USA, Histostain-Plus Kit	ready to use
biotinylated anti-goat IgG	rabbit	Invitrogen, Carlsbad, CA, USA, Histostain-Plus Kit	ready to use

2.1.5 Recombinant proteins

recombinant protein	company, catalog number
recombinant human DKK1	R&D Systems, Minneapolis, MN, USA, 1096-DK

2.1.6 Chemicals and reagents

product	company
Acrylamide solution, Rotiphorese® Gel 30	Carl Roth GmbH, Karlsruhe, Germany
Agarose	Promega, Madison, WI, USA
APS	Promega, Madison, WI, USA
β-Mercaptoethanol	Sigma-Aldrich, Saint Louis, MO, USA
Bromphenol Blue	Sigma-Aldrich, Saint Louis, MO, USA
BSA	Sigma-Aldrich, Saint Louis, MO, USA
Chemiluminescent Substrate SuperSignal® West Pico	Pierce Protein Research Products, USA
Citrate Buffer 20 x	Invitrogen, Carlsbad, CA, USA
Complete™ Protease Inhibitor	Roche, Basel, Switzerland
Dkk-1 DuoSet ELISA, human, DY1906	R&D Systems, Minneapolis, MN, USA
DNA Ladder 100 bp	Promega, Madison, WI, USA
DNA loading dye Blue/Orange, 6 x	Promega, Madison, WI, USA
dNTP PCR Nucleotide Mix 10 mM	Promega, Madison, WI, USA
EDTA	Promega, Madison, WI, USA

EGTA	Sigma-Aldrich, Saint Louis, MO, USA
Ethanol absolute	Sigma-Aldrich, St. Louis, MO, USA
Ethidium bromide	Carl Roth GmbH, Karlsruhe, Germany
Glycerol	Merck Biosciences, Darmstadt, Germany
Glycerol gelatine, Kaiser's	Merck Biosciences, Darmstadt, Germany
Glycine	Carl Roth GmbH, Karlsruhe, Germany
H_2O_2 30 % (w/w) Perdrogen®	Sigma-Aldrich, St. Louis, MO, USA
Hematoxylin, Mayer's	Sigma-Aldrich, St. Louis, MO, USA
HEPES Buffer solution 1 M	PAA Laboratories, Pasching, Austria
Histostain-Plus Kit	Invitrogen, Carlsbad, CA, USA
LHC-9	Invitrogen, Carlsbad, CA, USA
Methanol	Sigma-Aldrich, Saint Louis, MO, USA
$MgCl_2$ (25 mM)	Applied Biosystems, Wellesley, MA, USA
$MgCl_2$ (50 mM)	Invitrogen, Carlsbad, CA, USA
Milk powder (blotting grade)	Carl Roth GmbH, Karlsruhe, Germany
NaCl	Merck Biosciences, Darmstadt, Germany
Paraformaldehyde	Sigma-Aldrich, Saint Louis, MO, USA
PBS	PAA Laboratories, Pasching, Austria
PCR Buffer 10 x (without $MgCl_2$)	Applied Biosystems, Wellesley, MA, USA
Platinum® SYBR® Green qPCR SuperMix-UDG	Invitrogen, Carlsbad, CA, USA
Protein Standards Precision Plus, prestained	Bio-Rad, Hercules, CA, USA
Quick Start™ Bradford 1 x dye reagent	Bio-Rad, Hercules, CA, USA
Quick Start™ Bradford Protein Assay	Bio-Rad, Hercules, CA, USA
Random Hexamers (50 µM)	Applied Biosystems, Wellesley, MA, USA
Reverse Transcriptase MuLV RT (50 U/µl)	Applied Biosystems, Wellesley, MA, USA
RNase Inhibitor	Applied Biosystems, Wellesley, MA, USA
RNase-Free DNase Set	Qiagen, Venlo, Netherlands
RNase-Free Water	Qiagen, Venlo, Netherlands
RNeasy Mini Kit	Qiagen, Venlo, Netherlands
Roti®-Quick-Kit	Carl Roth GmbH, Karlsruhe, Germany

SDS Solution 10 % (w/v)	Promega, Madison, WI, USA
Streptavidin	Invitrogen, Carlsbad, CA, USA
TAE Buffer, Rotiphorese® 10 x	Carl Roth GmbH, Karlsruhe, Germany
TEMED	Bio-Rad, Hercules, CA, USA
Tris	Carl Roth GmbH, Karlsruhe, Germany
Triton® X-100	Promega, Madison, WI, USA
Trypsin EDTA 1 x	PAA Laboratories, Pasching, Austria
Tween® 20	Sigma-Aldrich, Saint Louis, MO, USA
Xylene	Sigma-Aldrich, St. Louis, MO, USA

2.1.7 Equipment and Software

product	**company**
Calibrated Densitometer GS-800™	Bio-Rad, Hercules, CA, USA
Chromatography paper 3MM CHR	Whatman International Ltd, Maidstone, UK
Developing machine; X Omat 2000	Kodak, Rochester, NY, USA
Electrophoresis and Western blot chambers	Bio-Rad, Hercules, CA, USA
Fusion A153601 microplate reader	Packard BioScience/PerkinElmer, Waltham, MA, USA
Light microscope Leica DMIL	Leica Microsystems, Wetzlar, Germany
Light microscope Olympus BX 51	Olympus, Hamburg, Germany
Microsoft Office Word/Excel/PowerPoint 2007	Microsoft Corp., Unterschleißheim, Germany
NanoDrop ND-100 Spectrophotometer	Peqlab, Erlangen, Germany
Nitrocellulose membrane	Bio-Rad, Hercules, CA, USA
PCR-Thermocycler	MJ Research, Waltham, MA, USA
Quantity One 1-D analysis software	Bio-Rad, Hercules, CA, USA
Sequence Detection System Fast 7500 and Software	Applied Biosystems, Wellesley, MA, USA
UV transilluminator	UVP, Upland, CA, USA
X-ray film AGFA Curix HT1000G Plus	AGFA-Gevaert, Mortsel, Belgium

2.2 Methods

2.2.1 Quantitative reverse transcription polymerase chain reaction (qRT-PCR)

2.2.1.1 RNA extraction from tissue

RNA was extracted from lung tissue homogenates with the Roti-Quick-Kit. Tissue samples were homogenized in liquid nitrogen with a pestle, 2 ml of the guanidinium thiocyanate containing solution were added per 0.2 g of tissue. After 20 min of incubation, samples were additionally homogenized with a syringe with a 0.9 mm needle. 2 ml of the phenol and chloroform containing solution were added per sample. Samples were incubated on ice for 10 min and vortexed every 2 min. After centrifugation at 13000 rpm for 15 min at a temperature of 4 °C, two phases were separated. The upper, RNA-containing phase was incubated with an equal volume of the isopropanol containing solution for 1 h, at a temperature of -80 °C. The centrifugation step was repeated and an RNA-containing pellet could be extracted. It was dissolved in a mixture of 150 µl of the guanidinium thiocyanate containing solution and 150 µl of the isopropanol containing solution and incubated for 1 h at -80 °C. Centrifugation and dissolving step were repeated. After that, samples were centrifuged at 13000 rpm for 20 min at a temperature of 4 °C. The supernatant was removed and 500 µl of ethanol (70 % v/v in RNase-free water) were added. Another centrifugation step was performed for 10 min and the supernatant was discarded. The RNA pellet was resuspended in 50 µl of RNase-free water and stored at a temperature of -80 °C.

2.2.1.2 RNA extraction from cells

Medium was removed from cell culture flasks and cells were washed with PBS twice. Cells were disrupted and detached from the plates by scraping with a rubber policeman after addition of β-mercaptoethanol containing RNeasy Lysis Buffer (RNeasy Mini Kit, preparation according to manufacturer's protocol) and they were homogenized with a syringe with 0.9 mm needle. RNA extraction was performed with the silica-membrane column system of the RNeasy Mini Kit according to the manufacturer´s instructions. This included an on-column DNase digestion using the RNase-free DNase Set to additionally remove DNA contaminant. Finally the RNA isolate was eluted from the column by adding 35 µl of RNase free water twice and then stored at a temperature of -80 °C.

2.2.1.3 RNA quantification

Quantification of the samples' RNA concentration was performed with the NanoDrop spectrophotometer. Therefore the optical density (OD) of 1.5 µl of the sample was determined at a wavelength of 260 nm, at which absorption correlates to the concentration of nucleic acids within the sample. Since the absorption at a wavelength of 280 nm correlates with protein concentration, sample purity could be verified by determination of the RNA/protein ratio (OD_{260nm}/OD_{280nm}). This ratio had to lie in between 1.8 and 2.0 to exclude a relevant protein contamination.

2.2.1.4 cDNA synthesis by reverse transcription

For analysis of the respective mRNA levels in a sample by qRT-PCR, the RNA had to be transcribed in complementary DNA (cDNA) by an RNA-dependent DNA polymerase (reverse transcriptase). For preparation of cDNA synthesis, 1 µg of total RNA was diluted with RNase-free water to a total volume of 20 µl. RNA denaturation was performed by a thermocycler at a temperature of 70 °C for 10 min, followed by cooling the samples down for 5 min at a temperature of 4 °C. For reverse transcription, 20 µl of the following RT Mastermix was added to each RNA sample:

component	volume	final concentration
10 x PCR Buffer (without $MgCl_2$)	4 µl	1 x
$MgCl_2$ (25 mM)	8 µl	5 mM
dNTP PCR Nucleotide Mix (10 mM)	2 µl	0.5 mM
Random Hexamers (50 µM)	2 µl	2.5 µM
RNase Inhibitor (20 U/µl)	1 µl	0.5 U/µl
Reverse Transcriptase MuLV RT (50 U/µl)	2 µl	2.5 U/µl
ddH_2O	1 µl	

Reverse transcription was performed with a thermocycler by the following steps at the indicated temperatures and durations:

step	temperature	duration
attachment of random hexamers	20 °C	10 min
reverse transcription	43 °C	75 min
inactivation of reverse transcriptase	99 °C	5 min
cooling down	4 °C	

The synthesized cDNA samples were stored at a temperature of -20 °C.

2.2.1.5 Quantitative reverse transcription polymerase chain reaction

Quantitative reverse transcription polymerase chain reaction (qRT-PCR) was performed using fluorogenic SYBR Green. 2 µl of the previously synthesized cDNA were transferred to the wells of a 96 well plate, each well filled with 23 µl of the following qRT-PCR Mastermix:

component	volume	final concentration
Platinum® SYBR® Green qPCR SuperMix-UDG	13 µl	
MgCl (50 mM)	1 µl	2 mM
forward primer (10 µM)	0.5 µl	200 nM
reverse primer (10 µM)	0.5 µl	200 nM
ddH_2O	8 µl	

Amplification and detection were carried out with the Sequence Detection System Fast 7500 via performance of 45 cycles of the following steps at the indicated temperatures and durations:

step	temperature	duration
activation of polymerase enzyme	50 °C	2 min
first denaturation	95 °C	5 min
second denaturation	95 °C	5 s
annealing	59 °C	5 s
elongation	72 °C	30 s
dissociation step 1	95 °C	15 s
dissociation step 2	60 °C	1 min
dissociation step 3	95 °C	15 s
dissociation step 4	60 °C	15 s

By denaturation, double-stranded DNA gets separated into single strands. During the annealing phase, primers bind to the respective sequences at the single DNA strands. A new DNA strand is synthesized by the DNA-dependent DNA polymerase enzyme during the elongation step.

2.2.1.6 Primers

GenBank from the National Center for Biotechnology Information (NCBI) and the primer express 3.0 software were used to create adequate primer sequences for target and reference genes. Detailed information on primer sequences are listed in ***table 3*** (chapter ***10.3***). Each primer was tested with an undiluted, a 1:8 and a 1:64 diluted sample to determine primer efficiency for a range of template concentrations. All primers were utilized at a final concentration of 200 nM.

2.2.1.7 Data evaluation

Since SYBR Green binds sequence independently to double stranded DNA and leads to an increase in fluorescence, the amount of synthesized DNA is proportional to the fluorescent signal. Fluorescence intensity is measured at the end of the elongation step of each cycle and a curve depicting the increase in DNA is created. Each sample was measured twice and the values were averaged. Empty controls containing the respective qRT-PCR Mastermix without addition of cDNA were measured at each plate.

Target-DNA levels of each sample were normalized to DNA levels of a reference gene within the respective sample amplified at the same plate. As reference gene, the constitutively and ubiquitously expressed hypoxanthine-guanine phosphoribosyltransferase 1 (*HPRT1*) [33,99] was used in all qRT-PCR reactions. Comparing measurement of target and reference DNA levels was performed in the exponentially increasing segment of the curve before saturation had occurred and a threshold was set in this area. For target and reference gene, the same threshold was used for all samples. The cycle number at which the fluorescent signal reached the threshold was expressed as Ct (threshold cycle). These Ct values are in inverse proportion to the initial amount of RNA within the sample. The relative transcript abundance in a sample is expressed as ΔCt value ($\Delta Ct = Ct^{reference} - Ct^{target}$). Therefore positive ΔCt values of the present study represent an elevated expression of the target gene compared to the reference gene, while negative ΔCt values depict a target gene expression lower than the expression of the reference gene. Relative changes of transcript levels in IPF samples compared to donor samples are given as ΔΔCt values ($\Delta\Delta Ct = \Delta Ct^{IPF} - \Delta Ct^{donor}$). The ΔΔCt values approximately correspond to the binary logarithm of the fold change.

The purity and length of the DNA products were verified by melting curve analysis and agarose gel electrophoresis.

2.2.1.8 Melting curve analysis

Melting curve analysis by the Fast 7500 System was used to verify the purity of the specific DNA product, since the melting temperature depends on product length and the amount of GC basepairs in the double stranded DNA. After 45 cycles, the melting point was identified by slowly increasing heat. The peak of fluorescence-intensity-change, induced by the release of SYBR Green during the melting process, indicated the specific melting temperature of one product.

2.2.1.9 DNA agarose gel electrophoresis

qRT-PCR products were displayed by agarose gel electrophoresis in order to check the product size to ensure that the correct template had been amplified. Therefore agarose gels were prepared:

2 % agarose gel: 1 x TAE buffer
2 % agarose (w/v)
0.5 µg/ml ethidium bromide

PCR product samples were mixed 5:1 with 6 x DNA loading dye Blue/Orange and transferred onto the gel. For each PCR product, two different samples as well as one empty control sample were applied. A 100 bp DNA ladder was run at the same gel. Gels were run in an electrophoresis chamber filled with 1x TAE buffer (Tris, acetic acid and EDTA) at 100 V for about 1 h. DNA bands were analyzed under ultraviolet lighting conditions.

2.2.2 Western blot analysis

Western blot analysis was performed on total protein extracts of lung tissue homogenates from donors and IPF patients.

2.2.2.1 Protein extraction and quantification

The lung tissue was homogenized in liquid nitrogen with a pestle and 1 ml lysis buffer was added per 0.1 g of tissue. After 5 min of incubation, a syringe with 0.9 mm needle was used for further homogenization. Samples were kept on ice for 30 min and vortexed every 5 min. By centrifugation at 12.000*g at a temperature of 4 °C for 10 min, the pro-

tein containing supernatant was separated from the tissue homogenate. The Supernatant was collected and stored at a temperature of -20 °C.

Lysis buffer: 20 mM Tris pH 7.5
150 mM NaCl
1 mM EDTA
1 mM EGTA
1 % Triton X-100
2 mM Na_3VO_4
1:25 Complete™, protease inhibitor mix

Protein quantification of each sample using the Quick Start Bradford Protein Assay was performed via spectrophotometric measurement with a Fusion A153601 Reader at a wavelength of 570 nm. Wells of a 96 well plate were filled with 200 µl of Quick Start Bradford dye reagent and 10 µl of the 1:20 diluted protein sample were added to a respective well. Additionally, six diluted BSA samples (0.05, 0.1, 0.2, 0.3, 0.4 and 0.5 µg/µl) as well as negative controls containing Bradford dye and 1:20 diluted protein lysis buffer were measured at the same plate. Measurement was done after an incubation period of 15 min. Duplicates of BSA standards, protein samples and controls were measured and values were averaged. By comparing protein sample values to the BSA standard curve via interpolation, the protein concentration of each sample was calculated.

2.2.2.2 SDS polyacrylamide gel electrophoresis (SDS-PAGE)

To separate proteins by size, SDS polyacrylamide gel electrophoresis was performed. Therefore, the required volume of each protein sample was calculated to reach a total amount of 25 µg protein for every loading sample. Equivalent volumes of SDS containing 2 x Sample Buffer were added to the proteins and samples were denaturated at a temperature of 95 °C for 10 min. Samples were loaded onto a polymerized gel, consisting of a 15-well stacking gel on top of a resolving gel. As molecular weight size markers, 5 µl of protein standards were run at the same gel. Proteins were kept on ice in between the working steps. Gels were run in an electrophoresis chamber filled with Running Buffer at 110 V.

Resolving gel:	Stacking gel:
10 % acrylamide/bisacrylamide	5 % acrylamide/bisacrylamide
375 mM Tris-HCl pH 8.8	125 mM Tris-HCl pH 6.8
0.1 % (w/v) SDS	0.1 % (w/v) SDS
0.1 % (w/v) APS	0.1 % (w/v) APS
0.1 % (v/v) TEMED	0.1 % (v/v) TEMED

The used acrylamide solution contained acrylamide : bisacrylamide in a 37.5 : 1 ratio.

2 x Sample Buffer:	Running Buffer:
100 mM Tris-HCl pH 6.8	25 mM Tris
4 % (w/v) SDS	250 mM glycine
0.2 % (w/v) bromphenol blue	0.1 % (w/v) SDS
20 % (v/v) glycerol	
100 nM DTT	

2.2.2.3 Immunoblotting

For further analyses, the separated proteins had to be transferred onto a nitrocellulose membrane by using a Western blot electrophoresis chamber. Packing of the gel and nitrocellulose membrane into a cassette with chromatography papers and sponges was performed in Transfer Buffer to avoid air bubbles. The cassette was put into an electrophoresis chamber filled with Transfer Buffer and the transfer was done at 120 V for 1 h. An icebox was used to cool the chamber during the blotting process.

2.2.2.4 Protein detection

Nitrocellulose membranes were washed in Washing Buffer (2 x 5 min) and kept in Blocking Buffer for about 1 h. Incubation with the primary antibody was performed overnight at a temperature of 4 °C with a specific dilution of each antibody in Blocking Buffer (primary antibodies and their dilutions are listed in chapter ***2.1.4.1***). After a washing step (3 x 10 min with Washing Buffer), the membrane was incubated with a dilution of the adequate horseradish peroxidase (HRP)-conjugated secondary antibody in Blocking Buffer for 1 h (secondary antibodies and their dilutions are listed in chapter ***2.1.4.2***). By performing these steps, primary and secondary antibodies got attached to the specific protein bands. After a second washing step (5 x 10 min), the membrane was

ready for protein detection. For visualization of protein bands, the Chemiluminescent Substrate SuperSignal West Pico was applied according to the manufacturer's instructions. An X-ray film was exposed to the membrane and developed. All incubation and washing steps were performed at room temperature unless it is indicated otherwise.
Before reusing the nitrocellulose membrane for an additional protein detection, they were incubated with Stripping Buffer in a water bath at a temperature of 52 °C for 8 min and were washed with Washing Buffer afterwards. Subsequent detection of β-actin at each membrane served as a control for an equal protein loading.

Transfer Buffer:
25 mM Tris
192 mM glycine
20 % (v/v) methanol

Washing Buffer:
PBS (1 x)
0.1 % (v/v) Tween 20

Blocking Buffer:
PBS (1 x)
0.1 % (v/v) Tween 20
5 % (w/v) skim milk powder

Stripping Buffer:
100 mM β-mercaptoethanol
62.5 mM Tris pH 6.8
2 % (w/v) SDS

2.2.2.5 Densitometry

Densitometric analysis of the developed X-ray films was performed using a GS-800 calibrated densitometer and the Quantity One 1-D analysis software. Optical density of β-actin loading control was used to equalize differences in total protein loading. Therefore the relative expression level of an indicated protein is calculated as relative optical density (OD) (optical density of indicated protein / optical density of β-actin) for each sample. Changes in expression levels between the indicated groups were calculated as fold change of the means ($OD_{(IPF)}$ / $OD_{(donor)}$) and were expressed as fold change ± SEM.

2.2.3 Immunohistochemistry

Paraffin embedded human lung tissue samples were cut to 3 µm sections and were mounted on slides. Immunohistochemical staining was performed with the Histostain Plus Kit. To remove the paraffin, slides were kept in an oven at a temperature of 48 °C

over night and were transferred to Xylene (3 x 10 min) afterwards. Incubation with decreasing ethanol dilutions (100 %, 95 %, 70 % of ethanol, 2 x 5 min each) and a washing step with PBS (2 x 5 min) followed, before tissue sections were treated for antigen retrieval. Therefore slides were placed in citrate buffer (1 x) and cooked in a water bath for 25 min. After cooling down, slides were washed with PBS again. Quenching of endogenous peroxidase activity was performed by incubation with 3 % (v/v) H_2O_2 for 20 min. After another washing step, the slides were incubated with serum blocking solution (Histostain Plus Kit, derived from a species different than the source of the intended primary antibody) for 10 min. Subsequently the primary antibody was prepared and applied over night at a temperature of 4 °C.

Primary antibody dilution:
PBS 1 x
1.5 % (v/v) serum blocking solution
1 % or 2 % (v/v) primary antibody solution*
*depending on the respective antibody dilution; primary antibodies and their dilutions are listed in chapter ***2.1.4.1***.

After 30 min at room temperature and a washing step with PBS, slides were incubated with the species-appropriate secondary biotinylated antibody (Histostain plus Kit, secondary biotinylated antibodies are listed in chapter ***2.1.4.2***) for 10 min. Another washing step and incubation with HRP-conjugated Streptavidin for 10 min followed. After removal of Streptavidin, the staining reaction was performed by incubating the slides with chromogen solution (Histostain Plus Kit) until red color staining was clearly visible under a microscope. Another washing step with PBS and counterstaining with hematoxylin for 8 min were performed subsequently. After washing the slides in running tap water for 10 min, coverslips were mounted via glycerol gelatine. The stained sections were examined using an Olympus BX51 microscope and pictures were taken in 3 different magnifications as indicated.

2.2.4 Cell culture

The human bronchial epithelial cell line BEAS-2B was maintained in 250 ml culture flasks filled with 10 ml LHC-9 medium in a 5 % CO_2 containing atmosphere of 95-

100 % air humidity at a temperature of 37 °C. The medium was changed every 3 days at least and passaging was performed at a confluence of 80-90 %. Therefore the medium was removed, cells were gently washed with PBS (1 x) and incubated with 3 ml of Trypsin EDTA. After detachment, 7 ml of fresh medium were added and 20 % of the cell suspension were transferred to a new culture flask. Then medium was added for a total amount of 10 ml suspension.

2.2.5 Enzyme-linked immunosorbent assay (ELISA)

A human DKK1 enzyme-linked immunosorbent assay was performed on BAL fluids (BALF) following the company's instructions. Wells of a 96-well microplate were coated with 100 µl of the diluted Capture Antibody and incubated for 12 h. Blocking was performed with 300 µl of Reagent Diluent for 1 h before incubating the wells with 100 µl of the BALF samples for 2 h. Additionally, seven 2-fold serial dilutions of recombinant DKK1 protein standard with a high standard of 4000 pg/ml were applied at the same plate. Each BALF sample and the standard dilutions were tested twice. After incubation with 100 µl of the Detection Antibody for 2 h, Streptavidin-HRP was added to each well for 20 min. Then 100 µl of Substrate Solution were applied to each well for another 20 min. Color reaction was stopped by adding 50 µl of Stop Solution. In between the working steps, washing steps were carried out following the company's instruction. Optical density was determined with a microplate reader at a wavelength of 450 nm. To minimize the optical influence of the plate, a second measurement was done at 570 nm and values were subtracted from the measurement at 450 nm. Double values of samples and standards were finally averaged and the DKK1 protein content of BAL fluids was calculated by interpolation on the basis of the seven point DKK1 protein standard curve.

2.2.6 Statistical analysis

All numerical data are presented as mean ± SEM. All experimental values were tested for normal distribution and the indicated groups were compared using a two-tailed, unpaired two-sample t-test for experiments with two groups of independent samples. Results were considered statistically significant when $p < 0.05$.

3 Results

3.1 Expression of Dickkopf proteins and their receptors in the lung

3.1.1 mRNA expression of Dickkopf proteins and their receptors

In order to quantify the relative Dickkopf (*DKK*) mRNA expression levels in donor and IPF lungs, quantitative (q)RT-PCR was performed on whole RNA-isolates of human lung tissue homogenates. Samples from donors and IPF patients were compared regarding their expression of *DKK1-4* (n=10, each). As demonstrated in ***figure 5A***, the mRNA of all four DKK proteins was detected in donor as well as in IPF specimens. While *DKK3* presented the highest relative mRNA expression level, *DKK4* showed the lowest mRNA expression in both, donor and IPF tissue samples. Comparison of IPF and donor lungs revealed significant differences in the relative transcript levels. While *DKK1* and *DKK4* presented a significantly increased mRNA expression in the fibrotic lung tissues (ΔΔCt (mean ± SEM): *DKK1*: 0.85 ± 0.36 and *DKK4*: 2.09 ± 0.88), *DKK2* mRNA was significantly decreased (ΔΔCt: -0.94 ± 0.34). The transcript levels of *DKK3* did not show a significant alteration (ΔΔCt: 0.02 ± 0.85).

The relative mRNA expression levels of the DKK receptors low density lipoprotein receptor-related protein (*LRP*) 5 and 6 and Kremen (*KRM*) 1 and 2 were examined likewise. As depicted in ***figure 5B***, all examined receptors were detected in donor as well as in IPF tissues. In both groups, *KRM2* presented a lower basal expression level than *KRM1* and the *LRP* receptors. While the expression of *KRM1* mRNA in IPF samples was significantly increased compared to the donor tissues (ΔΔCt: 1.31 ± 0.28), expression levels of *KRM2*, *LRP5* and *LRP6* were not significantly altered (ΔΔCt: *KRM2*: 1.19 ± 0.72, *LRP5*: 0.06 ± 0.63 and *LRP6*: 0.03 ± 0.37).

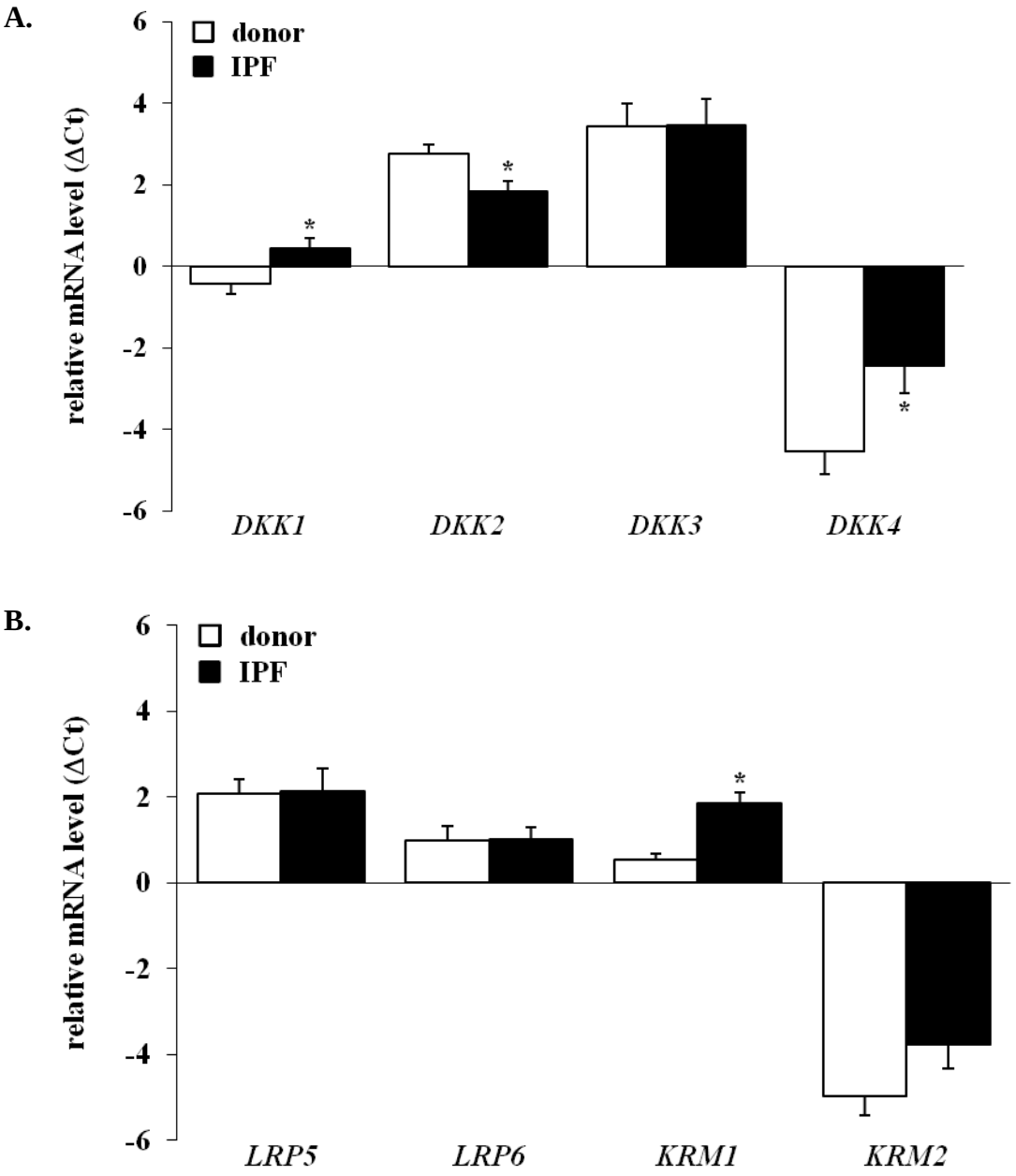

Figure 5. mRNA expression of Dickkopf (*DKK*), low density lipoprotein receptor-related protein (*LRP*) and Kremen (*KRM*) in donor and IPF lung tissue.
The mRNA expression of *DKK1-4* (**A**) and of the receptors *LRP5*, *LRP6*, *KRM1* and *KRM2* (**B**) was analyzed in human lung tissue homogenates derived from donors (open bars) and IPF patients (black bars) by quantitative (q)RT-PCR. Results of both groups (n=10, each) are shown as relative mRNA expression compared to the reference gene *HPRT1* (ΔCt), and presented as mean ± SEM, * = $p < 0.05$.

3.1.2 Protein expression of Dickkopf and Kremen

In order to examine whether the altered mRNA expression levels result in differences in protein expression, Western blot analysis was performed on whole protein extracts of donor and IPF lung tissue homogenates (n=5, each). The expression of the DKK proteins 1, 2 and 4, as well as of KRM1 and KRM2 was investigated. As depicted in

figure 6A, Western blotting revealed enhanced levels of all investigated DKK proteins in IPF. These results were confirmed by densitometric quantification of the respective protein immunoblots (***figure 6B***). Accordingly, DKK1 and DKK2 protein expression was significantly increased in IPF samples compared to donor samples (fold change ($OD_{(IPF)}$ / $OD_{(donor)}$) ± SEM: DKK1: 1.45 ± 0.09 and DKK2: 1.99 ± 0.13). DKK4 protein was not detected in donor tissue samples at all.

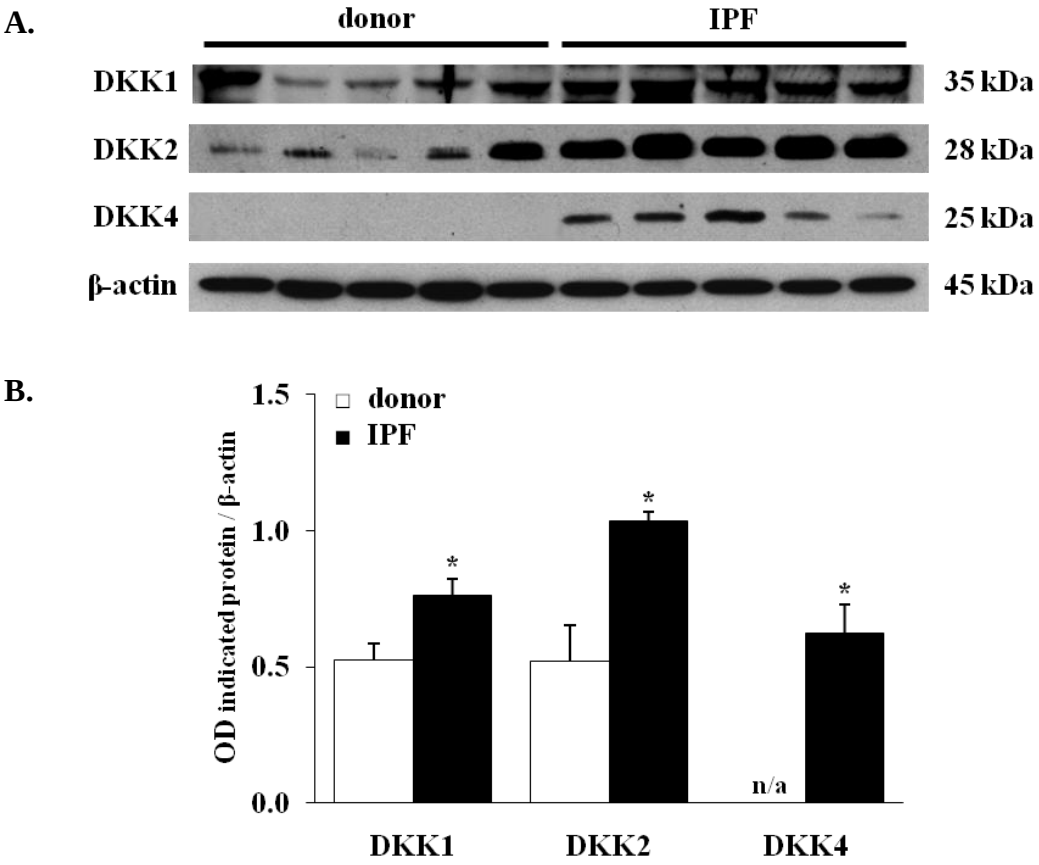

Figure 6. Protein expression of DKK in donor and IPF lung tissue.
(**A**) Expression of the proteins DKK1, DKK2 and DKK4 in human lung tissue homogenates derived from donors and IPF patients (n=5, each) was determined by Western blot analysis of whole protein extracts. Antibodies were used as indicated, β-actin served as loading control. Protein immunoblots were carried out twice, a representative blot is shown. (**B**) The densitometric analyses of the respective protein immunoblots are shown. The relative optical density (OD) (optical density of indicated protein / optical density of β-actin loading control) is presented for donor (open bars) and IPF (black bars) tissues as mean ± SEM. DKK4 protein was not detected in donor tissue samples, the respective OD was not available (n/a). * = $p < 0.05$.

The DKK receptors KRM1 and KRM2 were detected in lung tissue homogenates of both, donors and IPF patients (***figure 7A***). Both proteins depicted a high intra-group variability of expression levels. While the densitometric analysis of KRM1 protein revealed a significantly increased expression in IPF tissue samples (($OD_{(IPF)}$ / $OD_{(donor)}$):

1.92 ± 0.06), the expression of KRM2 protein was not significantly altered (($OD_{(IPF)}$ / $OD_{(donor)}$): 1.37 ± 0.40) (***figure 7B***).

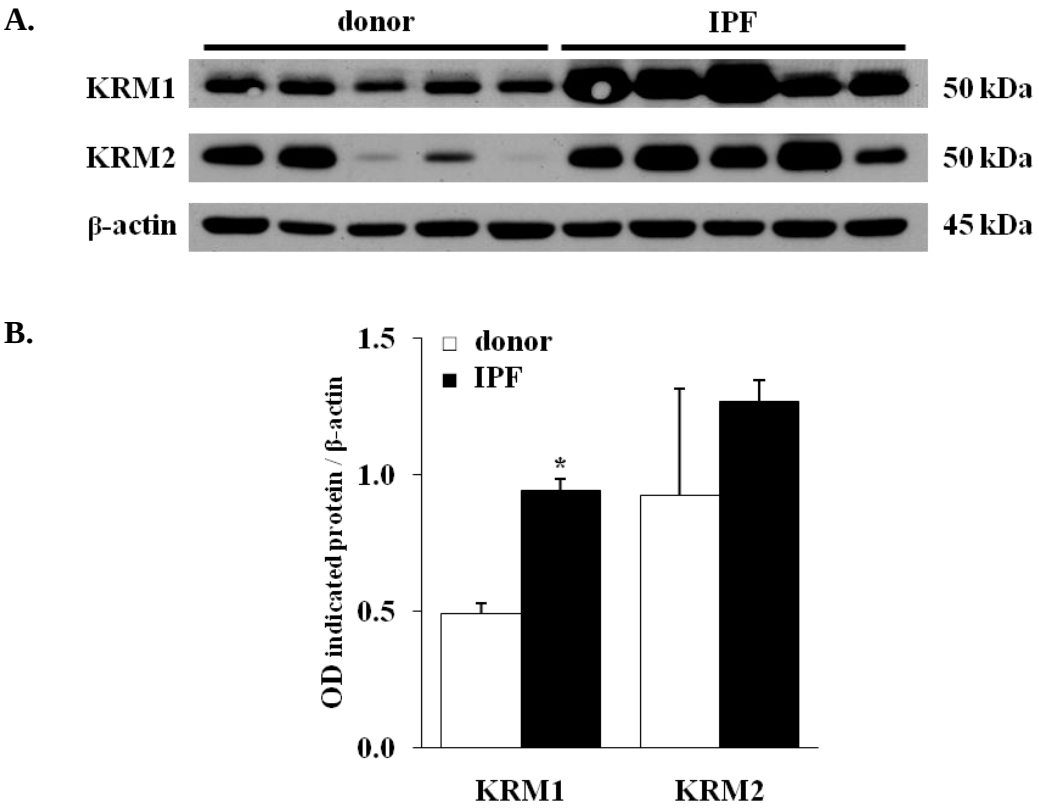

Figure 7. Protein expression of KRM in donor and IPF lung tissue.
(**A**) Expression of the proteins KRM1 and KRM2 in human lung tissue homogenates derived from donors and IPF patients (n=5, each) was determined by Western blot analysis of whole protein extracts. Antibodies were used as indicated, β-actin served as loading control. Protein immunoblots were carried out twice, a representative blot is shown. (**B**) The densitometric analyses of the respective protein immunoblots are shown. The relative optical density (OD) (optical density of indicated protein / optical density of β-actin loading control) is presented for donor (open bars) and IPF (black bars) tissues as mean ± SEM, * = $p < 0.05$.

3.2 Localization of Dickkopf proteins and their receptors in the lung

After investigations concerning the expression profile of Dickkopf proteins and receptors on mRNA and protein level, their actual localization in the human lung was examined. Immunohistochemical stainings were performed on donor and IPF lung tissue sections in order to identify cells that are actually expressing these proteins. Antibodies with reasonable and reproducible staining results could be found for DKK1 and DKK4 as well as for the receptors LRP5, KRM1 and KRM2. Stainings were performed at least twice using three different donor and IPF lung tissues for each antibody. Representative bronchial (A) and alveolar (B) regions are presented. As demonstrated in ***figure 8A***,

DKK1 was mainly located in bronchial epithelial cells in donor (left panel) and IPF lungs (right panel), with a pronounced accumulation of DKK1 in basal bronchial epithelial cells (***figure 8A***, arrows). In IPF lungs, DKK1 was furthermore located in hyperplastic alveolar epithelial cells (***figure 8B***, right panel, arrows). Besides, granulocytes presented staining of DKK1 protein in both, donor and IPF lung tissue sections (best recognizable in ***figure 8B***, left panel).

A.

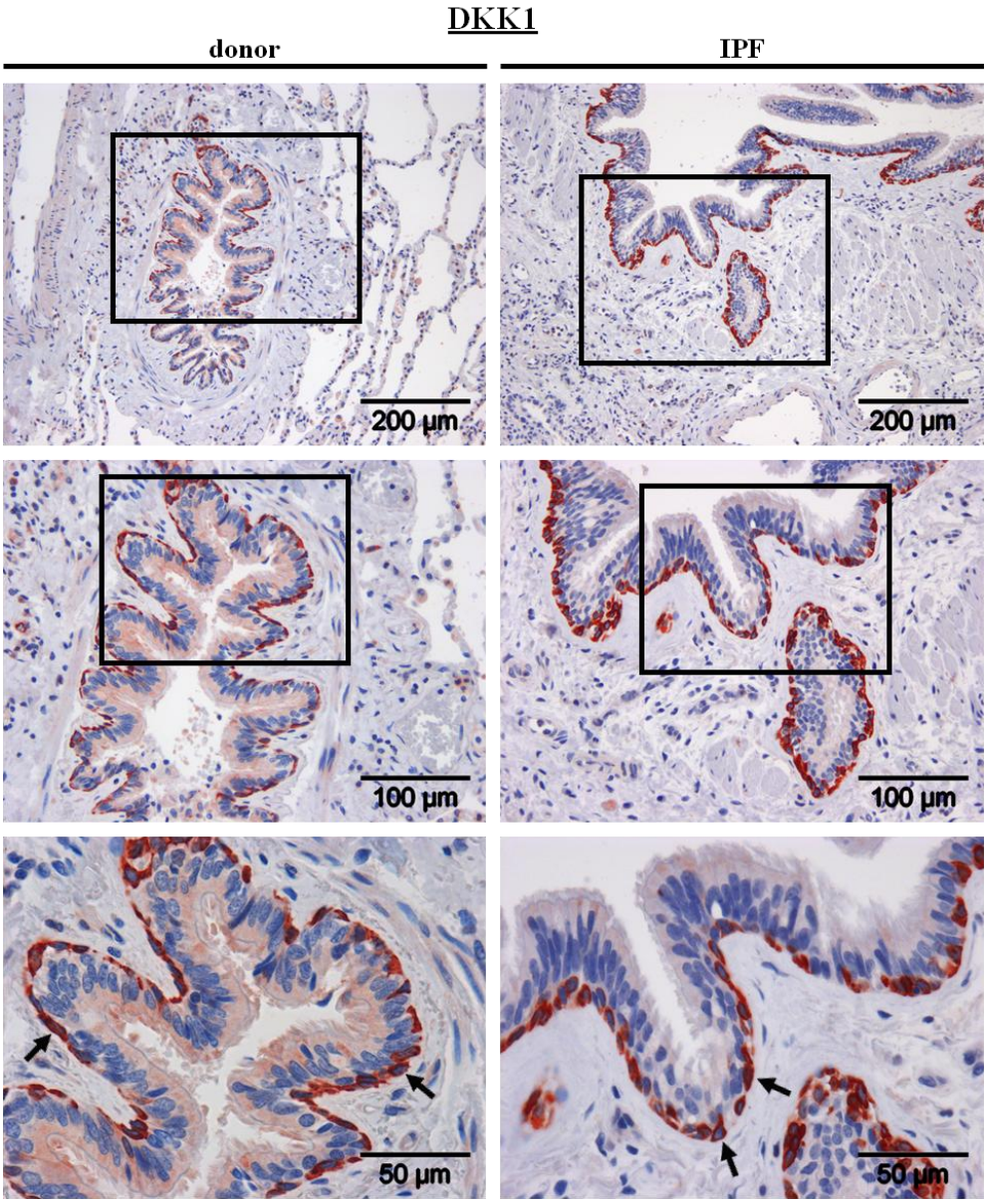

Figure 8A. Localization of DKK1 protein in donor and IPF lung tissue – bronchial regions.

Immunohistochemical staining for DKK1 protein was performed on lung tissue sections of donors and IPF patients. Stainings were performed at least twice using three different donor and IPF lung tissues. Representative **bronchial regions** of donor (**left panel**) and IPF (**right panel**) lungs are shown in three magnifications as indicated. Arrows indicate basal bronchial epithelial cells.

B.

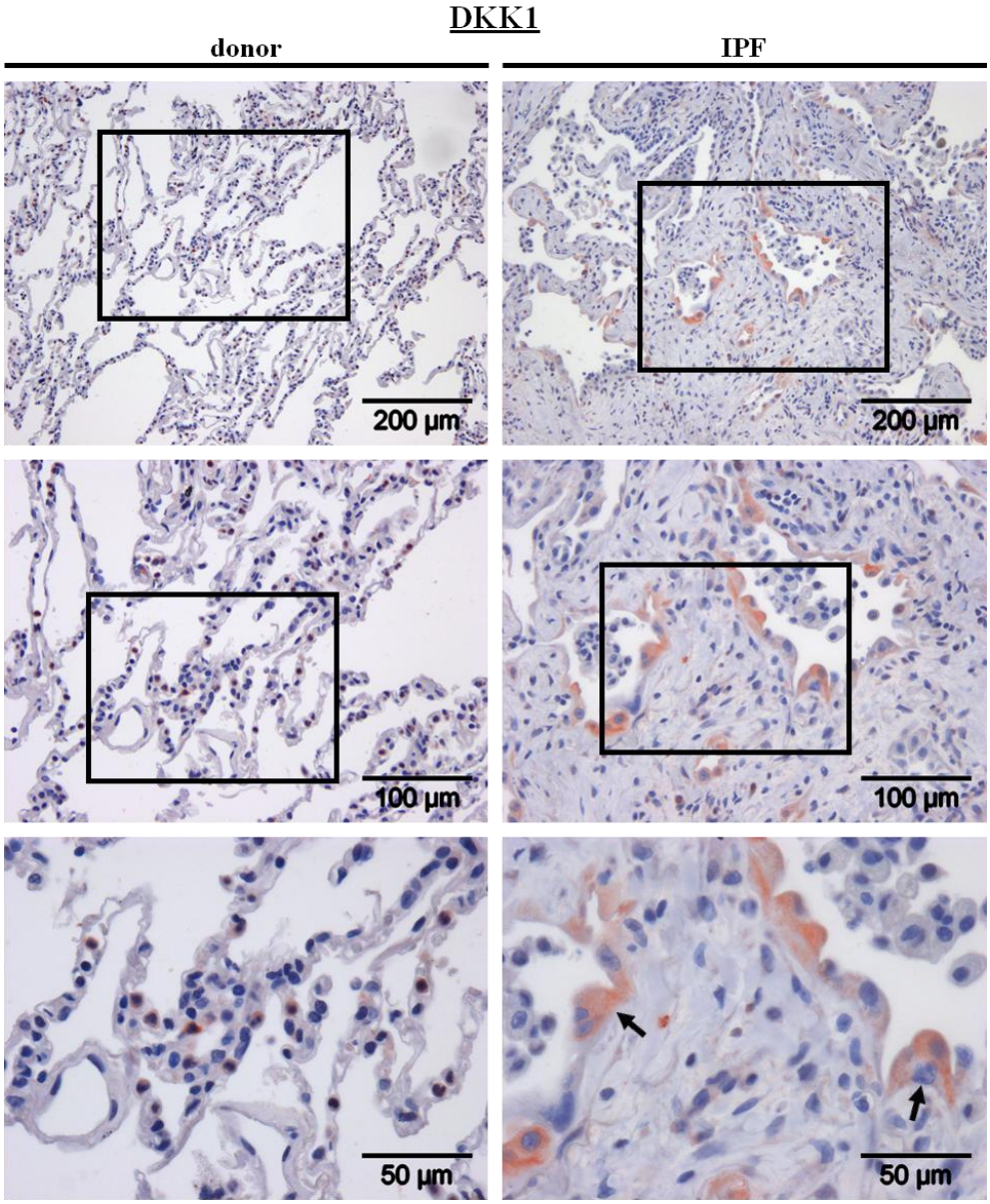

Figure 8B. Localization of DKK1 protein in donor and IPF lung tissue – alveolar regions.

Immunohistochemical staining for DKK1 protein was performed on lung tissue sections of donors and IPF patients. Stainings were performed at least twice using three different donor and IPF lung tissues. Representative **alveolar regions** of donor (**left panel**) and IPF (**right panel**) lungs are shown in three magnifications as indicated. Arrows indicate hyperplastic alveolar epithelial cells.

DKK4 protein was largely located in bronchial epithelial cells (***figure 9A***) and to a slighter extent in interstitial cells, in donor as well as in IPF lung tissues (***figure 9A and 9B***). In comparison to DKK1, DKK4 expression exhibited a more equal basal-apical intensity in the bronchial epithelium (***figure 9A***), whereas its general expression pattern was scattered. As depicted in ***figure 9B***, DKK4 was strongly expressed in hyperplastic alveolar epithelial cells in IPF (***figure 9B***, right panel, arrows).

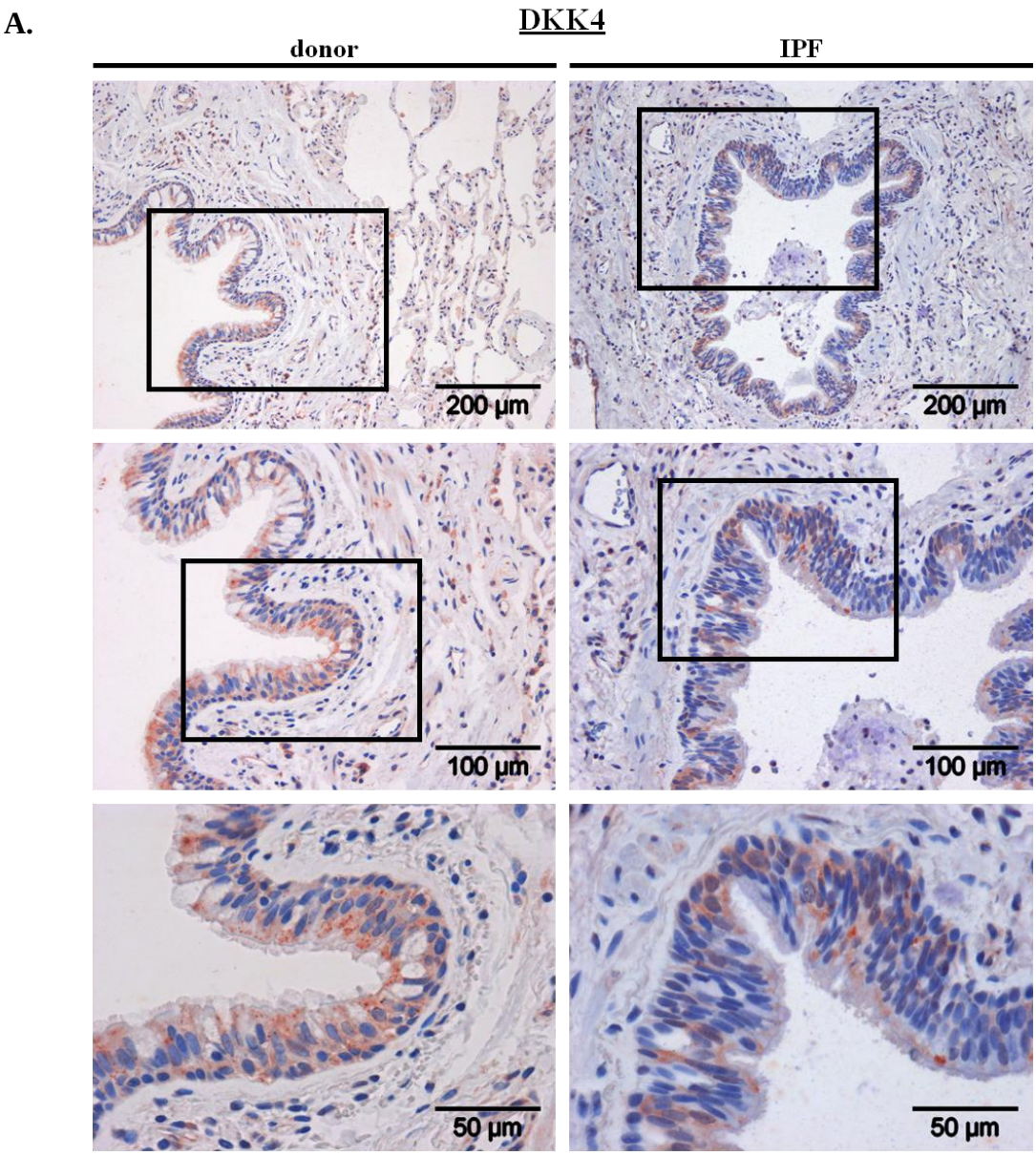

Figure 9A. Localization of DKK4 protein in donor and IPF lung tissue – bronchial regions.

Immunohistochemical staining for DKK4 protein was performed on lung tissue sections of donors and IPF patients. Stainings were performed at least twice using three different donor and IPF lung tissues. Representative **bronchial regions** of donor (**left panel**) and IPF (**right panel**) lungs are shown in three magnifications as indicated.

B.

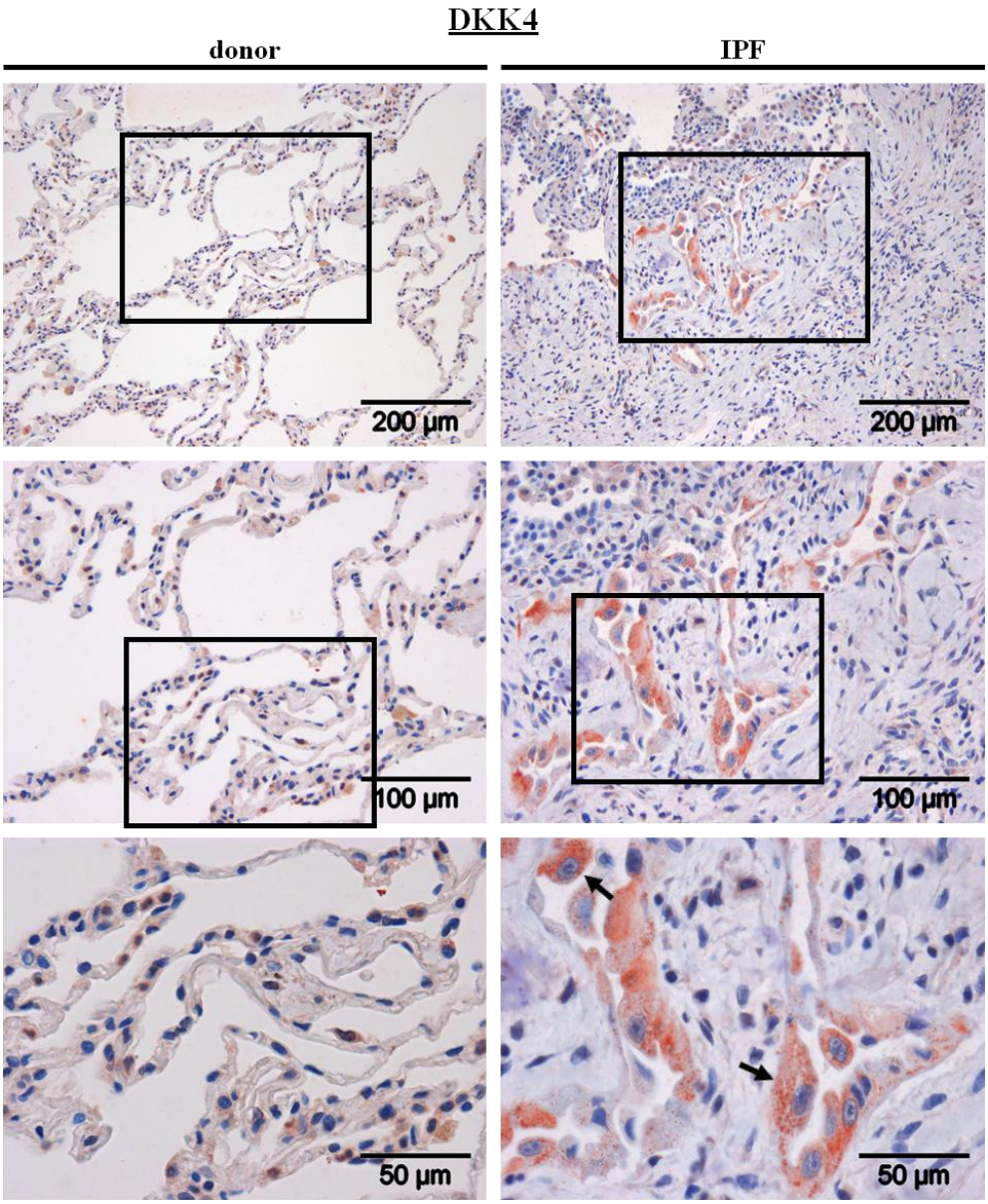

Figure 9B. Localization of DKK4 protein in donor and IPF lung tissue – alveolar regions.

Immunohistochemical staining for DKK4 protein was performed on lung tissue sections of donors and IPF patients. Stainings were performed at least twice using three different donor and IPF lung tissues. Representative **alveolar regions** of donor (**left panel**) and IPF (**right panel**) lungs are shown in three magnifications as indicated. Arrows indicate hyperplastic alveolar epithelial cells.

LRP5 receptor was detected in the bronchial epithelium of donor (***figure 10A***, left panel) and IPF tissues (***figure 10A***, right panel), with predominant staining of supranuclear regions in columnar bronchial epithelial cells (***figure 10A***, left and right panel, arrows). In IPF, LRP5 was slightly expressed in hyperplastic alveolar epithelial cells (***figure 10B***, right panel, arrows). Moreover, immune cells presented staining of LRP5 in donor and IPF lung tissue sections (best recognizable in ***figure 10B***, left panel).

A.

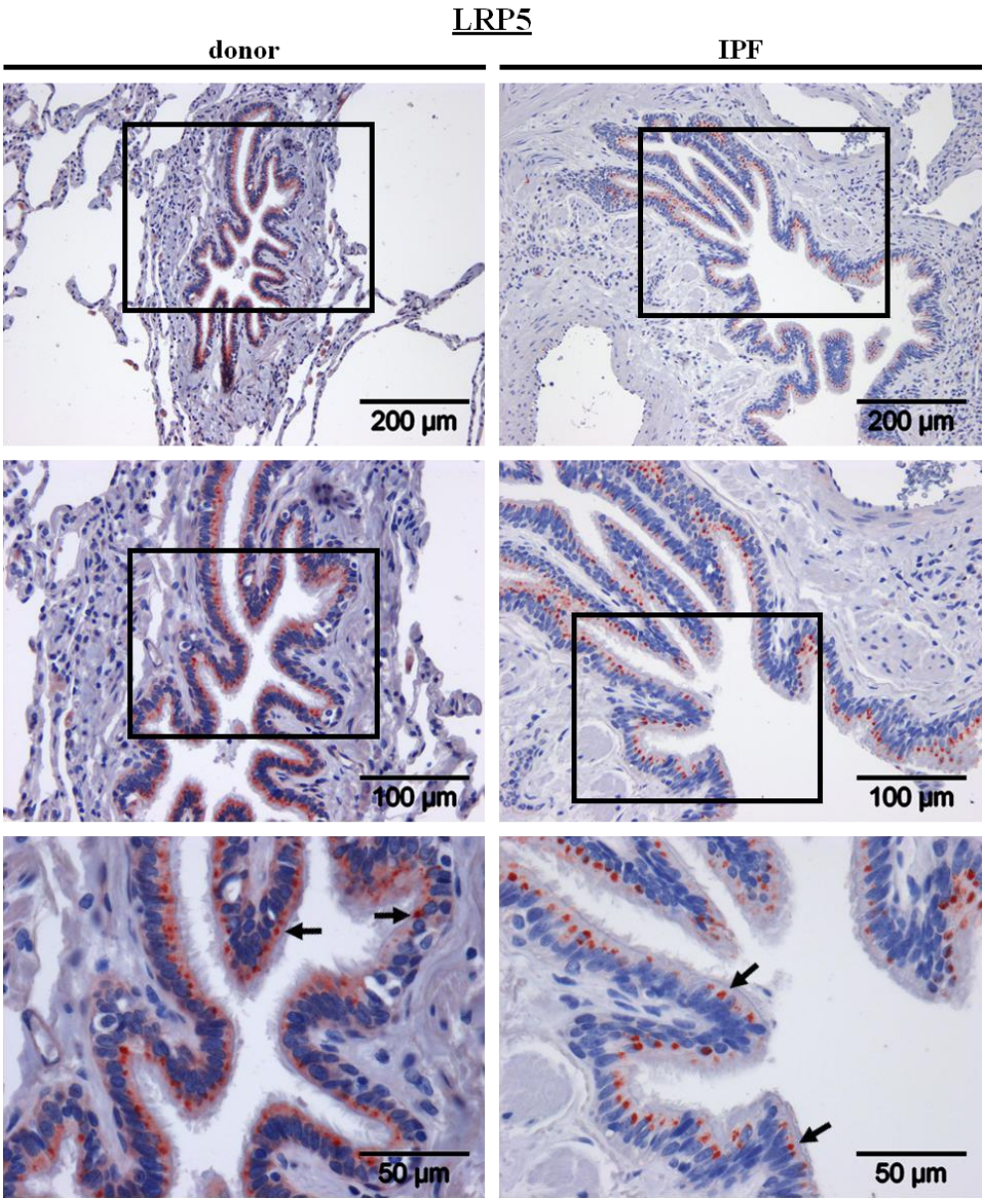

Figure 10A. Localization of LRP5 protein in donor and IPF lung tissue – bronchial regions.
Immunohistochemical staining for LRP5 protein was performed on lung tissue sections of donors and IPF patients. Stainings were performed at least twice using three different donor and IPF lung tissues. Representative **bronchial regions** of donor (**left panel**) and IPF (**right panel**) lungs are shown in three magnifications as indicated. Arrows indicate supranuclear staining in columnar bronchial epithelial cells.

B.

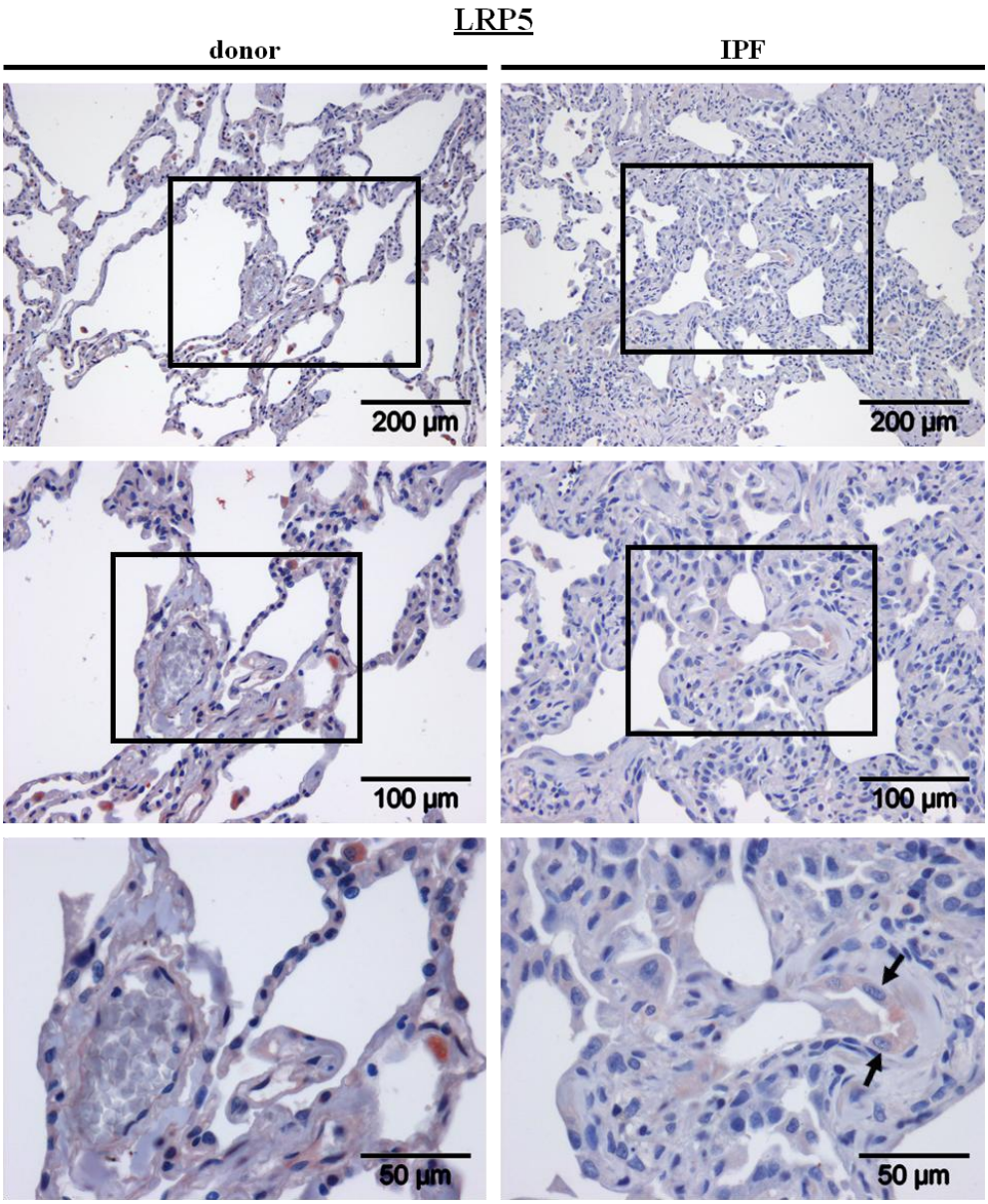

Figure 10B. Localization of LRP5 protein in donor and IPF lung tissue – alveolar regions.

Immunohistochemical staining for LRP5 protein was performed on lung tissue sections of donors and IPF patients. Stainings were performed at least twice using three different donor and IPF lung tissues. Representative **alveolar regions** of donor (**left panel**) and IPF (**right panel**) lungs are shown in three magnifications as indicated. Arrows indicate hyperplastic alveolar epithelial cells.

The DKK-binding receptors KRM1 and KRM2 could also be detected in the lung tissue sections. In detail, KRM1 protein was expressed in bronchial epithelial (***figure 11A***) and smooth muscle cells (best recognizable in ***figure 11A***, right panel, arrow) in donor and in IPF lungs. In IPF, the bronchial epithelium displayed a heterogeneous staining pattern (***figure 11A***, right panel) and hyperplastic alveolar epithelial cell regions showed expression of KRM1 protein (***figure 11B***, right panel, arrow). KRM1 was also found in alveolar macrophages (best recognizable in ***figure 11A and 11B***, left panels).

A.

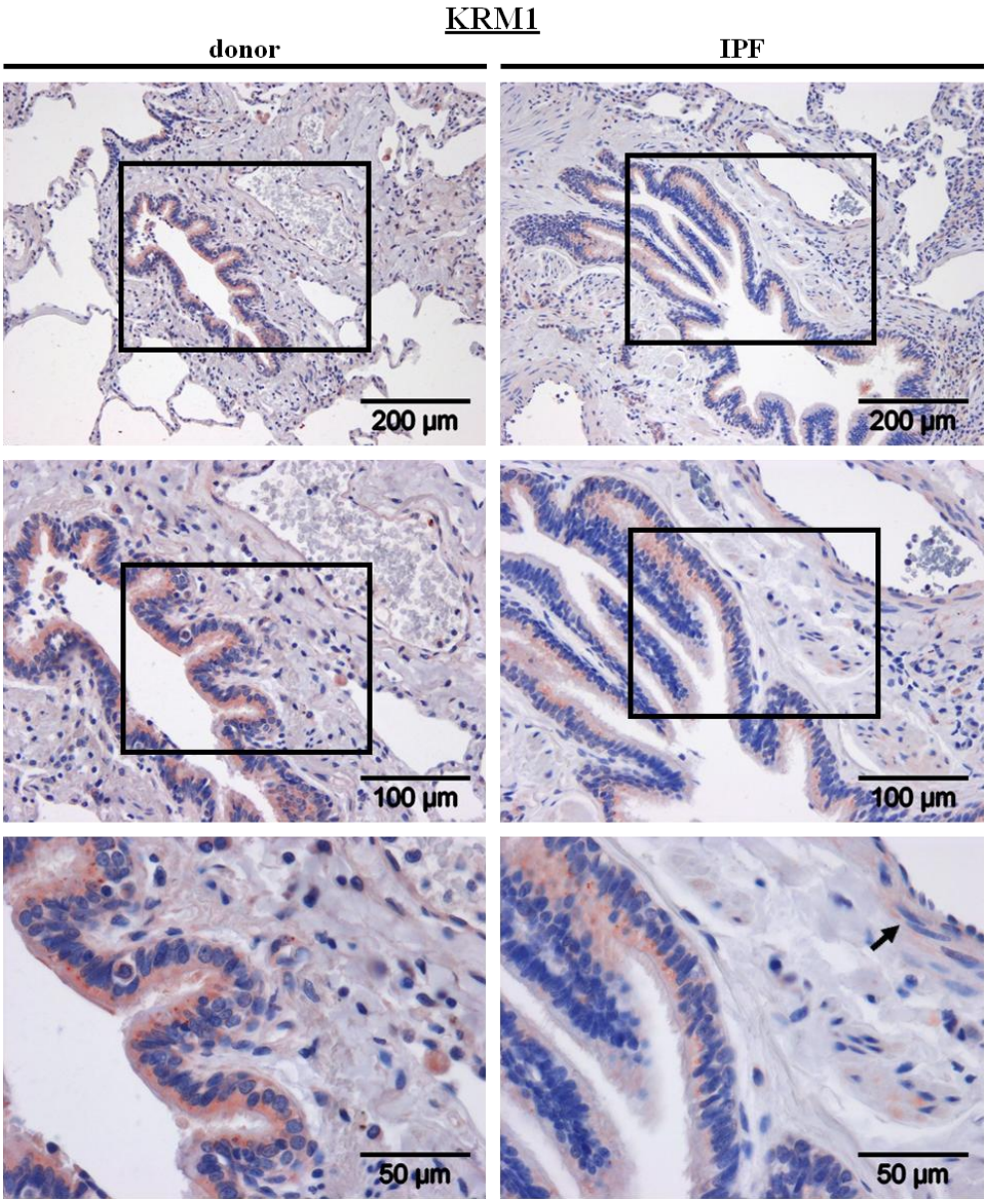

Figure 11A. Localization of KRM1 protein in donor and IPF lung tissue – bronchial regions.

Immunohistochemical staining for KRM1 protein was performed on lung tissue sections of donors and IPF patients. Stainings were performed at least twice using three different donor and IPF lung tissues. Representative **bronchial regions** of donor (**left panel**) and IPF (**right panel**) lungs are shown in three magnifications as indicated. An arrow indicates smooth muscle cells.

B.

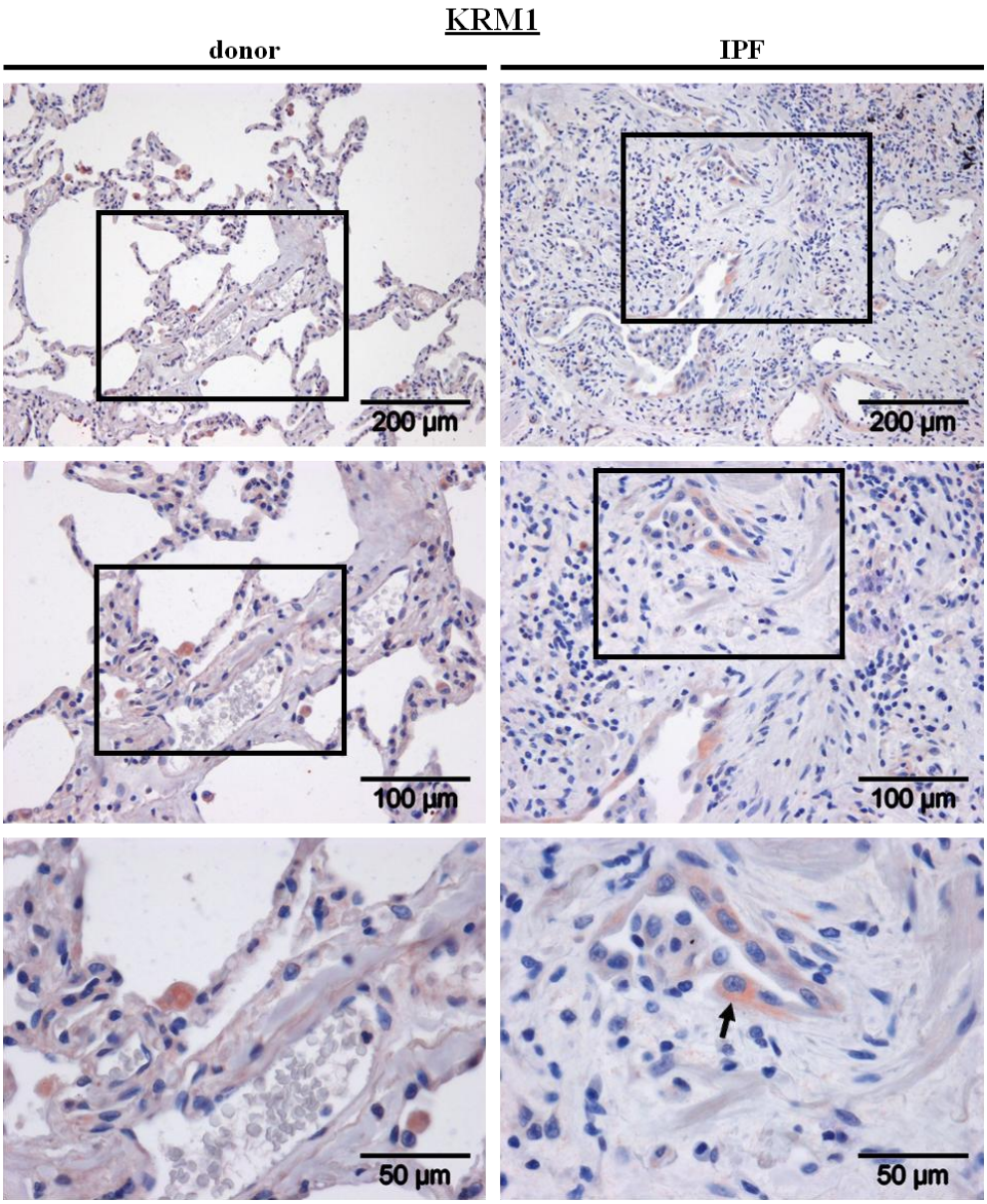

Figure 11B. Localization of KRM1 protein in donor and IPF lung tissue – alveolar regions.

Immunohistochemical staining for KRM1 protein was performed on lung tissue sections of donors and IPF patients. Stainings were performed at least twice using three different donor and IPF lung tissues. Representative **alveolar regions** of donor (**left panel**) and IPF (**right panel**) lungs are shown in three magnifications as indicated. An arrow indicates hyperplastic alveolar epithelial cells.

KRM2 protein was detected in bronchial epithelial cells (***figure 12A***) in donor and IPF lung tissue sections, with a more scattered expression in the IPF lungs. Mucus residuals within the epithelium and in the bronchial lumen also depicted intense staining when they were present on the tissue sections (***figure 12A***, right panel). In IPF, hyperplastic alveolar epithelial cells expressed KRM2 protein (***figure 12B***, right panel, arrow).

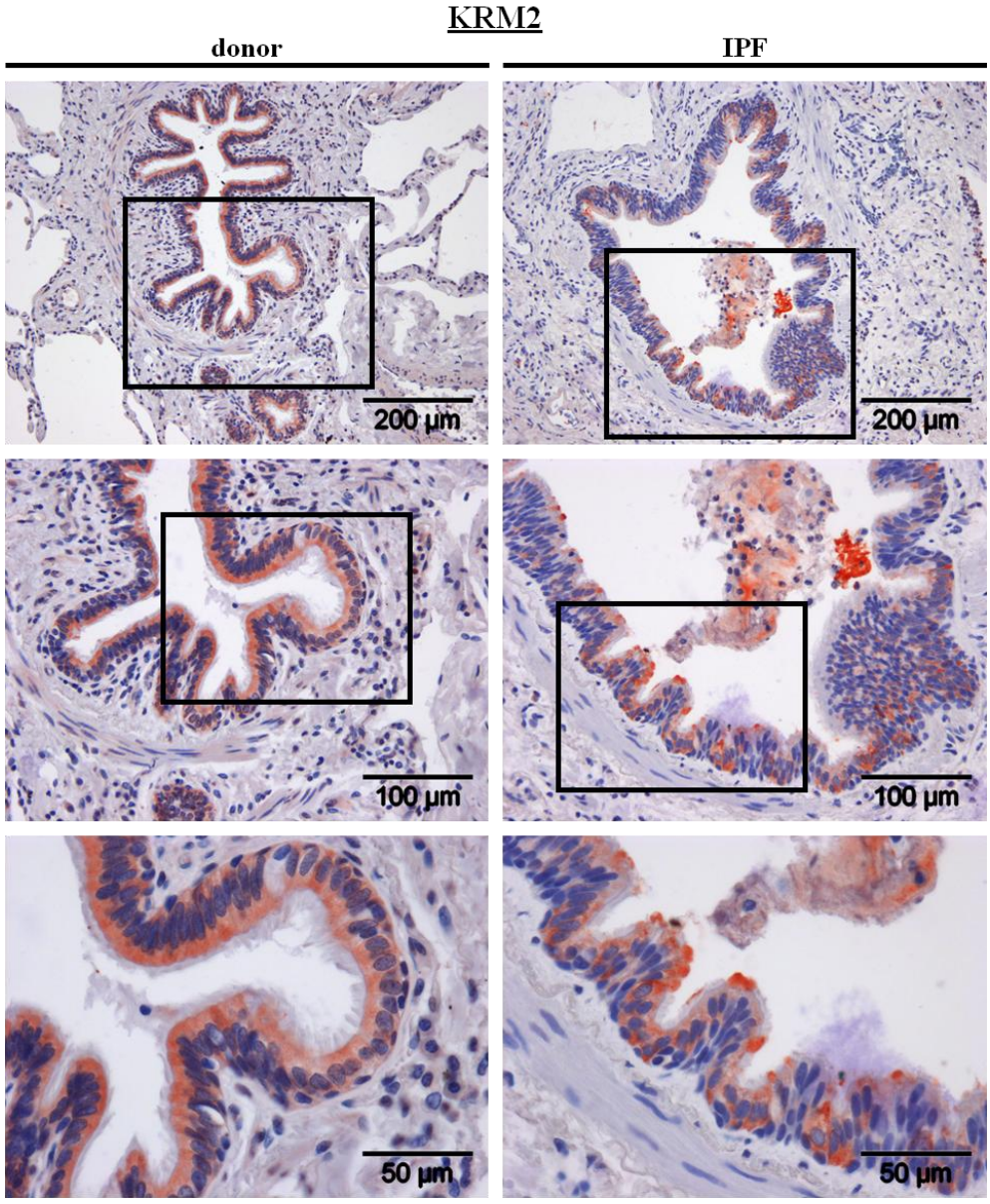

Figure 12A. Localization of KRM2 protein in donor and IPF lung tissue – bronchial regions.
Immunohistochemical staining for KRM2 protein was performed on lung tissue sections of donors and IPF patients. Stainings were performed at least twice using three different donor and IPF lung tissues. Representative **bronchial regions** of donor (**left panel**) and IPF (**right panel**) lungs are shown in three magnifications as indicated.

B.

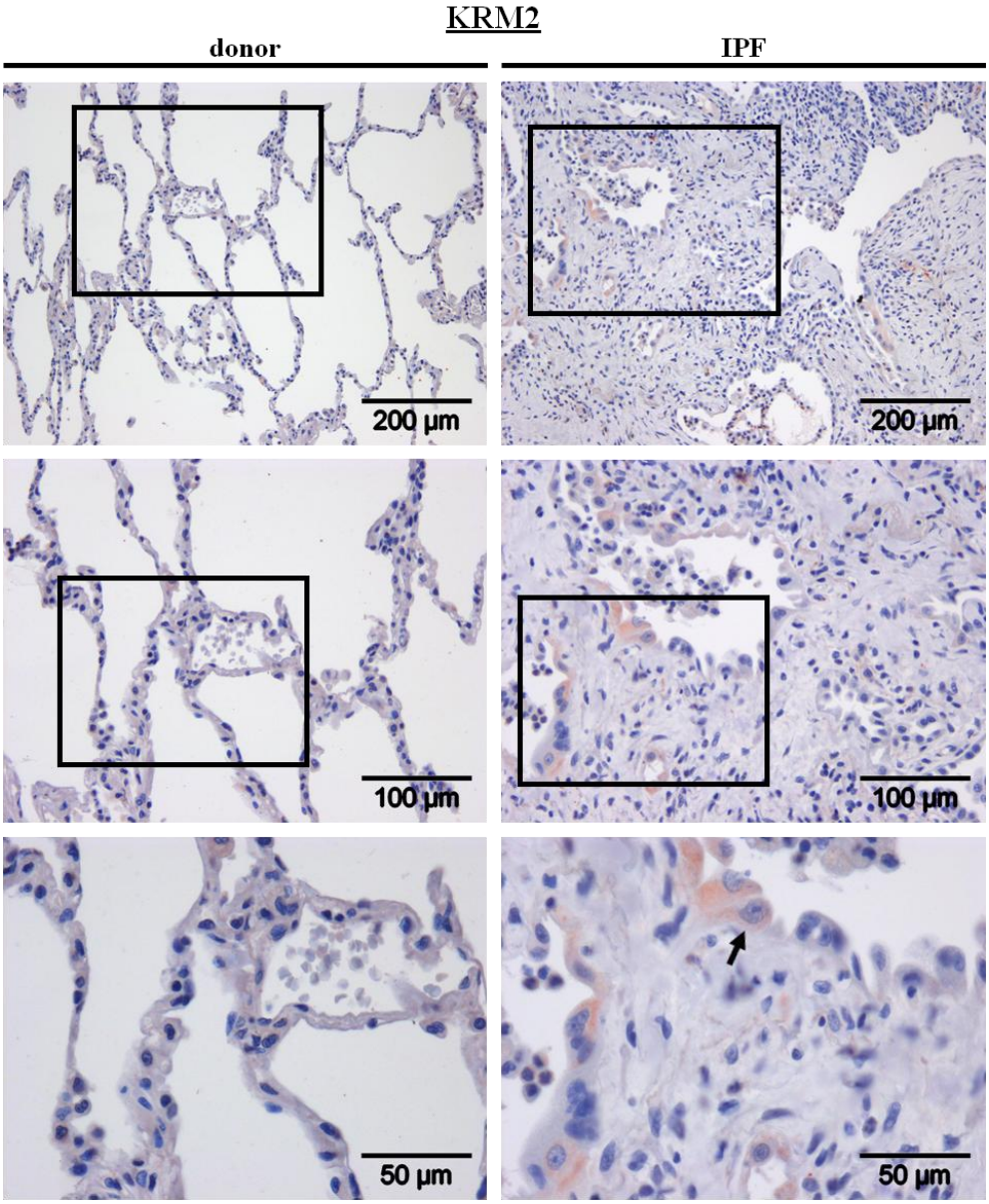

Figure 12B. Localization of KRM2 protein in donor and IPF lung tissue – alveolar regions.

Immunohistochemical staining for KRM2 protein was performed on lung tissue sections of donors and IPF patients. Stainings were performed at least twice using three different donor and IPF lung tissues. Representative **alveolar regions** of donor (**left panel**) and IPF (**right panel**) lungs are shown in three magnifications as indicated. An arrow indicates hyperplastic alveolar epithelial cells.

Immunohistochemical stainings of tissue sections from further donor and IPF lungs as supplement to the pictures illustrated here are depicted in chapter ***10.4*** for the respective antibodies.

3.3 WNT/β-catenin pathway components in bronchial epithelial cells

Immunohistochemistry detected DKK1 and DKK4 as well as their LRP and KRM receptors to be largely located in the bronchial epithelium of donor and IPF lungs. In order to investigate whether human bronchial epithelial cells can also express other key molecules of the WNT/β-catenin pathway and would therefore be basically capable of responding to WNT and DKK stimulation, the human bronchial epithelial cell line BEAS-2B was examined. RNA isolates of this cell line were analyzed for their mRNA expression of WNT/β-catenin signaling pathway components and DKK receptors by qRT-PCR (***figure 13A, B***). Additionally, the expression of *WNT* and *DKK* ligands was examined (***figure 13C, D***). Two flasks of BEAS-2B cells were tested and values were averaged. As depicted in ***figure 13A and 13B***, mRNA of the examined WNT receptors *FZD1-4*, of the WNT and DKK binding receptors *LRP5* and *LRP6*, as well as of the DKK receptors *KRM1* and *KRM2* was expressed by BEAS-2B cells (***figure 13A***). *LRP5* and *LRP6* displayed the highest expression levels of these receptors. Key components of the WNT/β-catenin signaling cascade were expressed as well, with a high relative mRNA expression of β-catenin (*β-CAT*) (***figure 13B***). Of the examined ligands (***figure 13C, D***), *WNT1*, *WNT7b*, *WNT10b*, as well as *DKK1* and *DKK3* could be detected. *WNT1* and *WNT10b* mRNA was only expressed on low levels. *WNT3a*, *DKK2* and *DKK4* did not show an evaluable mRNA expression in the BEAS-2B RNA isolates (***figure 13C, D***).

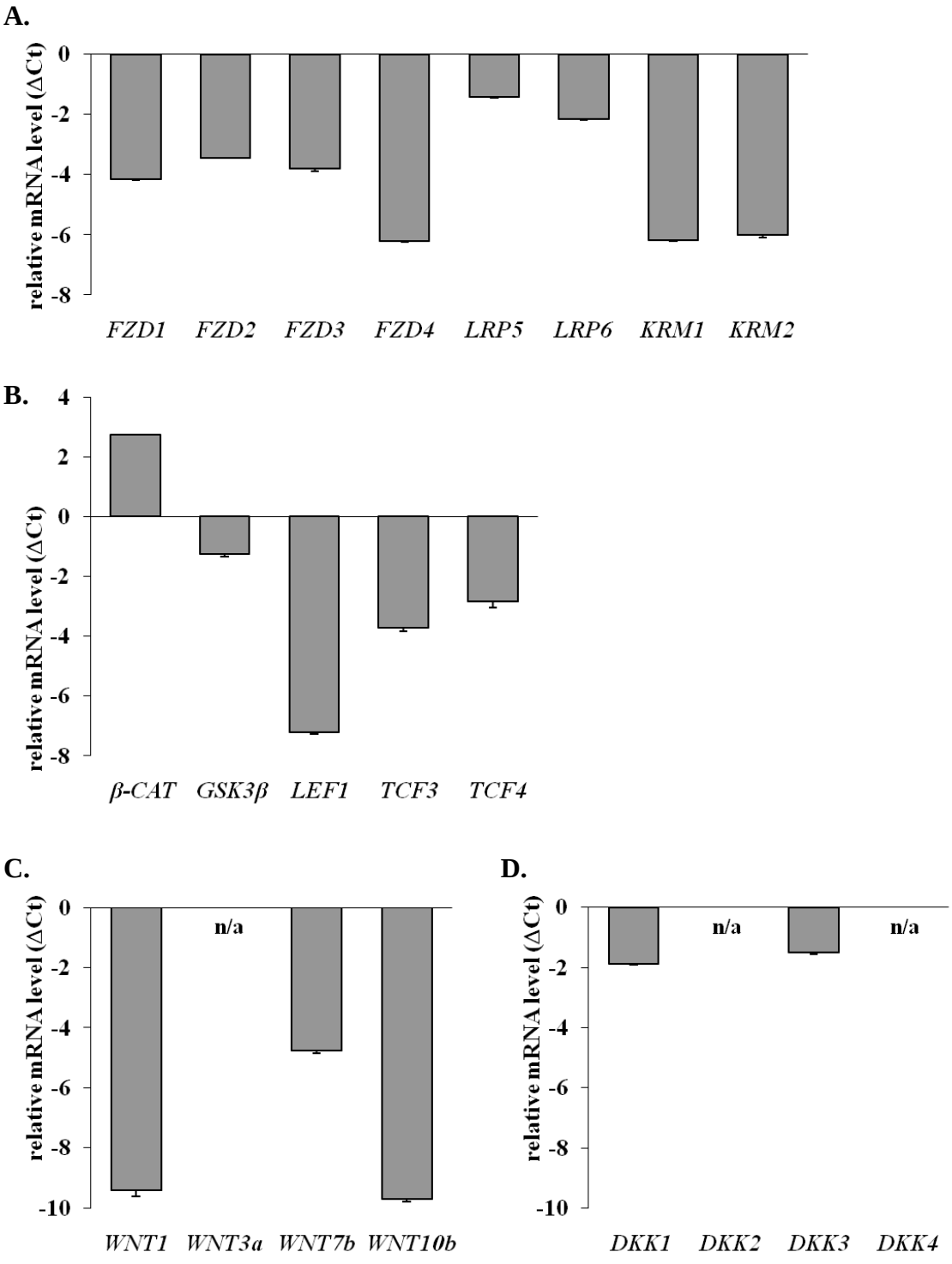

Figure 13. mRNA expression of WNT/β-catenin pathway components in the BEAS-2B cell line.

The mRNA expression of the receptors *FZD1-4*, *LRP5*, *LRP6*, *KRM1* and *KRM2* (**A**), of the WNT/β-catenin pathway components β-catenin (*β-CAT*), *GSK3β*, *LEF1*, *TCF3* and *TCF4* (**B**) and of the ligands *WNT1*, *WNT3a*, *WNT7b*, *WNT10b* (**C**) and *DKK1-4* (**D**) was analyzed in RNA isolates of the human bronchial epithelial cell line BEAS-2B by quantitative (q)RT-PCR. Averaged results of 2 isolates are shown as relative mRNA expression compared to the reference gene *HPRT1* (ΔCt) and are presented as mean ± SEM. *WNT3a*, *DKK2* and *DKK4* mRNA was not expressed, respective ΔCt values were not available (n/a).

3.4 DKK1 protein in bronchoalveolar lavage fluids

The present study demonstrated that DKK1 mRNA and protein expression are increased in IPF compared to donor lung tissues and that DKK1 is largely located in basal bronchial epithelial cells. To investigate whether the epithelial localization leads to occurrence of DKK1 in the bronchial lumen and whether there are measurable differences between IPF patients and healthy controls *in vivo*, bronchoalveolar lavage fluids (BALF) were analyzed. Therefore, DKK1 protein was quantified in BAL fluids of healthy volunteers (n=4) and IPF patients (n=9) using an enzyme-linked immunosorbent assay (ELISA). As depicted in ***figure 14***, DKK1 was expressed in the BAL fluids of both groups. While DKK1 levels in the BAL fluids of healthy volunteers showed a comparatively small divergence, the levels found in BAL fluids of IPF patients were widespread, varying up to a triplication of the absolute protein value between the lowest and the highest DKK1 concentration. However, the concentration of DKK1 protein in BAL fluids from IPF patients (mean ± SEM: 456 ± 55 pg/ml) was significantly increased compared to the healthy controls (266 ± 11 pg/ml).

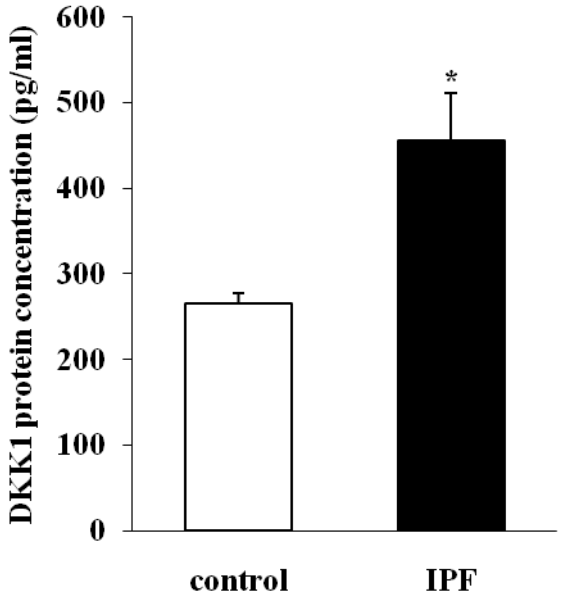

Figure 14. DKK1 protein concentration in bronchoalveolar lavage fluid.
The DKK1 protein concentration in bronchoalveolar lavage fluids (BALF) of healthy volunteers (control group, open bar, n=4) and IPF patients (black bar, n=9) was quantified using an enzyme-linked immunosorbent assay (ELISA). The concentration of DKK1 protein is given in pg/ml and is presented as mean ± SEM. * = $p < 0.05$.

4 Discussion

Idiopathic pulmonary fibrosis is a progressive and fatal lung disease that induces structural remodeling of the lungs' architecture, causes respiratory impairment and limits quality of life [36,133,158]. Due to the restricted response to pharmaceutical treatments, lung transplantation is currently the only option proven to notably prolong survival of IPF patients [112,168]. The mechanisms of IPF have not been fully elucidated yet and new insights into the pathogenesis may promote improvements of therapeutic strategies.

Recent studies have highlighted an involvement of WNT/β-catenin signaling in IPF. So far, an aberrant reactivation of this developmental pathway in IPF lung tissue has been demonstrated [26,86]. WNT/β-catenin signaling may contribute to disease progression, since knockout of the WNT target gene *MMP7* [183] as well as specific inhibition of WNT/β-catenin target gene transcription [63] or canonical pathway inhibition via β-catenin small interfering RNA [82] in the bleomycin mouse model attenuated pulmonary fibrosis. Although limitations concerning the transferability of this animal model to some aspects of IPF pathobiology have to be taken into account [113], modulators of WNT signaling represent an attractive target in IPF research. Dickkopf proteins with their ability to bind WNT coreceptors of the LRP family belong to the best studied regulators of WNT/β-catenin signal transduction [101].

An antifibrotic effect of DKK1 via WNT/β-catenin inhibition has already been reported in mouse models of cholestatic liver fibrosis [23] and renal fibrosis [62]. However, the role of DKK proteins in IPF had not been addressed before. Therefore, the present study focused on the expression and localization of DKK proteins and their receptors in the healthy adult lung and in the lungs of IPF patients.

4.1 Altered expression of DKK proteins and their receptors in IPF

The present study reveals a regulation of DKK and KRM expression in IPF. The mRNA expression of *DKK1* and *DKK4* was found to be increased in IPF compared to donor lung tissues, consistent with elevated protein levels of DKK1 and DKK4 detected by Western blot analysis. The increase in DKK2 protein expression however did not match the decreased *DKK2* mRNA levels in IPF lungs, suggesting differences in translational control mechanisms or protein stability. At first appearance, an increase of DKK1 and

DKK4 in IPF lungs seems to contradict the reported activation of WNT/β-catenin signaling in IPF, considering their WNT-inhibitory capability. But actually, this finding is consistent with an increased WNT activation, since *DKK1* [21,53,122] and *DKK4* [10,130] have been identified as downstream target genes of the WNT/β-catenin pathway, in terms of a negative feedback mechanism. For *DKK2* and *DKK3*, feedback-mechanisms have not been demonstrated yet.

Since availability of DKK receptors in the lung tissue represents a basic requirement for modulation of WNT/β-catenin signaling via secreted DKK proteins, the present study focused on the expression profile of these proteins as well. In both, donor and IPF lungs, mRNA expression of *LRP5* and *LRP6* could be confirmed by qRT-PCR. Additionally, LRP5 protein expression and localization could be demonstrated by immunohistochemistry. The presence of LRP6 protein in its phosphorylated form in homogenates of IPF and donor lungs has been described before by Western blot analysis [86]. *KRM1* and *KRM2* mRNA and the respective proteins KRM1 and KRM2 could also be detected, with an increased expression of KRM1 in IPF samples.

When interpreting the data, it has to be taken into account that mRNA and protein expression analyses were performed on lung tissue homogenates. As presence of DKK proteins and their receptors is cell type dependent, expression levels are subject to the cellular composition of each donor and IPF sample.

4.2 Localization of DKK proteins and their receptors in the lung tissue

Immunohistochemical analyses supplement the data derived from lung homogenates with the actual, cell-type dependent localization pattern. They revealed DKK1 and DKK4 to be largely located in the bronchial epithelium in donor as well as in IPF lung tissue sections. Additionally, hyperplastic alveolar epithelial cells in IPF exhibited intense staining for these DKK proteins. Regarding the WNT-target-gene character of *DKK1* and *DKK4*, this observation is compatible with the report on nuclear β-catenin accumulation and therefore with active WNT/β-catenin signaling within these cells [26]. It has to be mentioned that the observed expression of DKK4 protein is inconsistent with the protein expression pattern detected by Western blot analysis, which did not depict DKK4 protein expression in the donor samples. However, it has to be taken into consideration that samples of different donors had to be used for the two experiments, more-

over different DKK4 antibodies. For interpretation of the immunohistochemical data presented in the present study, it has to be noted that stainings of donor and IPF tissue sections are not quantitatively comparable, since exposure to the chromogen solution was performed until red color staining for each section was clearly visible under a microscope.

Interestingly, immunohistochemical staining for the receptors LRP5, KRM1 and KRM2 revealed striking similarities to the expression pattern of their own ligands. All of the investigated receptors were predominantly located in the bronchial epithelium in both, donor and IPF lungs and additionally in hyperplastic alveolar epithelial cells in the fibrotic lungs. This corresponds to the observed expression pattern of DKK1 and DKK4 in the present study. Furthermore, these observations are in line with the previously reported expression patterns of WNT1, WNT3a and GSK3β, whose presence in lung tissue also included the expression by bronchial epithelial cells and by hyperplastic ATII cells in IPF lungs [86]. Additionally, the analysis of the human bronchial epithelial cell line BEAS-2B in the present study demonstrated that human bronchial epithelial cells are able to express other key components of the WNT/β-catenin signaling cascade, as well. Taken together, these data indicate that autocrine and paracrine effects of the secreted DKK proteins are most likely the major type of interference with WNT in the lung epithelium.

The detection of KRM proteins in the lung epithelium has to be evaluated in the context of recent findings. While some authors support the theory of DKK, LRP and KRM forming a ternary complex that undergoes endocytosis [104,138], other authors favor the mere binding of DKK to LRP without enhanced removal of LRP from the plasma membrane as sufficient mechanism of WNT inhibition [148]. Additionally, recent investigations in *KRM*-knockout mice and cultured cells have highlighted that KRMs are not necessarily required for WNT modulation via DKK [40,169]. Another study in *Xenopus* even suggested a DKK-independent role for KRM in WNT modulation via direct binding to LRP, as KRM was able to activate WNT in the absence of DKK1 [60]. Nevertheless, KRM receptors bind DKK proteins [104,169] and their ability to enforce the WNT inhibitory function of DKK proteins has been demonstrated [103,104]. On that account it has been suggested that the exact impact of KRM on WNT modulation might depend on the level of LRP expression within the respective cells [169]. The present study detected both, KRM and LRP, in the lung epithelium. Therefore an involvement of KRM receptors in

WNT modulation of the lungs' epithelial cells seems probable, but further studies are needed to elucidate this topic in detail.

Notably, the bronchial epithelium partially depicted a heterogenous expression pattern for KRM1 and KRM2, and hyperplastic alveolar epithelial cells in IPF only exhibited a slight staining of LRP5. This emphasizes the importance of the microenvironmental composition for WNT modulation *in vivo*. LRP5 additionally revealed a distinct supranuclear accumulation in bronchial epithelial cells. This may be indicative of LRP5 containing vesicles and is possibly linked to internalization processes which have already been reported for LRP6. Besides the presumed LRP6 endocytosis upon DKK stimulation [12,104,139] in the context of WNT inhibition, further regulatory mechanisms of the WNT/β-catenin pathway that are based on alterations of LRP6 internalization processes have been described. Recent studies reported the internalization of LRP6 [78,97,176] as well as the inhibition of its transcription [78] upon stimulation with WNT3a. Furthermore, the endocytosis of LRP6 in *Xenopus* was suggested to be inhibited by KRM [60], but there are converse observations in transfected human cell lines [97].

Based on the distinct supranuclear localization of LRP5 demonstrated in the present study, similar internalization and regulation processes should be taken into consideration for LRP5 in the bronchial epithelium.

4.3 DKK in the conducting airways

Since DKK proteins were largely located in the lung epithelium, the present study investigated whether they appear in BAL fluids. DKK1 protein content was assessed using an enzyme-linked immunosorbent assay (ELISA) and could be detected in all samples tested. Interestingly, DKK1 expression was significantly increased in BAL fluids of IPF patients when compared to BAL fluids of healthy volunteers. This result is in line with the demonstrated increase of DKK1 mRNA and protein levels in IPF lungs. Nevertheless, it has to be mentioned that the study has limitations that have to be considered when interpreting the data. Since total cell number and protein content of the BAL fluids is an uncontrolled factor in this experiment, the increase in detected DKK1 could also reflect a higher occurrence of bronchial epithelial cell debris. Another important concern arises from the DKK1 expression pattern revealed by immunohistochemistry, where besides in the epithelium, staining was also present in neutrophil granulocytes. It remains unclear whether this finding depicts an endogenous expression, is a conse-

quence of their phagocytic capability or is just a remnant of endogenous peroxidase activity. These considerations are of interest, as neutrophils are known to be increased in BAL fluids of IPF patients [1]. In some of the other immunohistochemical experiments performed in the present study, immonureactive cells depicted staining as well (for example localization of LRP5 (***figure 10B***, left panel) and KRM1 (***figure 11A*** and ***11B***, left panels)). Therefore an insufficient quenching of peroxidase activity in the study protocol might after all be the cause for a staining of the neutrophils. More detailed studies are required for definite evaluation of these issues.

So far, BAL fluids are of subordinate use for the diagnosis of IPF. In some cases the examination of BAL fluid can contribute to the exclusion of differential diagnoses [1,133]. Interestingly, previous studies reported that the insulin-like growth factor binding protein 4 (IGFBP4), which has recently been identified as inhibitor of the WNT/β-catenin pathway [182], and MMP7, another WNT/β-catenin target [30], are also increased in BAL fluids of IPF patients [137,145]. It is further prominent that both proteins are located in basal bronchial / bronchiolar epithelial cells, according to the localization pattern of DKK1 in the present study [26,145].

4.4 DKK proteins and their receptors in the lung epithelium

The lung epithelium is of crucial interest for pathogenesis and disease progression in IPF, since repetitive epithelial microinjuries and inadequate repair mechanisms are considered as essential mechanisms of the fibrosing process [22,142]. Altered phenotypes of alveolar epithelial cells as well as of the bronchiolar epithelium are frequent findings in IPF lung tissues [25,144] and they have been associated with abnormal WNT/β-catenin signaling [26]. The present study revealed the expression of DKK proteins and their receptors in the lung epithelium and raises interesting questions about their influence on the cell-type dependent increase of WNT/β-catenin pathway activation in IPF.

4.4.1 DKK proteins and their receptors in alveolar epithelial cells

The present study identified expression of the WNT modulators DKK and KRM in hyperplastic alveolar epithelial cells of IPF patients. Alveolar epithelial cells (AEC) can be divided in type I cells (ATI), that account for 95 % of the AEC cells and type II cells (ATII), that account for 5 % of the AEC cells [170]. The function of ATII cells, which

among other capabilities are able to serve as progenitor cells for damaged ATI cells [163], is impaired in IPF [142]. Abnormal ATII cell proliferation, ATII cell apoptosis next to fibroblast foci and a hyperplastic phenotype of ATII cells are common findings in IPF lung histology [69,142,144]. Furthermore, the alveolar epithelium and especially ATII cells are an important source of cytokines, including profibrotic mediators [127,143,144]. Together with a dysregulation of apoptotic processes and a failure in alveolar re-epithelialization, these mediators are suggested to contribute to the fibrosing process [128,159]. An enhanced ATII cell proliferation has been reported in a mouse model of bleomycin induced pulmonary fibrosis [88] and in another recent study, the targeted injury of ATII cells in transgenic mice induced the occurrence of lung fibrosis [153].

For the abnormal hyperplastic ATII cell type in IPF, a nuclear accumulation of β-catenin indicating an activation of the WNT/β-catenin pathway has already been reported [26]. This observation seems to be rather specific to alveolar injury than disease-specific, since nuclear β-catenin accumulation also occurs in other lung diseases that go along with alveolar damage [26]. Additionally, components of the WNT β-catenin pathway as well as some of the WNTs themselves show an increased expression in primary ATII cells of IPF patients [86].

In the first place, the expression of DKK proteins in the hyperplastic cell type observed by the present study corresponds to the previously described activation of the WNT/β-catenin pathway within these cells, considering the target-gene-character of DKK1 and DKK4. But the DKK proteins may additionally be of interest in the autocrine or paracrine regulation of alveolar epithelial cell proliferation, as they were able to influence the proliferation of the human alveolar epithelial cell line A549 in a recent study performed by our workgroup [131]. A549 cells possess characteristics of alveolar epithelial type II cells [98] and WNT3a-responsiveness of A549 cells has been demonstrated before [86,94]. The proliferation of this cell line was increased upon WNT3a stimulation [86]. These data were supplemented by detection of a dose dependant inhibition of WNT-induced A549 cell proliferation by DKK1 [131]. Interpretation of these results is limited by the usage of a cell line. Especially A549 epithelial cells with their adenocarcinomatous origin may depict an altered cellular response upon WNT and DKK stimulation. A good possibility to clarify the impact of DKK proteins on alveolar epithelial cell proliferation would certainly be the stimulation of isolated primary ATII cells.

4.4.2 DKK proteins and their receptors in the bronchial epithelium

4.4.2.1 Proliferation and repair of the airway epithelium

In contrast to other epithelia like those of gut and skin, which exhibit a high cellular turnover, the unimpaired lung epithelium is renewing slowly [31,90,154]. However, the proliferative activity can be markedly increased in case of epithelial injury [31,136]. The regenerating strategies of the airway epithelium are still not fully elucidated. Most of the current knowledge is based on injury models performed in mice [32,52,100]. It is assumed that several resident cell populations can serve as potential progenitors for the lung epithelium and possibly, but controversially debated, also some non-local cell types such as bone marrow derived stem cells [52,90,100].

The resident progenitor cells include several cell types that are located at different compartments of the lung. As mentioned above, ATII cells are progenitor cells located in the alveoli [90,100,163]. But besides the repair mechanisms of the alveolar cell compartment, epithelial proliferation and repair processes of the conducting airways are of interest for IPF pathogenesis as well. Bronchiolar lesions and basal cell abnormalities including basal cell hyperplasia and abnormal bronchiolar proliferation are frequent and specific findings in IPF when compared to other diffuse parenchymal lung diseases [25]. In the bronchioles, specific types of Clara cells seem to possess proliferative capacity after epithelial injury [49,90]. At the bronchoalveolar junction, further cells that express Clara cell and ATII cell markers (bronchioalveolar stem cells, BASC) have been suggested to serve as epithelial progenitors [80], but their existence is critically discussed [90]. Additionally, multipotent resident stem cells have recently been identified in the distal airways of adult human lungs. These cells were able to generate bronchioles, alveoli and vasculature after injection into cryoinjured mouse lungs [74]. In the tracheal and bronchial epithelium, basal cells and cells that originate from submucosal airway glands are seen as potential progenitor populations [52,100]. It was proposed that ciliated cells themselves could serve for epithelial regeneration by transdifferentiation [129], but there are converse findings [134].

The present study identified Dickkopf proteins and their receptors to be largely located in the bronchial epithelium. An impact of WNT/β-catenin signaling on regeneration and proliferation of the bronchial and bronchiolar epithelium is recently under discussion. Concerning the bronchiolar epithelium, one recent study reported the WNT/β-catenin pathway to be activated during epithelial regeneration and to promote an expansion of

bronchoalveolar stem cells at the bronchoalveolar junction [181]. Conversely, another publication stated that β-catenin pathway activation is not necessary for bronchiolar epithelial proliferation or repair mechanisms [179]. Concerning the bronchial epithelium, an increased nuclear accumulation of β-catenin indicating an activated WNT/β-catenin signaling pathway was detected in an *in vitro* model of bronchial epithelial repair [156]. These studies were performed using human bronchial epithelial cell lines as well as primary human bronchial epithelial cells [156].

Therefore DKK proteins as modulators of the WNT/β-catenin signaling cascade are of interest concerning the regulation of maintenance and regeneration processes in the bronchial and bronchiolar epithelium. In the present study, all of the investigated DKK proteins and receptors were located in bronchial epithelial cells and interestingly, DKK1 depicted a pronounced and distinct accumulation in basal bronchial epithelial cells, one of the cell populations considered as epithelial progenitors.

4.4.2.2 DKK1 in basal cells of the bronchial system

The function of basal cells as bronchial epithelial progenitors was examined in mice [68,136], as well as in an *in vitro* assay of primary human basal bronchial epithelial cells [136]. A subset of them is considered to be capable of generating a differentiated airway epithelium after epithelial injury [68,136]. Basal bronchial epithelial cells can be found throughout the conducting airways of the human lung including the bronchioles, but occur less frequently in the distal parts of the bronchial tree [118,136]. Particularly with regard to the small airways, this cell population has gained interest in IPF histopathology. Proliferative bronchiolar abnormalities were demonstrated to be specific findings in IPF lungs when compared to other IIP entities and healthy lung tissue [25]. Those abnormalities included atypical and hyperplastic basal bronchiolar epithelial cells as well as an abnormal occurrence and superficial location of basal cells at the bronchoalveolar junctions [25,26]. These areas have been connected to the formation of characteristic histomorphological changes in IPF lungs like honeycomb cysts (dilated bronchioles) and bronchiolization (ectopic localization of bronchiolar epithelial cells in the alveolar space) [25,26]. Furthermore, those lesions and especially the basal cell population presented an accumulation of nuclear β-catenin and an elevated expression of the WNT/β-catenin target gene MMP7, indicating an activation of this signaling cascade [26].

Immunohistochemical stainings of the present study revealed an accumulation of DKK1 protein in basal epithelial cells of donor and IPF lungs and brought up the question on a possible influence of DKK1 on bronchial epithelial cell proliferation. It could be demonstrated that the human bronchial epithelial cell line BEAS-2B expresses mRNA of major components of the WNT/β-catenin pathway and of the DKK receptors. Therefore bronchial epithelial cells seem to be able to react on WNT and DKK stimulation. In consequence of the findings of the present study, our workgroup performed experiments on the proliferation of BEAS-2B cells and could demonstrate a dose-dependent regulation of WNT-induced BEAS-2B cell proliferation by DKK1 [131]. Stimulation with Wnt3a caused an increase of BEAS-2B cell proliferation and this effect could be inhibited by high concentrations of DKK1. Unexpectedly, low concentrations of DKK1 alone led to an increase in proliferation of BEAS-2B cells [131]. Whether this effect is accomplished by β-catenin pathway induced proliferation or is a WNT/β-catenin-independent action of DKK1 remains unclear. It was shown that DKK1 possesses WNT/β-catenin independent functions in the embryogenesis of *Xenopus* [89] and can also modulate non-canonical WNT signaling, what could be demonstrated in *Xenopus* embryos [19,20] and in human mesothelioma cell lines [92].

The results suggest that DKK proteins may be of interest for the molecular mechanisms underlying proliferation and maintenance of the bronchial epithelium and especially for IPF histopathology, where aberrantly activated canonical WNT signaling is found at sites of atypical and proliferative basal epithelial cell phenotypes [26]. However, interpretation of the results is limited by the usage of a cell line. As demonstrated by the present study, the mRNA expression profile of BEAS-2B cells does not exactly reflect the expression of WNT/β-catenin and DKK components in donor lungs revealed by immunohistochemistry. BEAS-2B cells express *LRP5*, *KRM1* and *KRM2* mRNA according to the immunohistochemical localization of the respective proteins in the bronchial epithelium. They also express mRNA of key components of the WNT/β-catenin pathway like β-catenin and GSK3β, consistent with a previous report on the localization of the respective proteins in bronchial epithelial cells [86]. But BEAS-2B cells exhibit some differences concerning the expression pattern of the ligands when compared to the bronchial epithelium of an adult lung. *WNT3a* was not detected in BEAS-2B RNA isolates in the present study, but WNT3a protein could be identified in selected bronchial epithelial cells of donor lung tissues by immunohistochemistry in a previous experiment [86]. Likewise, BEAS-2B cells did not express *DKK4* mRNA, while immunohistochemical

stainings of the present study identified DKK4 protein to be located in the bronchial epithelium of the adult lung. Basically, these findings should not influence the capability of BEAS-2B cells to react on WNT or DKK stimulation, but they indicate differences between this cell line and an entire bronchial epithelium. Therefore, further studies will have to be performed to elucidate the influence of DKK1 on bronchial and bronchiolar epithelial cell proliferation. Proliferation assays on primary basal bronchial epithelial cells would certainly contribute to a better understanding of WNT and DKK function in epithelial cell proliferation *in vivo*.

4.4.2.3 Basal bronchial epithelial cells and malignancies

Besides their physiological proliferative capacity, basal cells are considered as origin of squamous metaplasia and dysplasia, which are regarded as facultative preneoplastic lesions for the squamous cell carcinoma (SCC) of the lung [173]. Therefore, the distinct expression of DKK1 in basal bronchial epithelial cells and its influence on bronchial epithelial cell proliferation might also represent interesting aspects for lung cancer research. Especially since non-small-cell lung carcinomas (NSCLC), including SCC, have already been associated with an activation of WNT signaling [87,109,166]. WNT1 and WNT2 were found overexpressed in some NSCLCs / SCCs [61,177] and WNT1 was connected to NSCLC proliferation [71]. Other components of the WNT/β-catenin pathway like Dishevelled 3 (DSH3) and lymphoid enhancer-binding factor 1 (LEF1) were overexpressed as well [35,162], while the WNT inhibitors WNT inhibitory factor 1 (WIF1) and secreted frizzled-related protein 1 (SFRP1) were frequently found down-regulated in NSCLC tissues [35,46,109,110,166]. Furthermore, an inhibition of WNT1 and WNT2 proteins could induce apoptosis of NSCLC cell lines [61,177]. DKK1 expression has already been found increased in several lung cancer samples including SCC [175]. So DKK1 as inhibitor of WNT/β-catenin signaling might be of particular interest for the formation and growth of dysplasia and malignant transformations of the basal bronchial progenitor cell population.

Interestingly, metaplastic epithelia and in particular the squamous metaplasia are frequent findings in IPF lungs [25,65,85] and the squamous cell lung carcinoma is a frequently observed histological type of lung cancer in IPF patients [6,77]. Squamous metaplasia and invasive carcinoma in IPF patients are often located peripherally, in areas of fibrosis and honeycombing [6,25,65], a structural abnormality that has already been related to the

occurrence of atypical basal cells that depict an abnormal activation of WNT/β-catenin signaling [26].

4.5 Conclusions and future perspectives

Aim of the present study was to examine the expression and localization of the WNT modulatory DKK proteins and their LRP and KRM receptors in the adult lung and in IPF patients. Expression of these proteins could be confirmed in both examined groups. DKK1, DKK4 and KRM1 expression was significantly increased in IPF lung tissue homogenates on the mRNA as well as on the protein level. The enhanced expression of the DKK proteins underlines an aberrant WNT/β-catenin pathway activation in IPF, as they are known target genes of this signal transduction cascade [10,53,122,130]. However, this established negative-feedback-loop does not seem to be sufficient to effectively inhibit the abnormal activation of WNT/β-catenin signaling in IPF. Since DKK proteins and their receptors are mainly expressed in the lung epithelium, the homogenate derived data are subject to the cellular composition of the samples. As a next step, the results of the present study should be supplemented by expression analyses on isolated pulmonary epithelial cells.

The lung epithelium is of essential interest for the pathogenesis and disease progression in IPF [25,143,160] and it seems to be the center of DKK induced WNT modulation, as it expresses DKK ligands and receptors. Therefore, autocrine and paracrine effects appear to be the major type of DKK interference with WNT in the lung.

The distinct accumulation of DKK1 in basal bronchial epithelial cells and its influence on bronchial epithelial cell proliferation [131] underline this protein as an interesting research target concerning the maintenance and repair of the bronchial epithelium. Future experiments should focus on DKK1 influence in IPF, where aberrantly activated WNT/β-catenin signaling is present at proliferative lesions of atypical basal airway cells [26]. Moreover, the influence of DKK1 on formation and growth of squamous dysplasia and squamous cell carcinoma of the lung should be addressed. Future *in vitro* studies should focus on primary basal cells of the bronchial epithelium to elucidate the effects of DKK1 on bronchial epithelial cell proliferation.

Therapeutic antifibrotic capabilities of DKK1 via inhibition of WNT have already been stated in animal models of cholestatic liver fibrosis [23] and renal fibrosis [62]. Furthermore, the inhibition of WNT target gene transcription was able to suppress lung fibrosis in the

bleomycin mouse model [63,82,183]. Future *in vivo* studies about DKK1 in mice with bleomycin induced pulmonary fibrosis could possibly reveal whether this protein possesses therapeutic capabilities for IPF, while limitations of this animal model concerning the transferability to some aspects of IPF pathobiology [113] will have to be taken into account.

5 Summary

Idiopathic pulmonary fibrosis (IPF) is a severe interstitial lung disease that causes destruction of the lungs' architecture by accumulation of scar tissue. The prognosis of IPF is poor and currently the benefit of pharmaceutical treatment is very limited. The pathogenetic mechanisms underlying initiation and progression of the disease are still not completely elucidated and are subject of current investigations.

An aberrant activation of the WNT/β-catenin signaling pathway in the lung tissue of IPF patients has recently been reported and an inhibition of this signal transduction cascade was demonstrated to be able to attenuate bleomycin induced pulmonary fibrosis in mice. The present study focused on Dickkopf (DKK) proteins, potent modulators of the WNT/β-catenin pathway. An antifibrotic effect of these proteins via inhibition of WNT/β-catenin signaling has already been demonstrated in mouse models of other fibrosing diseases. However, the role of DKK proteins in IPF had not been addressed before. Therefore the aim of the present study was to investigate and to compare the expression and localization of DKK proteins and their receptors low density lipoprotein receptor-related protein (LRP) and Kremen (KRM) in the unaffected adult human lung and in IPF.

By quantitative reverse transcription polymerase chain reaction (qRT-PCR) and Western blot analysis, DKK proteins as well as their LRP and KRM receptors were found expressed in unaffected donor and in IPF lung tissues, with a significantly enhanced expression of DKK1, DKK4 and KRM1 in the fibrotic lungs.

Immunohistochemistry identified the bronchial epithelium of donors and IPF patients as well as hyperplastic alveolar epithelial cells of IPF patients as major sources for DKK proteins and their receptors in the lung tissue. A pronounced and distinct accumulation of DKK1 was observed in basal bronchial epithelial cells, one of the cell populations considered as epithelial progenitors.

Additionally, an enhanced DKK1 protein content was detected in bronchoalveolar lavage fluids of IPF patients by an enzyme-linked immunosorbent assay (ELISA).

Analysis of the human bronchial epithelial cell line BEAS-2B by qRT-PCR demonstrated that besides the DKK receptors, other key components of the WNT/β-catenin signaling cascade can be expressed by human bronchial epithelial cells as well.

Taken together, these data indicate an autocrine or paracrine mode of action for DKK at the bronchial epithelium.

In summary, DKK proteins and their receptors are largely located in the lung epithelium and their expression is altered in IPF. Since an impairment of epithelial functions is a key feature of IPF, DKK proteins may be of interest for the understanding of IPF pathogenesis and for treatment strategies of this fatal lung disease.

6 Zusammenfassung

Die idiopathische Lungenfibrose (IPF) ist eine schwerwiegende interstitielle Lungenerkrankung, bei welcher durch Anhäufung von Narbengewebe die Lungenarchitektur zerstört wird. Die IPF hat eine schlechte Prognose und derzeit ist der Nutzen von medikamentösen Behandlungen sehr begrenzt. Die Pathomechanismen, welche dem Beginn sowie dem Fortschreiten der Erkrankung zugrunde liegen, sind immer noch nicht vollständig aufgeklärt und sind Gegenstand der aktuellen Forschung.

Es wurde bereits über eine abnorme Aktivierung des WNT/β-catenin-Signalwegs im Lungengewebe von IPF Patienten berichtet und es konnte gezeigt werden, dass die Unterbindung dieser Signaltransduktionskaskade die Bleomycin-induzierte Lungenfibrose in Mäusen hemmt.

Die vorliegende Arbeit hat die Dickkopf (DKK) Proteine betrachtet, bei welchen es sich um potente Modulatoren des WNT/β-catenin-Signalwegs handelt. Ein antifibrotischer Effekt dieser Proteine mittels Hemmung der WNT/β-catenin-Signaltransduktion konnte bereits in Maus-Modellen anderer fibrosierender Erkrankungen gezeigt werden. Die Rolle von DKK Proteinen in der IPF war zuvor jedoch noch nicht untersucht worden. Ziel der gegenwärtigen Studie war es daher, die Expression und Lokalisation von DKK Proteinen und deren Rezeptoren Low Density Lipoprotein Receptor-related Protein (LRP) und Kremen (KRM) in der nicht betroffenen Erwachsenenlunge und in der IPF Lunge zu untersuchen und zu vergleichen.

Mittels quantitativer Real Time Polymerase-Kettenreaktion (qRT-PCR) und Western Blot Analyse konnte die Expression von DKK Proteinen und deren Rezeptoren im Lungengewebe von nicht betroffenen Spendern und IPF Patienten aufgezeigt werden, wobei DKK1, DKK4 und KRM1 in den fibrotischen Lungen signifikant verstärkt exprimiert wurden.

Immunhistochemische Untersuchungen identifizierten das Bronchialepithel von Spendern und IPF Patienten sowie hyperplastische Alveolarepithelzellen von IPF Patienten als Hauptquellen von DKK Proteinen und deren Rezeptoren im Lungengewebe. Es wurde eine deutlich verstärkte Anhäufung von DKK1 in basalen Bronchialepithelzellen beobachtet, eine der Zellpopulationen welche als epitheliale Vorläuferzellen angesehen werden.

Außerdem wurde mittels eines enzymgekoppelten Immunadsorptionstests (ELISA) ein erhöhter Gehalt an DKK1 Protein in bronchoalveolären Lavageflüssigkeiten von IPF Patienten festgestellt.

Die Untersuchung der humanen Bronchialepithelzelllinie BEAS-2B mittels qRT-PCR zeigte, dass außer den DKK-Rezeptoren auch weitere Schlüssel-Moleküle des WNT/β-catenin Signalwegs von humanen Bronchialepithelzellen exprimiert werden können.

In der Zusammenschau weisen diese Erkenntnisse auf eine autokrine oder parakrine Wirkungsweise von DKK am Bronchialepithel hin.

Zusammengefasst zeigen die Ergebnisse der vorliegenden Arbeit, dass DKK Proteine und deren Rezeptoren überwiegend im Lungenepithel vorkommen und dass ihre Expression in der IPF verändert ist. Da die Beeinträchtigung von epithelialen Funktionen ein Schlüsselmerkmal der IPF ist, könnten DKK Proteine für das Verständnis der IPF-Pathogenese und für Behandlungsstrategien dieser schwerwiegenden Lungenerkrankung von Interesse sein.

7 Abbreviations

A	ampere
AEC	alveolar epithelial cells
AIP	acute interstitial pneumonia
APC	adenomatous polyposis coli
APS	ammonium persulfate
ALAT	Latin American Thoracic Association
ATI cells	alveolar epithelial type I cells
ATII cells	alveolar epithelial type II cells
ATS	American Thoracic Society
BAL	bronchoalveolar lavage
BALF	bronchoalveolar lavage fluid
bp	base pair
BSA	bovine serum albumin
C	cytosine
°C	degree Celsius
Ca^{2+}	calcium
cDNA	complementary deoxyribonucleic acid
CK	casein kinase
CO	carbon monoxide
CO_2	carbon dioxide
COP	cryptogenic organizing pneumonia
Ct	threshold cycle
Δ	delta
dd	double distilled
DIP	desquamative interstitial pneumonia
DKK	Dickkopf
DL_{CO}	diffusing capacity of the lung for CO
DNA	deoxyribonucleic acid
dNTP	deoxynucleoside triphosphate
DPLD	diffuse parenchymal lung disease
DSH	Dishevelled
DTT	dithiothreitol
EDTA	ethylenediaminetetraacetic acid
EGTA	ethylene glycol tetraacetic acid
ELISA	enzyme-linked immunosorbent assay
EMT	epithelial-mesenchymal transition
ERS	European Respiratory Society
FEV_1	forced expiratory volume in 1 second
for	forward
FVC	forced vital capacity
FZD	Frizzled
g	gram
G	guanine
GSK	glycogen synthase kinase
h	hour
H_2O_2	hydrogen peroxide
HEPES	2-[4-(2-hydroxyethyl)piperazin-1-yl]ethanesulfonic acid
HPRT	hypoxanthine-guanine phosphoribosyltransferase

HRCT	high-resolution computed tomography
HRP	horseradish peroxidase
IgG	immunoglobulin G
IGFBP	insulin-like growth factor-binding protein
IHC	immunohistochemistry
IIP	idiopathic interstitial pneumonia
ILD	interstitial lung disease
IPF	idiopathic pulmonary fibrosis
JNK	c-Jun N-terminal kinase
JRS	Japanese Respiratory Society
kDA	kilo (10^3) Dalton
KRM	Kremen
l	liter
LEF	lymphoid enhancer-binding factor
LIP	lymphoid interstitial pneumonia
LRP	low density lipoprotein receptor-related protein
m	milli (10^{-3})
mm	millimeter
M	mol/l
µ	micro (10^{-6})
$MgCl_2$	magnesium chloride
mmHg	millimeter of mercury
min	minutes
MMP	matrix metalloproteinase
mRNA	messenger RNA
MuLV	murine leukemia virus
n	nano (10^{-9})
n/a	not available
NaCl	sodium chloride
NCBI	National Center for Biotechnology Information
no.	number
NSCLC	non-small-cell lung carcinoma
NSIP	nonspecific interstitial pneumonia
O_2	(di)oxygen
OD	optical density
p	pico (10^{-12})
Pa_{O2} / Pa_{CO2}	partial pressure of O_2 / CO_2 in the arterialized ear lobe blood sample
PBS	phosphate buffered saline
PCR	polymerase chain reaction
q	quantitative
qRT-PCR	quantitative reverse transcription PCR
RB-ILD	respiratory bronchiolitis-associated interstitial lung disease
rev	reverse
RNA	ribonucleic acid
rpm	rounds per minute
RT	reverse transcription / reverse transcriptase
s	seconds
SCC	squamous cell carcinoma
SDS	sodium dodecyl sulfate
SDS-PAGE	SDS polyacrylamide gel electrophoresis

SEM	standard error of the mean
SFRP	secreted frizzled-related protein
stdev	standard deviation
TAE	Tris, acetic acid and EDTA
TCF	T-cell-specific transcription factor
TGF	transforming growth factor
TEMED	tetramethylethylenediamine
TLC	total lung capacity
Tris	trishydroxymethylaminomethane
U	enzyme unit
UDG	uracil-DNA glycosylase
UIP	usual interstitial pneumonia
UV	ultraviolet
V	volt
VA	alveolar volume
VC	vital capacity
v/v	volume fraction
WB	Western blot
WIF	WNT inhibitory factor
WISP	WNT1-inducible-signaling pathway protein
w/v	mass concentration (mass / volume percentage)

8 List of Figures

9 References

1. American Thoracic Society. Idiopathic pulmonary fibrosis: diagnosis and treatment. International consensus statement. American Thoracic Society (ATS), and the European Respiratory Society (ERS). Am J Respir Crit Care Med 161:646-664, 2000
2. American Thoracic Society/European Respiratory Society International Multidisciplinary Consensus Classification of the Idiopathic Interstitial Pneumonias. This joint statement of the American Thoracic Society (ATS), and the European Respiratory Society (ERS) was adopted by the ATS board of directors, June 2001 and by the ERS Executive Committee, June 2001. Am J Respir Crit Care Med 165:277-304, 2002
3. Adamali HI, Maher TM: Current and novel drug therapies for idiopathic pulmonary fibrosis. Drug Des Devel Ther 6:261-271, 2012
4. Akhmetshina A, Palumbo K, Dees C, et al: Activation of canonical Wnt signalling is required for TGF-beta-mediated fibrosis. Nat Commun 3:735, 2012
5. Angers S, Moon RT: Proximal events in Wnt signal transduction. Nat Rev Mol Cell Biol 10:468-477, 2009
6. Aubry MC, Myers JL, Douglas WW, et al: Primary pulmonary carcinoma in patients with idiopathic pulmonary fibrosis. Mayo Clin Proc 77:763-770, 2002
7. Baarsma HA, Konigshoff M, Gosens R: The WNT signaling pathway from ligand secretion to gene transcription: molecular mechanisms and pharmacological targets. Pharmacol Ther 138:66-83, 2013
8. Bafico A, Liu G, Yaniv A, et al: Novel mechanism of Wnt signalling inhibition mediated by Dickkopf-1 interaction with LRP6/Arrow. Nat Cell Biol 3:683-686, 2001
9. Baumgartner KB, Samet JM, Stidley CA, et al: Cigarette smoking: a risk factor for idiopathic pulmonary fibrosis. Am J Respir Crit Care Med 155:242-248, 1997
10. Bazzi H, Fantauzzo KA, Richardson GD, et al: The Wnt inhibitor, Dickkopf 4, is induced by canonical Wnt signaling during ectodermal appendage morphogenesis. Dev Biol 305:498-507, 2007
11. Behr J, Thannickal VJ: Update in diffuse parenchymal lung disease 2008. Am J Respir Crit Care Med 179:439-444, 2009
12. Binnerts ME, Tomasevic N, Bright JM, et al: The first propeller domain of LRP6 regulates sensitivity to DKK1. Mol Biol Cell 20:3552-3560, 2009
13. Bjoraker JA, Ryu JH, Edwin MK, et al: Prognostic significance of histopathologic subsets in idiopathic pulmonary fibrosis. Am J Respir Crit Care Med 157:199-203, 1998
14. Borchers AT, Chang C, Keen CL, et al: Idiopathic Pulmonary Fibrosis-an Epidemiological and Pathological Review. Clin Rev Allergy Immunol 40:117-134, 2011
15. Brabletz T, Jung A, Dag S, et al: beta-catenin regulates the expression of the matrix metalloproteinase-7 in human colorectal cancer. Am J Pathol 155:1033-1038, 1999
16. Brembeck FH, Rosario M, Birchmeier W: Balancing cell adhesion and Wnt signaling, the key role of beta-catenin. Curr Opin Genet Dev 16:51-59, 2006
17. Brott BK, Sokol SY: Regulation of Wnt/LRP signaling by distinct domains of Dickkopf proteins. Mol Cell Biol 22:6100-6110, 2002

18. Cadigan KM, Liu YI: Wnt signaling: complexity at the surface. J Cell Sci 119:395-402, 2006
19. Caneparo L, Huang YL, Staudt N, et al: Dickkopf-1 regulates gastrulation movements by coordinated modulation of Wnt/beta catenin and Wnt/PCP activities, through interaction with the Dally-like homolog Knypek. Genes Dev 21:465-480, 2007
20. Cha SW, Tadjuidje E, Tao Q, et al: Wnt5a and Wnt11 interact in a maternal Dkk1-regulated fashion to activate both canonical and non-canonical signaling in Xenopus axis formation. Development 135:3719-3729, 2008
21. Chamorro MN, Schwartz DR, Vonica A, et al: FGF-20 and DKK1 are transcriptional targets of beta-catenin and FGF-20 is implicated in cancer and development. Embo J 24:73-84, 2005
22. Chapman HA: Disorders of lung matrix remodeling. J Clin Invest 113:148-157, 2004
23. Cheng JH, She H, Han YP, et al: Wnt antagonism inhibits hepatic stellate cell activation and liver fibrosis. Am J Physiol Gastrointest Liver Physiol 294:G39-49, 2008
24. Chilosi M, Doglioni C, Murer B, et al: Epithelial stem cell exhaustion in the pathogenesis of idiopathic pulmonary fibrosis. Sarcoidosis Vasc Diffuse Lung Dis 27:7-18, 2010
25. Chilosi M, Poletti V, Murer B, et al: Abnormal re-epithelialization and lung remodeling in idiopathic pulmonary fibrosis: the role of deltaN-p63. Lab Invest 82:1335-1345, 2002
26. Chilosi M, Poletti V, Zamo A, et al: Aberrant Wnt/beta-catenin pathway activation in idiopathic pulmonary fibrosis. Am J Pathol 162:1495-1502, 2003
27. Clevers H: Wnt/beta-catenin signaling in development and disease. Cell 127:469-480, 2006
28. Collard HR, Moore BB, Flaherty KR, et al: Acute exacerbations of idiopathic pulmonary fibrosis. Am J Respir Crit Care Med 176:636-643, 2007
29. Cong F, Schweizer L, Varmus H: Wnt signals across the plasma membrane to activate the beta-catenin pathway by forming oligomers containing its receptors, Frizzled and LRP. Development 131:5103-5115, 2004
30. Crawford HC, Fingleton BM, Rudolph-Owen LA, et al: The metalloproteinase matrilysin is a target of beta-catenin transactivation in intestinal tumors. Oncogene 18:2883-2891, 1999
31. Crosby LM, Waters CM: Epithelial repair mechanisms in the lung. Am J Physiol Lung Cell Mol Physiol 298:L715-731, 2010
32. Crystal RG, Randell SH, Engelhardt JF, et al: Airway epithelial cells: current concepts and challenges. Proc Am Thorac Soc 5:772-777, 2008
33. de Kok JB, Roelofs RW, Giesendorf BA, et al: Normalization of gene expression measurements in tumor tissues: comparison of 13 endogenous control genes. Lab Invest 85:154-159, 2005
34. De Langhe SP, Sala FG, Del Moral PM, et al: Dickkopf-1 (DKK1) reveals that fibronectin is a major target of Wnt signaling in branching morphogenesis of the mouse embryonic lung. Dev Biol 277:316-331, 2005
35. Dehan E, Ben-Dor A, Liao W, et al: Chromosomal aberrations and gene expression profiles in non-small cell lung cancer. Lung Cancer 56:175-184, 2007
36. Dempsey OJ: Clinical review: idiopathic pulmonary fibrosis--past, present and future. Respir Med 100:1871-1885, 2006

37. Diarra D, Stolina M, Polzer K, et al: Dickkopf-1 is a master regulator of joint remodeling. Nat Med 13:156-163, 2007
38. du Bois RM: Strategies for treating idiopathic pulmonary fibrosis. Nat Rev Drug Discov 9:129-140, 2010
39. Eickelberg O, Laurent GJ: The quest for the initial lesion in idiopathic pulmonary fibrosis: gene expression differences in IPF fibroblasts. Am J Respir Cell Mol Biol 42:1-2, 2010
40. Ellwanger K, Saito H, Clement-Lacroix P, et al: Targeted disruption of the Wnt regulator Kremen induces limb defects and high bone density. Mol Cell Biol 28:4875-4882, 2008
41. Enomoto N, Suda T, Kato M, et al: Quantitative analysis of fibroblastic foci in usual interstitial pneumonia. Chest 130:22-29, 2006
42. Fernandez IE, Eickelberg O: New cellular and molecular mechanisms of lung injury and fibrosis in idiopathic pulmonary fibrosis. Lancet 380:680-688, 2012
43. Flaherty KR, Colby TV, Travis WD, et al: Fibroblastic foci in usual interstitial pneumonia: idiopathic versus collagen vascular disease. Am J Respir Crit Care Med 167:1410-1415, 2003
44. Forget MA, Turcotte S, Beauseigle D, et al: The Wnt pathway regulator DKK1 is preferentially expressed in hormone-resistant breast tumours and in some common cancer types. Br J Cancer 96:646-653, 2007
45. Frankel SK, Schwarz MI: Update in idiopathic pulmonary fibrosis. Curr Opin Pulm Med 15:463-469, 2009
46. Fukui T, Kondo M, Ito G, et al: Transcriptional silencing of secreted frizzled related protein 1 (SFRP 1) by promoter hypermethylation in non-small-cell lung cancer. Oncogene 24:6323-6327, 2005
47. Gauldie J: Pro: Inflammatory mechanisms are a minor component of the pathogenesis of idiopathic pulmonary fibrosis. Am J Respir Crit Care Med 165:1205-1206, 2002
48. Gharaee-Kermani M, Hu B, Thannickal VJ, et al: Current and emerging drugs for idiopathic pulmonary fibrosis. Expert Opin Emerg Drugs 12:627-646, 2007
49. Giangreco A, Reynolds SD, Stripp BR: Terminal bronchioles harbor a unique airway stem cell population that localizes to the bronchoalveolar duct junction. Am J Pathol 161:173-182, 2002
50. Giles RH, van Es JH, Clevers H: Caught up in a Wnt storm: Wnt signaling in cancer. Biochim Biophys Acta 1653:1-24, 2003
51. Glinka A, Wu W, Delius H, et al: Dickkopf-1 is a member of a new family of secreted proteins and functions in head induction. Nature 391:357-362, 1998
52. Gomperts BN, Strieter RM: Stem cells and chronic lung disease. Annu Rev Med 58:285-298, 2007
53. Gonzalez-Sancho JM, Aguilera O, Garcia JM, et al: The Wnt antagonist DICKKOPF-1 gene is a downstream target of beta-catenin/TCF and is downregulated in human colon cancer. Oncogene 24:1098-1103, 2005
54. Gordon MD, Nusse R: Wnt signaling: multiple pathways, multiple receptors, and multiple transcription factors. J Biol Chem 281:22429-22433, 2006
55. Goss AM, Tian Y, Tsukiyama T, et al: Wnt2/2b and beta-catenin signaling are necessary and sufficient to specify lung progenitors in the foregut. Dev Cell 17:290-298, 2009
56. Gross TJ, Hunninghake GW: Idiopathic pulmonary fibrosis. N Engl J Med 345:517-525, 2001

57. Grutters JC, du Bois RM: Genetics of fibrosing lung diseases. Eur Respir J 25:915-927, 2005
58. Gunther A, Markart P, Eickelberg O, et al: [Pulmonary fibrosis--a therapeutic dilemma?]. Med Klin (Munich) 101:308-312, 2006
59. Gurung A, Uddin F, Hill RP, et al: Beta-catenin is a mediator of the response of fibroblasts to irradiation. Am J Pathol 174:248-255, 2009
60. Hassler C, Cruciat CM, Huang YL, et al: Kremen is required for neural crest induction in Xenopus and promotes LRP6-mediated Wnt signaling. Development 134:4255-4263, 2007
61. He B, You L, Uematsu K, et al: A monoclonal antibody against Wnt-1 induces apoptosis in human cancer cells. Neoplasia 6:7-14, 2004
62. He W, Dai C, Li Y, et al: Wnt/beta-catenin signaling promotes renal interstitial fibrosis. J Am Soc Nephrol 20:765-776, 2009
63. Henderson WR, Jr., Chi EY, Ye X, et al: Inhibition of Wnt/beta-catenin/CREB binding protein (CBP) signaling reverses pulmonary fibrosis. Proc Natl Acad Sci U S A 107:14309-14314, 2010
64. Hilberg O, Simonsen U, du Bois R, et al: Pirfenidone: significant treatment effects in idiopathic pulmonary fibrosis. Clin Respir J 6:131-143, 2012
65. Hironaka M, Fukayama M: Pulmonary fibrosis and lung carcinoma: a comparative study of metaplastic epithelia in honeycombed areas of usual interstitial pneumonia with or without lung carcinoma. Pathol Int 49:1060-1066, 1999
66. Hoang BH, Kubo T, Healey JH, et al: Dickkopf 3 inhibits invasion and motility of Saos-2 osteosarcoma cells by modulating the Wnt-beta-catenin pathway. Cancer Res 64:2734-2739, 2004
67. Hodgson U, Laitinen T, Tukiainen P: Nationwide prevalence of sporadic and familial idiopathic pulmonary fibrosis: evidence of founder effect among multiplex families in Finland. Thorax 57:338-342, 2002
68. Hong KU, Reynolds SD, Watkins S, et al: Basal cells are a multipotent progenitor capable of renewing the bronchial epithelium. Am J Pathol 164:577-588, 2004
69. Horowitz JC, Thannickal VJ: Epithelial-mesenchymal interactions in pulmonary fibrosis. Semin Respir Crit Care Med 27:600-612, 2006
70. Hsieh JC, Kodjabachian L, Rebbert ML, et al: A new secreted protein that binds to Wnt proteins and inhibits their activities. Nature 398:431-436, 1999
71. Huang CL, Liu D, Ishikawa S, et al: Wnt1 overexpression promotes tumour progression in non-small cell lung cancer. Eur J Cancer 44:2680-2688, 2008
72. Itasaki N, Jones CM, Mercurio S, et al: Wise, a context-dependent activator and inhibitor of Wnt signalling. Development 130:4295-4305, 2003
73. Johnston ID, Prescott RJ, Chalmers JC, et al: British Thoracic Society study of cryptogenic fibrosing alveolitis: current presentation and initial management. Fibrosing Alveolitis Subcommittee of the Research Committee of the British Thoracic Society. Thorax 52:38-44, 1997
74. Kajstura J, Rota M, Hall SR, et al: Evidence for human lung stem cells. N Engl J Med 364:1795-1806, 2011
75. Katzenstein AL, Myers JL: Idiopathic pulmonary fibrosis: clinical relevance of pathologic classification. Am J Respir Crit Care Med 157:1301-1315, 1998
76. Kawano Y, Kypta R: Secreted antagonists of the Wnt signalling pathway. J Cell Sci 116:2627-2634, 2003

77. Kawasaki H, Nagai K, Yokose T, et al: Clinicopathological characteristics of surgically resected lung cancer associated with idiopathic pulmonary fibrosis. J Surg Oncol 76:53-57, 2001
78. Khan Z, Vijayakumar S, de la Torre TV, et al: Analysis of endogenous LRP6 function reveals a novel feedback mechanism by which Wnt negatively regulates its receptor. Mol Cell Biol 27:7291-7301, 2007
79. Kikuchi A, Yamamoto H, Kishida S: Multiplicity of the interactions of Wnt proteins and their receptors. Cell Signal 19:659-671, 2007
80. Kim CF, Jackson EL, Woolfenden AE, et al: Identification of bronchioalveolar stem cells in normal lung and lung cancer. Cell 121:823-835, 2005
81. Kim DS, Collard HR, King TE, Jr.: Classification and natural history of the idiopathic interstitial pneumonias. Proc Am Thorac Soc 3:285-292, 2006
82. Kim TH, Kim SH, Seo JY, et al: Blockade of the Wnt/beta-catenin pathway attenuates bleomycin-induced pulmonary fibrosis. Tohoku J Exp Med 223:45-54, 2011
83. King TE, Jr., Pardo A, Selman M: Idiopathic pulmonary fibrosis. Lancet 378:1949-1961, 2011
84. King TE, Jr., Schwarz MI, Brown K, et al: Idiopathic pulmonary fibrosis: relationship between histopathologic features and mortality. Am J Respir Crit Care Med 164:1025-1032, 2001
85. Konigshoff M: Lung cancer in pulmonary fibrosis: tales of epithelial cell plasticity. Respiration 81:353-358, 2011
86. Konigshoff M, Balsara N, Pfaff EM, et al: Functional Wnt signaling is increased in idiopathic pulmonary fibrosis. PLoS One 3:e2142, 2008
87. Konigshoff M, Eickelberg O: WNT signaling in lung disease: a failure or a regeneration signal? Am J Respir Cell Mol Biol 42:21-31, 2010
88. Konigshoff M, Kramer M, Balsara N, et al: WNT1-inducible signaling protein-1 mediates pulmonary fibrosis in mice and is upregulated in humans with idiopathic pulmonary fibrosis. J Clin Invest 119:772-787, 2009
89. Korol O, Gupta RW, Mercola M: A novel activity of the Dickkopf-1 amino terminal domain promotes axial and heart development independently of canonical Wnt inhibition. Dev Biol 324:131-138, 2008
90. Kotton DN, Fine A: Lung stem cells. Cell Tissue Res 331:145-156, 2008
91. Krupnik VE, Sharp JD, Jiang C, et al: Functional and structural diversity of the human Dickkopf gene family. Gene 238:301-313, 1999
92. Lee AY, He B, You L, et al: Dickkopf-1 antagonizes Wnt signaling independent of beta-catenin in human mesothelioma. Biochem Biophys Res Commun 323:1246-1250, 2004
93. Lee HL, Ryu JH, Wittmer MH, et al: Familial idiopathic pulmonary fibrosis: clinical features and outcome. Chest 127:2034-2041, 2005
94. Li C, Chen H, Hu L, et al: Ror2 modulates the canonical Wnt signaling in lung epithelial cells through cooperation with Fzd2. BMC Mol Biol 9:11, 2008
95. Li C, Xiao J, Hormi K, et al: Wnt5a participates in distal lung morphogenesis. Dev Biol 248:68-81, 2002
96. Li L, Mao J, Sun L, et al: Second cysteine-rich domain of Dickkopf-2 activates canonical Wnt signaling pathway via LRP-6 independently of dishevelled. J Biol Chem 277:5977-5981, 2002
97. Li Y, Lu W, King TD, et al: Dkk1 stabilizes Wnt co-receptor LRP6: implication for Wnt ligand-induced LRP6 down-regulation. PLoS One 5:e11014, 2010

98. Lieber M, Smith B, Szakal A, et al: A continuous tumor-cell line from a human lung carcinoma with properties of type II alveolar epithelial cells. Int J Cancer 17:62-70, 1976
99. Liu DW, Chen ST, Liu HP: Choice of endogenous control for gene expression in nonsmall cell lung cancer. Eur Respir J 26:1002-1008, 2005
100. Liu X, Engelhardt JF: The glandular stem/progenitor cell niche in airway development and repair. Proc Am Thorac Soc 5:682-688, 2008
101. Logan CY, Nusse R: The Wnt signaling pathway in development and disease. Annu Rev Cell Dev Biol 20:781-810, 2004
102. MacDonald BT, Tamai K, He X: Wnt/beta-catenin signaling: components, mechanisms, and diseases. Dev Cell 17:9-26, 2009
103. Mao B, Niehrs C: Kremen2 modulates Dickkopf2 activity during Wnt/LRP6 signaling. Gene 302:179-183, 2003
104. Mao B, Wu W, Davidson G, et al: Kremen proteins are Dickkopf receptors that regulate Wnt/beta-catenin signalling. Nature 417:664-667, 2002
105. Mao B, Wu W, Li Y, et al: LDL-receptor-related protein 6 is a receptor for Dickkopf proteins. Nature 411:321-325, 2001
106. Mao J, Wang J, Liu B, et al: Low-density lipoprotein receptor-related protein-5 binds to Axin and regulates the canonical Wnt signaling pathway. Mol Cell 7:801-809, 2001
107. Marshall RP, Puddicombe A, Cookson WO, et al: Adult familial cryptogenic fibrosing alveolitis in the United Kingdom. Thorax 55:143-146, 2000
108. Martinez FJ, Safrin S, Weycker D, et al: The clinical course of patients with idiopathic pulmonary fibrosis. Ann Intern Med 142:963-967, 2005
109. Mazieres J, He B, You L, et al: Wnt signaling in lung cancer. Cancer Lett 222:1-10, 2005
110. Mazieres J, He B, You L, et al: Wnt inhibitory factor-1 is silenced by promoter hypermethylation in human lung cancer. Cancer Res 64:4717-4720, 2004
111. McNeill H, Woodgett JR: When pathways collide: collaboration and connivance among signalling proteins in development. Nat Rev Mol Cell Biol 11:404-413, 2010
112. Meltzer EB, Noble PW: Idiopathic pulmonary fibrosis. Orphanet J Rare Dis 3:8, 2008
113. Moeller A, Ask K, Warburton D, et al: The bleomycin animal model: a useful tool to investigate treatment options for idiopathic pulmonary fibrosis? Int J Biochem Cell Biol 40:362-382, 2008
114. Moon RT, Kohn AD, De Ferrari GV, et al: WNT and beta-catenin signalling: diseases and therapies. Nat Rev Genet 5:691-701, 2004
115. Morvan F, Boulukos K, Clement-Lacroix P, et al: Deletion of a single allele of the Dkk1 gene leads to an increase in bone formation and bone mass. J Bone Miner Res 21:934-945, 2006
116. Mucenski ML, Nation JM, Thitoff AR, et al: Beta-catenin regulates differentiation of respiratory epithelial cells in vivo. Am J Physiol Lung Cell Mol Physiol 289:L971-979, 2005
117. Mucenski ML, Wert SE, Nation JM, et al: beta-Catenin is required for specification of proximal/distal cell fate during lung morphogenesis. J Biol Chem 278:40231-40238, 2003
118. Nakajima M, Kawanami O, Jin E, et al: Immunohistochemical and ultrastructural studies of basal cells, Clara cells and bronchiolar cuboidal cells in normal human airways. Pathol Int 48:944-953, 1998

119. Nakamura T, Aoki S, Kitajima K, et al: Molecular cloning and characterization of Kremen, a novel kringle-containing transmembrane protein. Biochim Biophys Acta 1518:63-72, 2001
120. Nicholson AG, Fulford LG, Colby TV, et al: The relationship between individual histologic features and disease progression in idiopathic pulmonary fibrosis. Am J Respir Crit Care Med 166:173-177, 2002
121. Niehrs C: Function and biological roles of the Dickkopf family of Wnt modulators. Oncogene 25:7469-7481, 2006
122. Niida A, Hiroko T, Kasai M, et al: DKK1, a negative regulator of Wnt signaling, is a target of the beta-catenin/TCF pathway. Oncogene 23:8520-8526, 2004
123. Noble PW, Homer RJ: Back to the future: historical perspective on the pathogenesis of idiopathic pulmonary fibrosis. Am J Respir Cell Mol Biol 33:113-120, 2005
124. Noth I, Martinez FJ: Recent advances in idiopathic pulmonary fibrosis. Chest 132:637-650, 2007
125. Nusse R: The Wnt Homepage, 1997-2013, Vol 2013
126. Nusse R, Fuerer C, Ching W, et al: Wnt signaling and stem cell control. Cold Spring Harb Symp Quant Biol 73:59-66, 2008
127. Pan LH, Yamauchi K, Uzuki M, et al: Type II alveolar epithelial cells and interstitial fibroblasts express connective tissue growth factor in IPF. Eur Respir J 17:1220-1227, 2001
128. Pardo A, Selman M: Idiopathic pulmonary fibrosis: new insights in its pathogenesis. Int J Biochem Cell Biol 34:1534-1538, 2002
129. Park KS, Wells JM, Zorn AM, et al: Transdifferentiation of ciliated cells during repair of the respiratory epithelium. Am J Respir Cell Mol Biol 34:151-157, 2006
130. Pendas-Franco N, Garcia JM, Pena C, et al: DICKKOPF-4 is induced by TCF/beta-catenin and upregulated in human colon cancer, promotes tumour cell invasion and angiogenesis and is repressed by 1alpha,25-dihydroxyvitamin D3. Oncogene 27:4467-4477, 2008
131. Pfaff EM, Becker S, Gunther A, et al: Dickkopf proteins influence lung epithelial cell proliferation in idiopathic pulmonary fibrosis. Eur Respir J 37:79-87, 2011
132. Pinzone JJ, Hall BM, Thudi NK, et al: The role of Dickkopf-1 in bone development, homeostasis, and disease. Blood 113:517-525, 2009
133. Raghu G, Collard HR, Egan JJ, et al: An official ATS/ERS/JRS/ALAT statement: idiopathic pulmonary fibrosis: evidence-based guidelines for diagnosis and management. Am J Respir Crit Care Med 183:788-824, 2011
134. Rawlins EL, Ostrowski LE, Randell SH, et al: Lung development and repair: contribution of the ciliated lineage. Proc Natl Acad Sci U S A 104:410-417, 2007
135. Rijsewijk F, Schuermann M, Wagenaar E, et al: The Drosophila homolog of the mouse mammary oncogene int-1 is identical to the segment polarity gene wingless. Cell 50:649-657, 1987
136. Rock JR, Onaitis MW, Rawlins EL, et al: Basal cells as stem cells of the mouse trachea and human airway epithelium. Proc Natl Acad Sci U S A 106:12771-12775, 2009
137. Rosas IO, Richards TJ, Konishi K, et al: MMP1 and MMP7 as potential peripheral blood biomarkers in idiopathic pulmonary fibrosis. PLoS Med 5:e93, 2008

138. Rothbacher U, Lemaire P: Creme de la Kremen of Wnt signalling inhibition. Nat Cell Biol 4:E172-173, 2002
139. Sakane H, Yamamoto H, Kikuchi A: LRP6 is internalized by Dkk1 to suppress its phosphorylation in the lipid raft and is recycled for reuse. J Cell Sci 123:360-368, 2010
140. Sato N, Yamabuki T, Takano A, et al: Wnt inhibitor Dickkopf-1 as a target for passive cancer immunotherapy. Cancer Res 70:5326-5336, 2010
141. Scotton CJ, Chambers RC: Molecular targets in pulmonary fibrosis: the myofibroblast in focus. Chest 132:1311-1321, 2007
142. Selman M, King TE, Pardo A: Idiopathic pulmonary fibrosis: prevailing and evolving hypotheses about its pathogenesis and implications for therapy. Ann Intern Med 134:136-151, 2001
143. Selman M, Pardo A: Idiopathic pulmonary fibrosis: an epithelial/fibroblastic cross-talk disorder. Respir Res 3:3, 2002
144. Selman M, Pardo A: Role of epithelial cells in idiopathic pulmonary fibrosis: from innocent targets to serial killers. Proc Am Thorac Soc 3:364-372, 2006
145. Selman M, Pardo A, Barrera L, et al: Gene expression profiles distinguish idiopathic pulmonary fibrosis from hypersensitivity pneumonitis. Am J Respir Crit Care Med 173:188-198, 2006
146. Selman M, Pardo A, Kaminski N: Idiopathic pulmonary fibrosis: aberrant recapitulation of developmental programs? PLoS Med 5:e62, 2008
147. Semenov MV, Tamai K, Brott BK, et al: Head inducer Dickkopf-1 is a ligand for Wnt coreceptor LRP6. Curr Biol 11:951-961, 2001
148. Semenov MV, Zhang X, He X: DKK1 antagonizes Wnt signaling without promotion of LRP6 internalization and degradation. J Biol Chem 283:21427-21432, 2008
149. Sheng SL, Huang G, Yu B, et al: Clinical significance and prognostic value of serum Dickkopf-1 concentrations in patients with lung cancer. Clin Chem 55:1656-1664, 2009
150. Shtutman M, Zhurinsky J, Simcha I, et al: The cyclin D1 gene is a target of the beta-catenin/LEF-1 pathway. Proc Natl Acad Sci U S A 96:5522-5527, 1999
151. Shu W, Guttentag S, Wang Z, et al: Wnt/beta-catenin signaling acts upstream of N-myc, BMP4, and FGF signaling to regulate proximal-distal patterning in the lung. Dev Biol 283:226-239, 2005
152. Shu W, Jiang YQ, Lu MM, et al: Wnt7b regulates mesenchymal proliferation and vascular development in the lung. Development 129:4831-4842, 2002
153. Sisson TH, Mendez M, Choi K, et al: Targeted injury of type II alveolar epithelial cells induces pulmonary fibrosis. Am J Respir Crit Care Med 181:254-263, 2010
154. Snyder JC, Teisanu RM, Stripp BR: Endogenous lung stem cells and contribution to disease. J Pathol 217:254-264, 2009
155. Spagnolo P, Del Giovane C, Luppi F, et al: Non-steroid agents for idiopathic pulmonary fibrosis. Cochrane Database Syst Rev:CD003134, 2010
156. Steel MD, Puddicombe SM, Hamilton LM, et al: Beta-catenin/T-cell factor-mediated transcription is modulated by cell density in human bronchial epithelial cells. Int J Biochem Cell Biol 37:1281-1295, 2005
157. Strieter RM: Pathogenesis and natural history of usual interstitial pneumonia: the whole story or the last chapter of a long novel. Chest 128:526S-532S, 2005

158. Swigris JJ, Kuschner WG, Jacobs SS, et al: Health-related quality of life in patients with idiopathic pulmonary fibrosis: a systematic review. Thorax 60:588-594, 2005
159. Thannickal VJ, Horowitz JC: Evolving concepts of apoptosis in idiopathic pulmonary fibrosis. Proc Am Thorac Soc 3:350-356, 2006
160. Thannickal VJ, Toews GB, White ES, et al: Mechanisms of pulmonary fibrosis. Annu Rev Med 55:395-417, 2004
161. Turner-Warwick M, Burrows B, Johnson A: Cryptogenic fibrosing alveolitis: clinical features and their influence on survival. Thorax 35:171-180, 1980
162. Uematsu K, He B, You L, et al: Activation of the Wnt pathway in non small cell lung cancer: evidence of dishevelled overexpression. Oncogene 22:7218-7221, 2003
163. Uhal BD: Cell cycle kinetics in the alveolar epithelium. Am J Physiol 272:L1031-1045, 1997
164. Uren A, Reichsman F, Anest V, et al: Secreted frizzled-related protein-1 binds directly to Wingless and is a biphasic modulator of Wnt signaling. J Biol Chem 275:4374-4382, 2000
165. van Amerongen R, Nusse R: Towards an integrated view of Wnt signaling in development. Development 136:3205-3214, 2009
166. Van Scoyk M, Randall J, Sergew A, et al: Wnt signaling pathway and lung disease. Transl Res 151:175-180, 2008
167. Visscher DW, Myers JL: Histologic spectrum of idiopathic interstitial pneumonias. Proc Am Thorac Soc 3:322-329, 2006
168. Walter N, Collard HR, King TE, Jr.: Current perspectives on the treatment of idiopathic pulmonary fibrosis. Proc Am Thorac Soc 3:330-338, 2006
169. Wang K, Zhang Y, Li X, et al: Characterization of the Kremen-binding site on Dkk1 and elucidation of the role of Kremen in Dkk-mediated Wnt antagonism. J Biol Chem 283:23371-23375, 2008
170. Welsch U: Lehrbuch Histologie: Urban & Fischer Verlag, 2003, Vol 1
171. White ES, Lazar MH, Thannickal VJ: Pathogenetic mechanisms in usual interstitial pneumonia/idiopathic pulmonary fibrosis. J Pathol 201:343-354, 2003
172. Williams TJ, Wilson JW: Challenges in pulmonary fibrosis: 7--Novel therapies and lung transplantation. Thorax 63:277-284, 2008
173. Wistuba, II, Gazdar AF: Lung cancer preneoplasia. Annu Rev Pathol 1:331-348, 2006
174. Wu W, Glinka A, Delius H, et al: Mutual antagonism between dickkopf1 and dickkopf2 regulates Wnt/beta-catenin signalling. Curr Biol 10:1611-1614, 2000
175. Yamabuki T, Takano A, Hayama S, et al: Dikkopf-1 as a novel serologic and prognostic biomarker for lung and esophageal carcinomas. Cancer Res 67:2517-2525, 2007
176. Yamamoto H, Sakane H, Yamamoto H, et al: Wnt3a and Dkk1 regulate distinct internalization pathways of LRP6 to tune the activation of beta-catenin signaling. Dev Cell 15:37-48, 2008
177. You L, He B, Xu Z, et al: Inhibition of Wnt-2-mediated signaling induces programmed cell death in non-small-cell lung cancer cells. Oncogene 23:6170-6174, 2004
178. Yue W, Sun Q, Dacic S, et al: Downregulation of Dkk3 activates beta-catenin/TCF-4 signaling in lung cancer. Carcinogenesis 29:84-92, 2008

179. Zemke AC, Teisanu RM, Giangreco A, et al: beta-Catenin is not necessary for maintenance or repair of the bronchiolar epithelium. Am J Respir Cell Mol Biol 41:535-543, 2009
180. Zeng X, Tamai K, Doble B, et al: A dual-kinase mechanism for Wnt co-receptor phosphorylation and activation. Nature 438:873-877, 2005
181. Zhang Y, Goss AM, Cohen ED, et al: A Gata6-Wnt pathway required for epithelial stem cell development and airway regeneration. Nat Genet 40:862-870, 2008
182. Zhu W, Shiojima I, Ito Y, et al: IGFBP-4 is an inhibitor of canonical Wnt signalling required for cardiogenesis. Nature 454:345-349, 2008
183. Zuo F, Kaminski N, Eugui E, et al: Gene expression analysis reveals matrilysin as a key regulator of pulmonary fibrosis in mice and humans. Proc Natl Acad Sci U S A 99:6292-6297, 2002

10 Appendix

10.1 Table 1 Lung tissue biopsies

Characteristics of IPF patients.

VC = vital capacity, TLC = total lung capacity, DL_{CO}/VA = diffusing capacity of the lung for CO per unit of alveolar volume (all in % predicted), O_2 = additional nasal oxygen supplementation during blood gas analysis, Pa_{O2} / Pa_{CO2} = partial pressure of O_2 / CO_2 in the arterialized ear lobe blood sample, n/a = not available.

no.	diagnosis	gender	age (years)	VC (%)	TLC (%)	DL_{CO}/VA (%)	O_2 (l/min)	Pa_{O2} (mmHg)	Pa_{CO2} (mmHg)
1	IPF/UIP	male	63	56	48	33	3	52	33
2	IPF/UIP	male	62	50	52	26	3	49	38
3	IPF/UIP	male	58	49	n/a	n/a	n/a	n/a	n/a
4	IPF/UIP	male	65	59	42	20	3	53	38
5	IPF/UIP	male	65	59	42	20	4	69	41
6	IPF/UIP	male	43	48	51	27	n/a	n/a	n/a
7	IPF/UIP	male	71	40	46	24	n/a	n/a	n/a
8	IPF/UIP	male	64	59	52	22	2	58	38
9	IPF/UIP	male	60	51	49	18	2	59	39
10	IPF/UIP	male	65	51	66	20	2	53	38
11	IPF/UIP	male	44	47	55	25	2	36	35
12	IPF/UIP	female	43	40	n/a	n/a	2	54	35
13	IPF/UIP	female	42	50	58	17	3	52	36
14	IPF/UIP	female	66	29	45	23	4	56	45
15	IPF/UIP	female	62	27	48	n/a	4	71	65

10.2 Table 2 Bronchoalveolar lavage fluids (BALF)

Characteristics of IPF patients.

VC = vital capacity, TLC = total lung capacity, DL_{CO}/VA = diffusing capacity of the lung for CO per unit of alveolar volume (all in % predicted), O_2 = additional nasal oxygen supplementation during blood gas analysis, Pa_{O2} / Pa_{CO2} = partial pressure of O_2 / CO_2 in the arterialized ear lobe blood sample, n/a = not available.

no.	diagnosis	gender	age (years)	VC (%)	TLC (%)	DL_{CO}/VA (%)	O_2 (l/min)	Pa_{O2} (mmHg)	Pa_{CO2} (mmHg)
1	IPF/UIP	male	66	86	78	56	2	90	41
2	IPF/UIP	male	76	41	47	73	-	79	38
3	IPF/UIP	male	68	57	55	37	-	51	34
4	IPF/UIP	male	60	33	42	n/a	5	69	41
5	IPF/UIP	male	64	69	71	54	-	70	35
6	IPF/UIP	male	79	81	75	42	-	45	37
7	IPF/UIP	male	65	60	62	48	-	61	34
8	IPF/UIP	male	65	64	58	75	-	78	35
9	IPF/UIP	male	69	36	41	n/a	n/a	71	46

10.3 Table 3 qRT-PCR primer

Sequences were taken from the NCBI GenBank. All accession numbers are listed.

gene	**accession**		**sequences (5´ → 3´)**	**length**	**amplicon**
β-CAT human	NM001904	for	AAGTGGGTGGTATAGAGGCTCTTG	24bp	77bp
		rev	GATGGCAGGCTCAGTGATGTC	21bp	
DKK1 human	NM012242	for	CGCCGAAAACGCTGCAT	17bp	109bp
		rev	TTTCCTCAATTTCTCCTCGGAA	22bp	
DKK2 human	NM014421	for	TCAGGCCGCCAATCGA	16bp	85bp
		rev	GTAGGCCTGCCCCAGGTT	18bp	
DKK3 human	NM015881	for	GCTTCTGGACCTCATCACCTG	21bp	119bp
		rev	TCGGCTTGCACACATACACC	20bp	
DKK4 human	NM014420	for	GAAGGGCTCACAGTGCCTGT	20bp	131bp
		rev	AGCACATGGCATCTCGCTG	19bp	
FZD1 human	NM003505	for	AGCGCCGTGGAGTTCGT	17bp	64bp
		rev	CGAAAGAGAGTTGTCTAGTGAGGAAAC	27bp	
FZD2 human	NM001466	for	CACGCCGCGCATGTC	15bp	63bp
		rev	ACGATGAGCGTCATGAGGTATTT	23bp	
FZD3 human	NM017412	for	GGTGTTCCTTGGCCTGAAGA	20bp	72bp
		rev	CACAAGTCGAGGATATGGCTCAT	23bp	
FZD4 human	NM12193	for	GACAACTTTCACACCGCTCATC	22bp	164bp
		rev	CCTTCAGGACGGGTTCACA	19bp	

GSK3β human	NM002093	for	CTCATGCTCGGATTCAAGCA	20bp	86bp
		rev	GGTCTGTCCACGGTCTCCAGTA	22bp	
HPRT1 human	NM000194	for	AAGGACCCCACGAAGTGTTG	20bp	157bp
		rev	GGCTTTGTATTTTGCTTTTCCA	22bp	
KRM1 human	NM001039570	for	TGGAAGCCACAGAGTTGAAGG	21bp	146bp
		rev	GACAATCCCTAAGGTCCCCTG	21bp	
KRM2 human	NM172229	for	CTGGCGCTACTGCGACATC	19bp	62bp
		rev	AGTCCACAAAGCATCCCAGGTA	22bp	
LEF1 human	NM016269	for	CATCAGGTACAGGTCCAAGAATGA	24bp	93bp
		rev	GTCGCTGCCTTGGCTTTG	18bp	
LRP5 human	NM002335	for	GACCCAGCCCTTTGTTTTGAC	21bp	134bp
		rev	TGTGGACGTTGATGGTATTGGT	22bp	
LRP6 human	NM002336	for	GATTCAGATCTCCGGCGAATT	21bp	83bp
		rev	GGCTGCAAGATATTGGAGTCTTCT	24bp	
TCF3 human	NM031283	for	ACCATCTCCAGCACACTTGTCTAATA	26bp	71bp
		rev	GAGTCAGCGGATGCATGTGA	20bp	
TCF4 human	NM030756	for	GCGCGGGATAACTATGGAAAG	21bp	89bp
		rev	GGATTTAGGAAACATTCGCTGTGT	24bp	
WNT1 human	NM005430	for	CTCATGAACCTTCACAACAACGA	23bp	80bp
		rev	ATCCCGTGGCACTTGCA	17bp	
WNT3a human	NM033131	for	GCCCCACTCGGATACTTCTTACT	23bp	98bp
		rev	GAGGAATACTGTGGCCCAACA	21bp	
WNT7b human	NM058238	for	GCAAGTGGATTTTCTACGTGTTTCT	25bp	65bp
		rev	TGACAGTGCTCCGAGCTTCA	20bp	
WNT10b human	NM003394	for	GCGCCAGGTGGTAACTGAA	19bp	59bp
		rev	TGCCTGATGTGCCATGACA	19bp	

10.4 Immunohistochemistry - supplements

Immunohistochemical stainings of tissue sections from further donor and IPF lungs are presented on the following pages. Representative bronchial and alveolar regions of lungs other than depicted in the results chapter (chapter ***3.2***) are shown for each antibody.

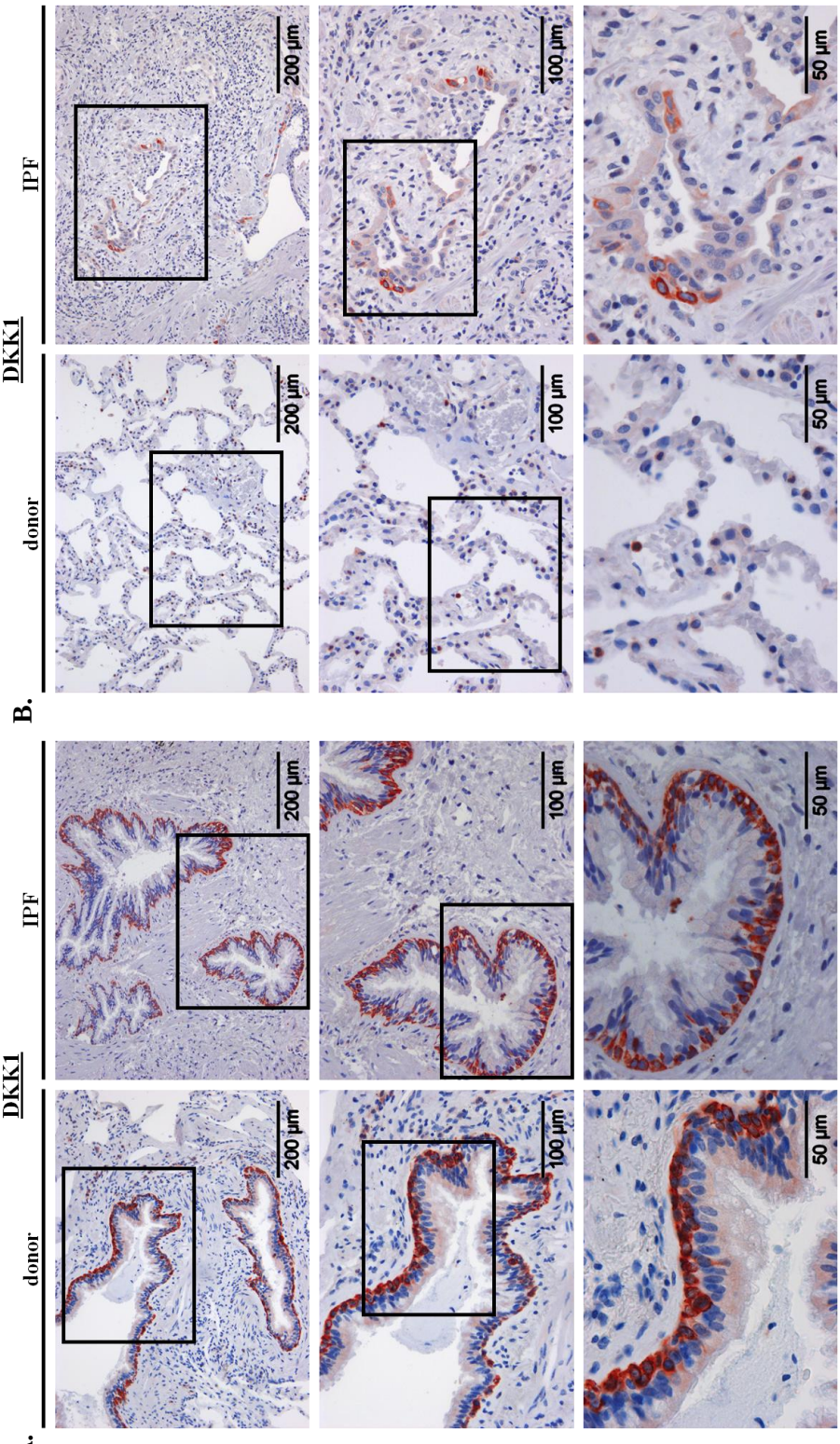

Figure 15. Localization of DKK1 protein in donor and IPF lung tissue.
Immunohistochemical staining for DKK1 protein was performed on lung tissue sections of donors and IPF patients. Stainings were performed at least twice using three different donor and IPF lung tissues. Representative **bronchial (A)** and **alveolar (B)** regions of donor **(left panels)** and IPF **(right panels)** lungs are shown in three magnifications as indicated.

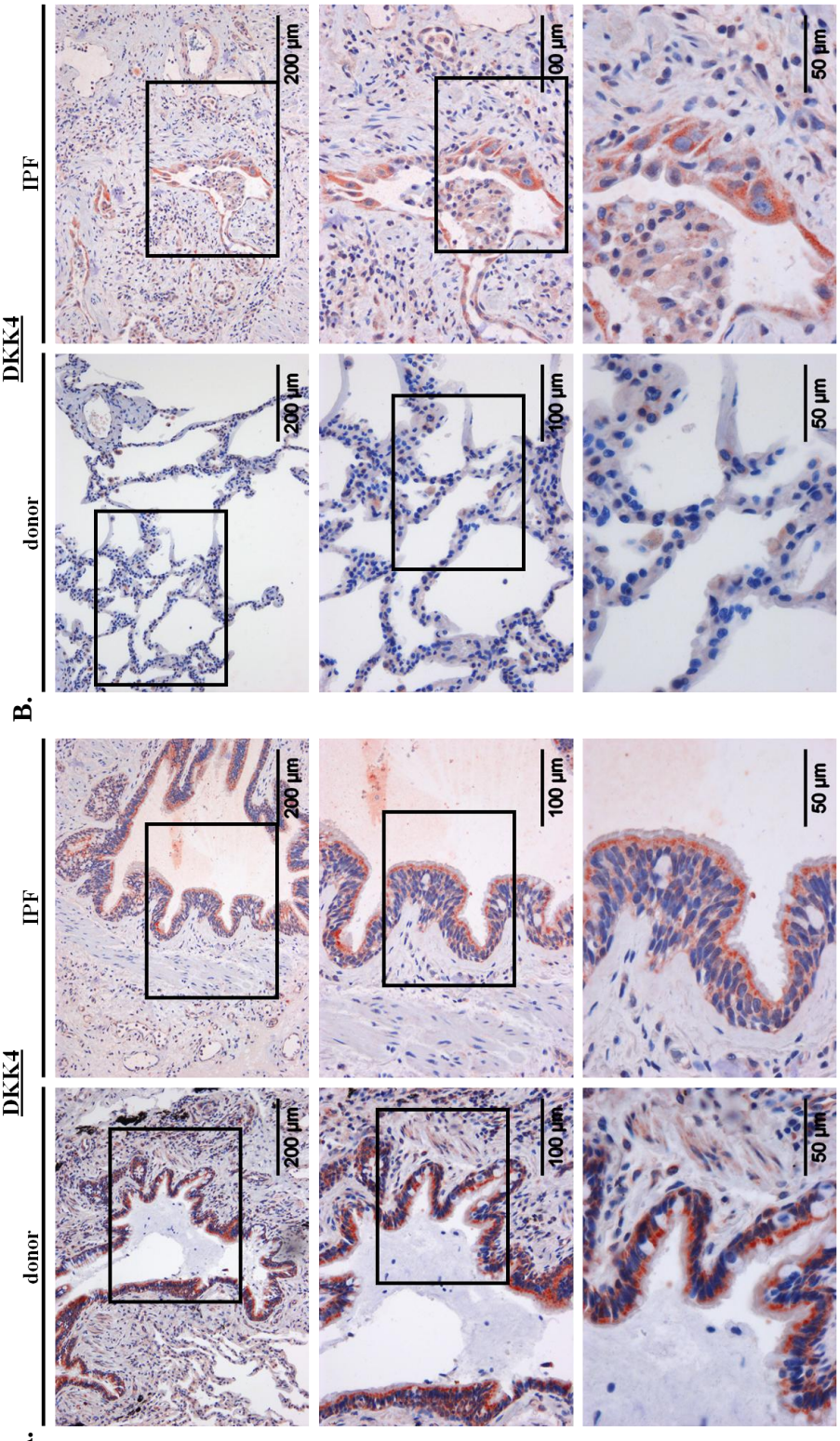

Figure 16. Localization of DKK4 protein in donor and IPF lung tissue.
Immunohistochemical staining for DKK4 protein was performed on lung tissue sections of donors and IPF patients. Stainings were performed at least twice using three different donor and IPF lung tissues. Representative **bronchial (A)** and **alveolar (B)** regions of donor **(left panels)** and IPF **(right panels)** lungs are shown in three magnifications as indicated.

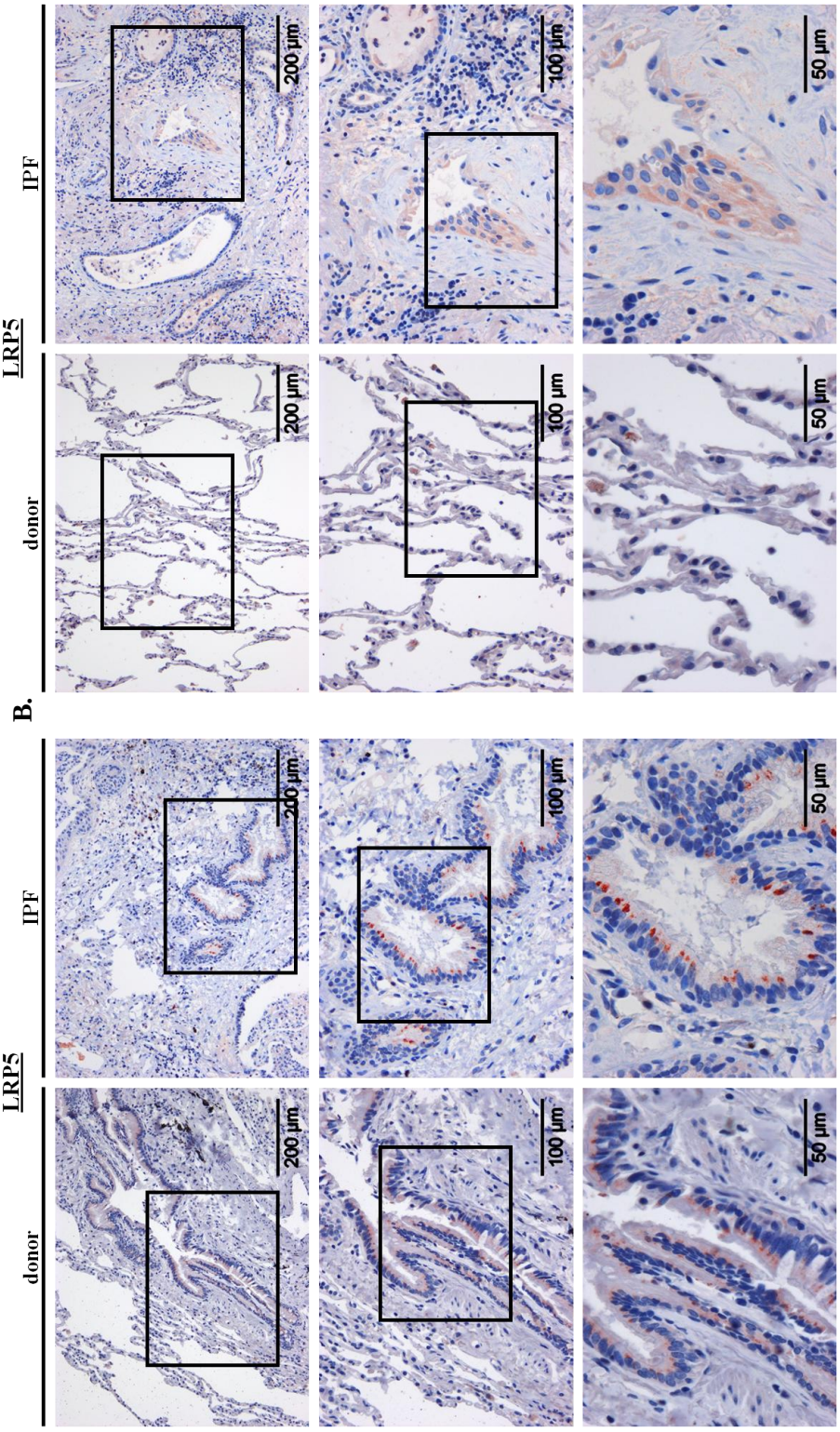

Figure 17. Localization of LRP5 protein in donor and IPF lung tissue.
Immunohistochemical staining for LRP5 protein was performed on lung tissue sections of donors and IPF patients. Stainings were performed at least twice using three different donor and IPF lung tissues. Representative **bronchial (A)** and **alveolar (B)** regions of donor **(left panels)** and IPF **(right panels)** lungs are shown in three magnifications as indicated.

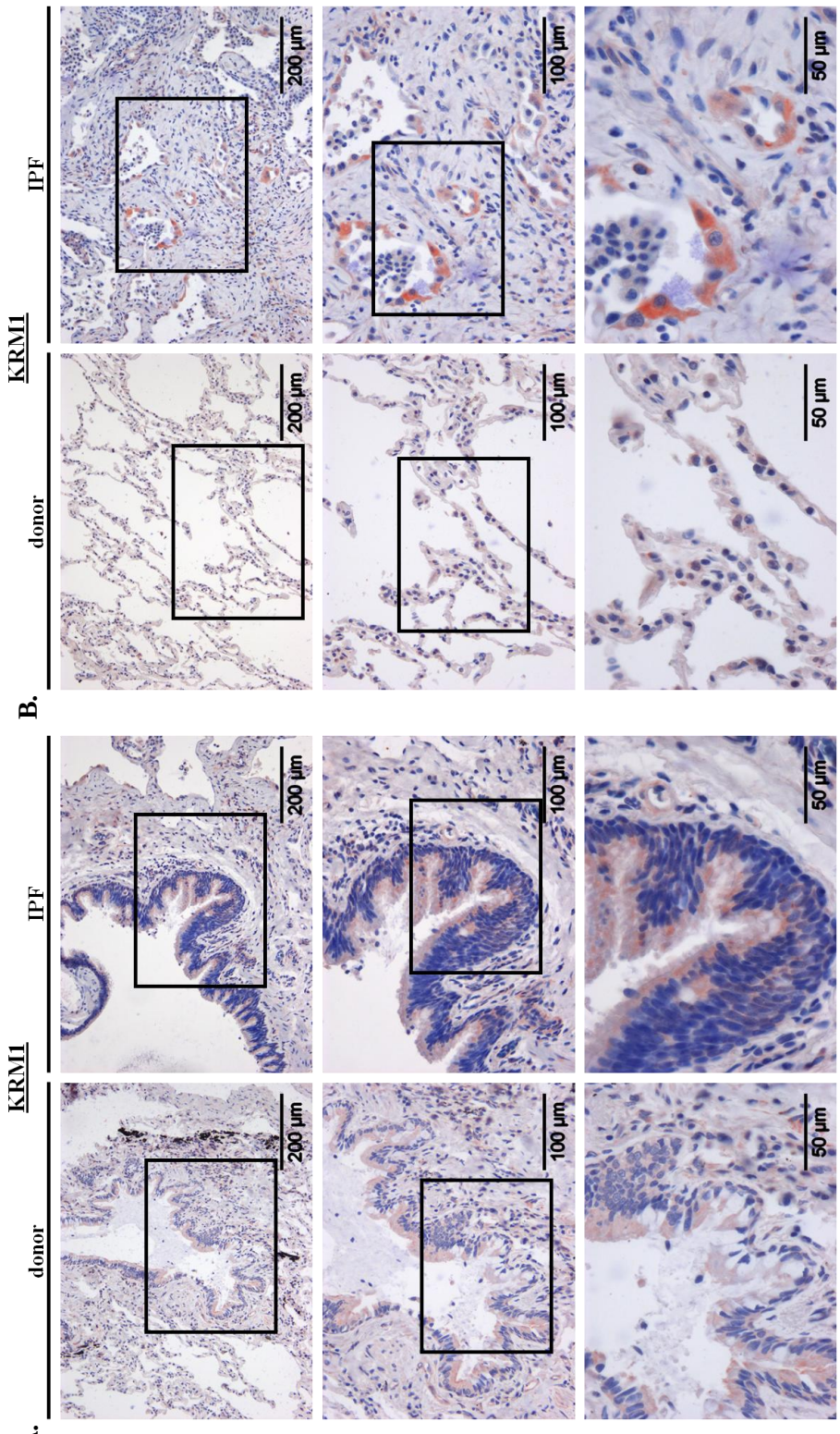

Figure 18. Localization of KRM1 protein in donor and IPF lung tissue.
Immunohistochemical staining for KRM1 protein was performed on lung tissue sections of donors and IPF patients. Stainings were performed at least twice using three different donor and IPF lung tissues. Representative **bronchial (A)** and **alveolar (B)** regions of donor **(left panels)** and IPF **(right panels)** lungs are shown in three magnifications as indicated.

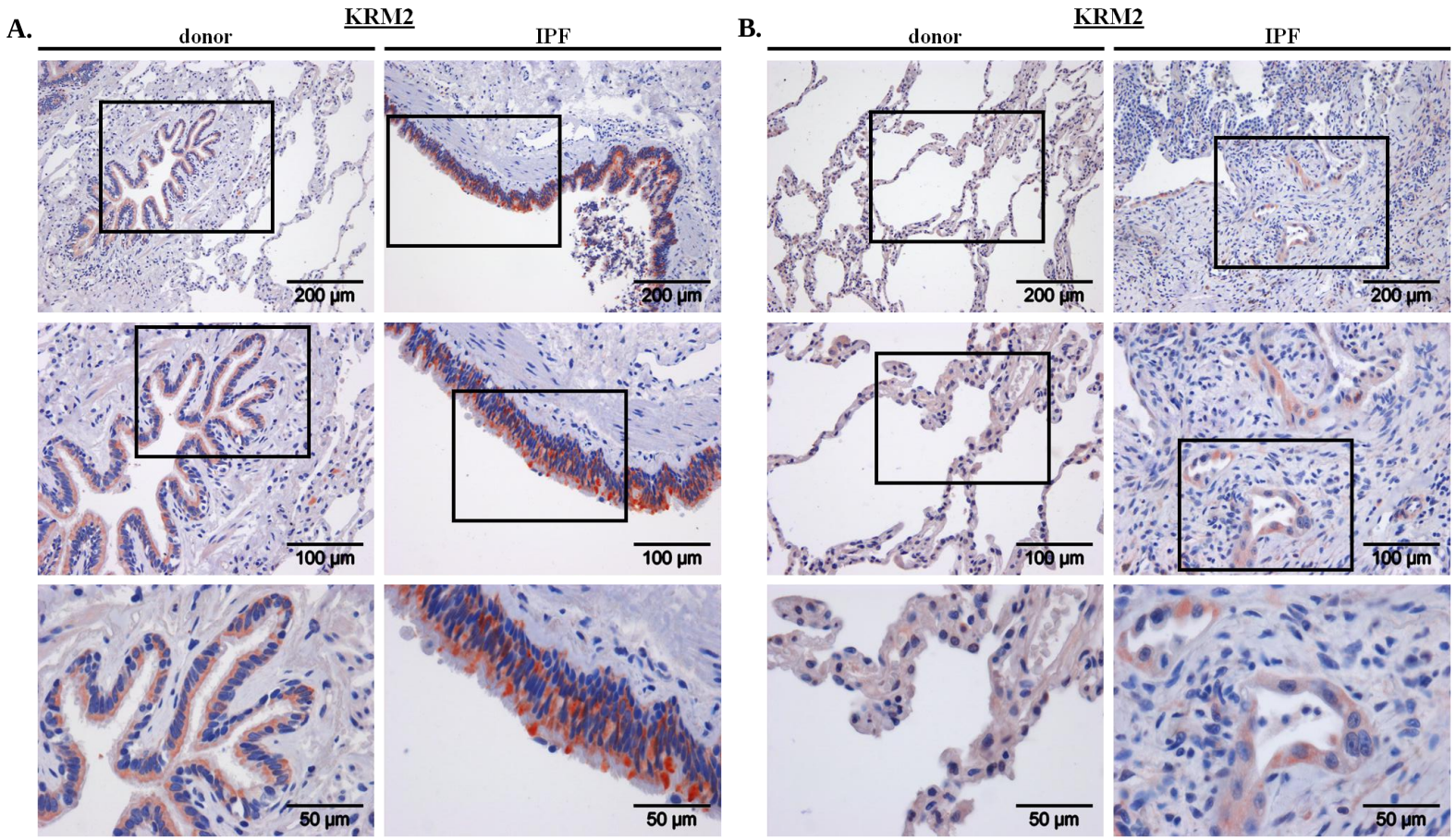

Figure 19. Localization of KRM2 protein in donor and IPF lung tissue.
Immunohistochemical staining for KRM2 protein was performed on lung tissue sections of donors and IPF patients. Stainings were performed at least twice using three different donor and IPF lung tissues. Representative **bronchial (A)** and **alveolar (B)** regions of donor (**left panels**) and IPF (**right panels**) lungs are shown in three magnifications as indicated.

11 Publications and presentations

11.1 Publications

1. **Pfaff EM**, Becker S, Gunther A, et al: Dickkopf proteins influence lung epithelial cell proliferation in idiopathic pulmonary fibrosis. Eur Respir J 37:79-87, 2011

2. Konigshoff M, Balsara N, **Pfaff EM**, et al: Functional Wnt signaling is increased in idiopathic pulmonary fibrosis. PLoS One 3:e2142, 2008

11.2 Oral presentation

Freier Vortrag, Sektion Zellbiologie, 49. Kongress der Deutschen Gesellschaft für Pneumologie und Beatmungsmedizin e.V., Lübeck, April 2008. **E. Pfaff**/Gießen, N. Balsara, O. Eickelberg, M. Königshoff. Expression und Lokalisation von Wnt-Inhibitoren in der idiopathischen Lungenfibrose.

12 Erklärung zur Dissertation

„Hiermit erkläre ich, dass ich die vorliegende Arbeit selbständig und ohne unzulässige Hilfe oder Benutzung anderer als der angegebenen Hilfsmittel angefertigt habe. Alle Textstellen, die wörtlich oder sinngemäß aus veröffentlichten oder nichtveröffentlichten Schriften entnommen sind, und alle Angaben, die auf mündlichen Auskünften beruhen, sind als solche kenntlich gemacht. Bei den von mir durchgeführten und in der Dissertation erwähnten Untersuchungen habe ich die Grundsätze guter wissenschaftlicher Praxis, wie sie in der „Satzung der Justus-Liebig-Universität Gießen zur Sicherung guter wissenschaftlicher Praxis“ niedergelegt sind, eingehalten sowie ethische, datenschutzrechtliche und tierschutzrechtliche Grundsätze befolgt. Ich versichere, dass Dritte von mir weder unmittelbar noch mittelbar geldwerte Leistungen für Arbeiten erhalten haben, die im Zusammenhang mit dem Inhalt der vorgelegten Dissertation stehen, oder habe diese nachstehend spezifiziert. Die vorgelegte Arbeit wurde weder im Inland noch im Ausland in gleicher oder ähnlicher Form einer anderen Prüfungsbehörde zum Zweck einer Promotion oder eines anderen Prüfungsverfahrens vorgelegt. Alles aus anderen Quellen und von anderen Personen übernommene Material, das in der Arbeit verwendet wurde oder auf das direkt Bezug genommen wird, wurde als solches kenntlich gemacht. Insbesondere wurden alle Personen genannt, die direkt und indirekt an der Entstehung der vorliegenden Arbeit beteiligt waren. Mit der Überprüfung meiner Arbeit durch eine Plagiatserkennungssoftware bzw. ein internetbasiertes Softwareprogramm erkläre ich mich einverstanden.“

_____ _____

Ort, Datum Unterschrift

13 Danksagung

Besonders bedanken möchte ich mich bei Dr. Dr. Melanie Königshoff für die Betreuung während der Zeit in der ehemaligen Arbeitsgruppe und auch bei der nachfolgenden Ausarbeitung. Ich bin ihr sehr dankbar für die Unterstützung in den vielen theoretischen und praktischen Fragen sowie für ihre Begeisterungsfähigkeit, womit sie mich immer wieder motiviert hat.

Besonderer Dank geht auch an Prof. Dr. Oliver Eickelberg. Er hat mir ermöglicht, in einer engagierten Arbeitsgruppe das wissenschaftliche Arbeiten zu erlernen. Ich danke ihm für das Schaffen eines besonders angenehmen und motivierenden Arbeitsumfeldes mit vielen Möglichkeiten zur produktiven Diskussion.

Bei Simone Becker möchte ich mich herzlich für die geduldige Unterstützung bei den praktischen Schwierigkeiten und ihre stete Hilfsbereitschaft bedanken.

Anna Lühring, Nisha Balsara und Monika Kramer danke ich für freundliche Worte an anstrengenden Tagen und fürs Zuhören.

Der gesamten ehemaligen Arbeitsgruppe gilt ein großer Dank für ihre Hilfsbereitschaft, für anregende Diskussionen und für das freundliche Miteinander.